INVESTIGATION OF RESIDUAL STRENGTH AND FATIGUE LIFE OF UNSTIFFINED ALUMINUM PANELS WITH MULTIPLE SITE DAMAGE

THESIS

Mark C. Cherry
Captain, USAF

AFIT/GAE/ENY/95D-06

DEPARTMENT OF THE AIR FORCE
AIR UNIVERSITY
AIR FORCE INSTITUTE OF TECHNOLOGY

Wright-Patterson Air Force Base, Ohio

INVESTIGATION OF RESIDUAL STRENGTH AND FATIGUE LIFE OF UNSTIFFINED ALUMINUM PANELS WITH MULTIPLE SITE DAMAGE

THESIS

Mark C. Cherry
Captain, USAF

AFIT/GAE/ENY/95D-06

AFIT/GAE/ENY/95D-06

INVESTIGATION OF RESIDUAL STRENGTH AND FATIGUE LIFE OF UNSTIFFINED ALUMINUM PANELS WITH MULTIPLE SITE DAMAGE

THESIS

Mark C. Cherry
Captain, USAF

AFIT/GAE/ENY/95D-06

AFIT/GAE/ENY/95D-06

INVESTIGATION OF RESIDUAL STRENGTH AND FATIGUE LIFE OF UNSTIFFINED ALUMINUM PANELS WITH MULTIPLE SITE DAMAGE

THESIS

Presented to the Faculty of the Graduate School of Engineering

of the Air Force Institute of Technology

Air University

In Partial Fulfillment of the

Requirements for the Degree of

Master of Science in Aeronautical Engineering

Mark C. Cherry, B.S.E.M.

Captain, USAF

December 1995

Approved for public release; distribution unlimited

Acknowledgments

As with any research effort, a single name on the title sheet does not lend the proper credit to the number of people who have worked to accomplish the project. This study has been no exception. I would like to give thanks to all those individuals who have lent their time and effort to help me complete this study.

I would like to thank Capt Karl Hart of Wright Labs FIBEC for providing the sponsorship for this research. Special thanks goes to Dr. Mall who provided research direction, answers to questions, and many hours of proofreading.

Many people helped with the successful accomplishment of this study. I would like to specifically mention Mr. Mark Derriso, who helped me immeasurably with the testing of my material specimens. Mr. Larry Mack provided timely support in final fabrication of test specimens. The technicians working in the AFIT lab unselfishly lent their time to answer questions or track down any number of problems I had while testing. I would like to extend a special thanks to the AFIT Model Shop for the many designs and redesigns of the test specimens used in this study. Without their effort, this research would not have been possible.

Mr. Markus Heinimann of Purdue University deserves special mention. He provided a wealth of knowledge in the setup and analysis of the tests within this study. I would like to thank him for his time, effort, and e-mails.

Finally, I am forever grateful to my family. Their continual love, and support has always provided me with a foundation from which I could accomplish my goals. This effort has been no exception.

Mark C. Cherry

Table of Contents

List of Figures

List of Tables

Abstract

Multiple Site Damage (MSD) is the occurrence of small fatigue cracks at several sites within aircraft structures. This is important since it may lower the residual strength and fatigue life of the structure beyond what can be predicted using the damage tolerance technique based on a single crack, currently in use to design aircraft structures.

This study investigated the effects of MSD on unstiffined panels. MSD usually occurs at rivet holes, or other stress concentration locations within an aircraft structure. This study simulated rivet holes with MSD, by using holes of constant diameter with small cracks, evenly spaced across the midspan of specimens. The objective of the study was to test the validity of the available analytical methods to predict the residual strength and fatigue life of panels with MSD.

Residual strengths of large specimens with MSD were measured in two different configurations to test the applicability of five failure criteria. A total of ten residual strength tests were conducted using panels of 1.016 mm (0.04 in) thick 2024-T3 Aluminum. These panels had two configurations with each having two variations. These configurations were prepared by either fatiguing MSD damage at rivet holes, or simulating fatigue damage by sawcuts at each hole. Each residual strength specimen was subjected to a constantly increasing tensile load until failure occurred across the midspan of the gauge section. Five different failure criteria were used for each specimens geometry and material properties. When specimens were assumed to behave in a linear elastic manner, failure criteria overestimated the residual strength of specimens. Failure criterion which included consideration for crack interaction effects consistently predicted conservative

failure loads. A failure criterion which was based on the plastic zone size of MSD cracks gave the accurate prediction for failure load in panels with MSD damage.

Fatigue tests were also conducted in three configurations to test the ability of analytical methods to predict fatigue life. Three failure criteria were incorporated into a computer program, that was developed for this study. The purpose of this program was to use the three failure criteria to determine if fatigue life could be adequately predicted by analytical methods. Crack growth behavior and material property characteristics were used in conjunction with the three criteria to predict fatigue life of the tested specimens. The two failure criteria which relied on linear elastic material assumptions consistently overestimated the fatigue life of the tested specimens. When MSD interaction effects were included in these linear elastic criteria, fatigue life prediction remained unconservative. A failure criteria that accounted for crack interaction effects as well as the MSD cracks plastic zone size produced the better prediction of fatigue life.

The analytical methods investigated in this study can provide an aircraft designer with a conservative estimate of the residual strength of aircraft structures with MSD damage. However, the three failure criteria considered in this study produced unconservative fatigue life predictions.

INVESTIGATION OF RESIDUAL STRENGTH AND FATIGUE LIFE OF UNSTIFFINED ALUMINUM PANELS WITH MULTIPLE SITE DAMAGE

I. Introduction

Multiple Site damage (MSD) is a type of widespread damage due to fatigue, and corrosion effects. It is characterized by the simultaneous presence of several cracks at various sites, such as at different holes in the structural element (28). This may become significant and critical when cracks are of sufficient size and density whereby the structure will no longer meet its damage tolerance requirements. MSD may reduce the residual strength and fatigue life of an aerospace structural component below that predicted by simple analytical techniques, which is currently based on a single crack approach without consideration of interaction with the surrounding cracks. For the purposes of this study, residual strength is defined as the maximum stress a component can sustain before complete failure occurs in the presence of damage, and fatigue life is defined as the number of cycles a component can sustain while subjected to a constant amplitude loading before failure occurs.

Increasingly aircraft, both military and commercial, are being used beyond their designed lifetime. The average age of U.S. jetliners now stands at 12.67 years, but it is not uncommon to see 25-30 year old aircraft flying with some commercial fleets (5). As aircraft age, structural degradation presents a risk to safety in the form of fatigue and corrosion. The most widely known failure attributed to MSD is the Aloha Airlines incident. On April 28, 1988 an Aloha Airlines Boeing 737 experienced an in-flight

structural failure when the upper fuselage ripped open and a 15 foot section of the skin peeled away. This accident resulted in the death of a flight attendant , and nearly many others aboard the aircraft (12). This incident spawned an increased interest in the structural integrity of aging aircraft. Numerous incidents since the Aloha Airlines accident have served to reinforce the need for extensive study of this phenomenon.

MSD poses a significant challenge to those who must assure the structural integrity of aging aircraft. Most commercial aircraft are designed and maintained according to the "damage tolerance" philosophy that is based on the principles of fracture mechanics (16). The damage tolerance philosophy is based on a single lead crack in a structure. Several small MSD cracks, however, can cause a structure to catastrophically fail when these cracks are smaller than a single critical crack which the maintenance crew is looking for.

Several studies have been done to investigate various MSD conditions, as discussed in Chapter 2. There are various levels of testing required to achieve a full understanding of the structural components with MSD. These include: small coupon specimens, large flat panels with MSD, curved panels, subscale models, and finally aircraft prototypes (12). NASA, in cooperation with the Boeing™ Commercial Airplane Company and Douglas™ Aircraft Company, has sponsored extensive research of curved panels and subscale models. The goal of NASA airframe structural integrity program (ASIP) is to achieve the verification of a structural analysis methodology through testing of the curved panel and subscale barrel-test article level (12). Moukawsher (18) investigated 2024-T3 aluminum panels to study if analytical methods could be used to

adequately predict residual strength, and fatigue life of panels with MSD. This study involved the relatively small panels. Jeong and Brewer (13), also investigated small panels with MSD to compare analytical techniques for predicting failure due to MSD. Therefore, a need exists to investigate the large flat panels with MSD which are bigger than the coupon type panels studied by other researchers (13,18), but smaller than the large subscale models currently under study by NASA. This research fills this need of the testing and analysis of these large panels with MSD. And, it can be extended in the future to incorporate the larger panels as sponsored by NASA.

The objective of this study was, therefore, to gain a better understanding of the effects of MSD and how cracks coalesce in the presence of other cracks in large flat panels. This was accomplished by testing and applying various failure criteria to 381 mm (15 in) wide specimens with MSD to determine if width and thickness affect the validity of presently available analytical prediction methods. This study also investigated the effects of using sawcuts to simulate fatigue cracks in the measurement of residual strength with MSD.

The objective was accomplished by testing ten specimens for residual strength in two different configurations. The first configuration, Type A, had a lead crack with no other additional holes or MSD. It was used to obtain an average stress intensity factor for the material. The second configuration, Type B, included a lead crack and holes with MSD. It was used to validate failure criteria for MSD. Additionally four specimens' fatigue lives were tested in three different configurations to investigate the applicability of using three analytical techniques to predict fatigue life. The first configuration, Type A,

had holes spanning the specimen with MSD at every hole. The second configuration, Type B, had a lead crack and holes without MSD. The final configuration, Type C, had a lead crack and holes with MSD.

The effects of MSD damage on residual strength and fatigue life is described in this study. Chapter 2 provides the background and the previous works related to this study. Chapter 3 describes the procedures which were used to gather data for the fourteen tests used in this study. Failure strength, crack growth, and fatigue life data were obtained to establish residual strength and fatigue life of the aluminum panels. Two residual strength, and three fatigue life configurations were used to make comparisons among different analytical models. Chapter 4 gives a detailed description of the analytical models used to predict both residual strength and fatigue life. Chapters 5 and 6 detail the results and analysis of the fourteen tests used in this study. Finally, Chapter 7 provides the conclusions and recommendations of the investigation of MSD damage on residual strength and fatigue life.

The results of this study coupled with the earlier studies by other researchers should become a basis from which a new damage tolerance philosophy can be integrated, and implemented within the aircraft industry. The long term goal of this study is to get a firm understanding of the failure of aircraft structures subjected to MSD, thereby aircraft manufacturers and operators will be able to take steps to mitigate the influence of MSD on the operational life of aircraft.

Introduction

MSD occurs within structures in three different stages, Local stage, Crack Growth, and Linkup and Failure. These stages differ mainly by the mechanisms which drive the crack growth.

1) Local Stage - It is the period when cracks are too small to influence adjacent cracks and the development of each crack is dominated by the influence of its local structural details (7). This period begins with the initiation of a crack such as from a rivet hole, or structural flaw. It ends when the crack has reached sufficient size that interaction effects from other cracks, or structural inclusions affect the crack growth. In a study by Moukawsher (18) as well as in this study, this length, a_t, is taken from a method proposed by Dowling (9):

$$a_t = \frac{r}{\left[(1.12 * K_t)^2 - 1\right]} \tag{1}$$

where: r = the radius of the hole
a_t = the transition crack length
K_t = the stress concentration factor

2) Crack Growth - This period is when cracks have reached their transition length and are of sufficient length such that they interact . To be able to model cracks in this stage, one has to consider both crack interactions as well as local geometry (7).

3) Linkup and Failure - The linkup and failure criteria is the most important stage. It determines when and at what load the cracks will cause a catastrophic failure (7). For this purpose, several different failure criteria have been proposed (3,13,27).

The previous works pertinent to this study include MSD studies dealing with crack growth and interactions, and crack linkup and failure. These studies incorporate either analytical techniques, or analysis coupled with specimen testing. Most of the previous works in this chapter employed 2024-T3 aluminum, unless mentioned otherwise, as the testing material. A brief background of these studies is presented in this chapter which are related to the present work. These studies are separated into two parts involving investigation of crack growth, or investigation of crack linkup and failure.

Crack Growth

The analysis of the growth of a crack in a structure requires knowledge of local and remote stress concentration factors. Various analytical methods have been used to investigate this phenomenon.

Finite Element Method with Alternating Technique: This method is based on the principle of superposition of stresses associated with cracks and free boundaries. The stresses in the uncracked body are analyzed first by using finite element or boundary element methods. The effects of cracks are assessed by erasing the traction at the crack location in the otherwise uncracked body. To accomplish this, the finite body is replaced by an infinite one, with the stresses going to zero at infinity. This infinite body problem has an analytical solution, but the far field stresses do not satisfy the boundary conditions. To account for this , the residual traction's at the boundaries are erased, first by solving an uncracked infinite body with the residual boundary tractions, and then by erasing the crack tractions in the uncracked body. This iterating loop is repeated until the analytical solution

for this infinite body also satisfies the zero traction condition of the finite body. Once the solution has converged, the stress intensity factor may be obtained.

The alternating technique has been employed by Dawicke and Newman (19), Tong and Atluri (2), and Park and Atluri (20). Dawicke and Newman (6) used boundary elements to analyze different types of MSD specimens with open holes and uniaxial loading. They report fatigue lives of their crack configurations agree within 20% of their analysis of the configurations using boundary elements.

Crack Tip Opening Angle Approach: Newman, Dawicke, Sutton and Bigelow (19) investigated critical crack tip opening angle, with an elastic-plastic finite element analysis. They were able to predict the stable tearing behavior of large lead cracks in the presence of stable tearing of MSD cracks. Further analysis of crack tip opening angle criterion by Dawicke and Sutton (19) shows that stable tearing behavior of thin sheets of 2024-T3 is influenced by stress history. Specifically, the initial stable tearing behavior of low and high fatigue stress tests is significantly different.

Hybrid finite element method: This method is based on a variational formulation in which relevant field variables in the element need not satisfy the requirements of inter-element displacement compatibility and inter-element traction reciprocity (7). The constraint condition can then be included in the functional by the use of Lagrange multipliers, which are the additional variables at the element boundary. The method can provide directly the solution for the strength singularities (such as stress intensity factors at the tips of a crack). Hybrid finite element methods (30) are directly applicable to crack

growth analysis. This method is reported to be extremely accurate and efficient in comparison to the standard finite element method to predict growth of cracks.

Finite element analysis with super-convergent methods: This analysis method, like other finite element analysis has been used to predict growth of cracks initiated from stress concentrations. Actis and Szabo (1) used finite element analyses with super-convergent methods to solve for the stress intensity factors at MSD crack tips. The solution was obtained using the p-version program "PEGASYS" which allows extraction of the stress concentration on an arbitrary circular path around the crack tip. The advanced development of computational speed will allow more complicated codes to be used.

Compound methods: For an array of collinear cracks in structural components the common approach currently being used in the aircraft industry is the compounding solution method (7). The principle of the compounding method is to obtain a solution for the stress intensity factor of a complex geometric configuration by superimposing a set of appropriate assisting solutions, usually associated with simple configurations of cracks and component boundaries and having known solutions. An assisting configuration usually contains only one boundary which interacts with the crack. Combining the effects of each boundary on individual cracks is subject to the principle of superposition with the addition of an interaction effect between the separate boundaries. The compound method has been used by Partl and Schijve (21) to analyze a collinear row of open holes with the center three cracked. They report agreement within 14% with experimental results. Although this is a simplified case, their results show that simple compounding techniques based on superposition produce very acceptable results for MSD analysis.

Linkup and Failure

The linkup and failure criteria is extremely important. It determines at what load a structure will fail. Consequently it effects the inspection intervals and the size of cracks which would be deemed critical during the inspection.

Swift (28) has proposed a criteria based on the gross stress level which will cause a specimen with an existing lead crack to coalesce with surrounding cracks. Specifically, he calculated the load at which the plastic zone size of lead cracks, which is based on half of the Irwin plastic zone size, will touch the plastic zone caused by a MSD crack. Swift postulated that the link-up of a lead crack with a MSD crack would occur when the intact ligament stress between the lead crack tip and the MSD crack tip reaches the typical yield strength of the material. The ligament between the two cracks will fail when the plastic zones of the two cracks touch. The interactions between the two crack tips can be determined for the Swift criteria from analyses by Rooke and Cartwright (22) or Kamei and Yokobori (14).

Moukawsher (18) found that Swift's residual strength criterion (28) produces a good estimate of the residual strength of small panels with a central lead crack and nearly uniform MSD. For panels without MSD, the classical fracture mechanics approach is suitable. However, the fracture mechanics and net ligament loss methods are not well-suited for making MSD residual strength predictions. He also found that the interaction of cracks significantly increases the rate of crack growth and reduces the overall fatigue lives of panels with extensive MSD, even when the MSD cracks are initially small in length (1.27 mm to 2.54 mm (0.5 in to 0.1 in)).

Dahr, Gallagher and Berens made a comparison of three fracture criteria: R-curve analysis, Swift's method, and the fracture mechanics method (11). Their conclusions based on this analysis were that these three criteria imply that crack coalescence is influenced by the distance between the adjacent crack tips. The ratios of crack length between small and large cracks does not effect crack coalescence when the distance between crack tips is less than 0.254 cm (0.1 in). The effect of fracture toughness on the residual strength and the crack coalescence is more severe than the yield strength of the material. The lower bound for the residual strength is decided by the fracture mechanics method or R-curve criterion for large distances between the crack tips, but as this distance approaches zero, Swift's criterion dominates.

Jeong and Brewer (13), proposed two criteria for multiple crack linkup. These are based on solutions for displacements and stresses in the presence of multiple cracks. These criteria are the average displacement criterion, and the average stress criterion. The average displacement criterion assumes that the stress across a ligament is uniformly equal to the material's ultimate stress at failure. Linkup is assumed when the remote tension is such that the crack tip openings cannot be kept closed by the material. The average stress criterion models the various cracks individually and is based upon the stress distribution between neighboring crack tips. Linkup between two adjacent cracks is assumed to occur when the average stress in the ligament between the crack tips reaches the ultimate stress of the material. Results from using these criterion show that the average stress criterion compares closely with the Swift criterion when stable tearing is assumed, i.e. 5.7% for the

average stress criterion compared to 1.9% for the Swift criterion from experimental data. The displacement criterion averages a 17.5% difference from experimental tests.

It is clear that there is limited research in the area of crack linkup and failure. The need to further validate analytical methods for large flat panel subjected to MSD has spawned this research. The current research in this study is part of an attempt to gain a better understanding of the coalescence of multiple cracks within an aircraft structure.

III. Experimental Set-up and Procedures

The purpose of this study, as mentioned earlier, was to investigate the residual strength, and fatigue characteristics of wide, but thin aluminum panels with MSD. This chapter describes the specimen details, material, preparation, and testing procedures used for this study. Specifically, this chapter will discuss the preparation of specimens to measure the residual strength, and fatigue behavior, procedures for gathering data on both types of specimens, and procedures for gathering material property data.

Material

The material chosen for this study was 2024-T3 Aluminum with a thickness of 1.016 mm (0.04 in). 2024 is a heat treatable aluminum copper alloy. The T3 temper designation means that the material is cold worked to improve strength after solution heat-treatment. 2024-T3 is noteworthy for its high toughness (17). 2024-T3 is used extensively in the airline industry for various aircraft structures. It was first developed for use on the Douglas DC-3 in the late 1930's (18).

Specimen Preparation

All specimens used in this study were cut from sheets of 2024-T3 Aluminum 1.219 m (48 in) x 3.657 m (144 in) with a 1.016 mm (0.04 in) thickness by the AFIT Model Fabrication Shop.

There were four types of specimens employed in this study. Tensile specimens were used to measure both yield and ultimate strength of the batch of aluminum material used in this study. Middle Tension (MT) specimens were tested to establish the crack growth behavior, ΔK vs da/dN curve, for this material lot (24). Residual Strength (RS) specimens were used to find the ultimate strength of panels with MSD. Finally, fatigue (FAT) specimens were tested to determine the fatigue life of panels containing MSD in three different configurations. All specimens were fabricated such that the material rolling or grain direction was perpendicular to the intended loading. According to Luzar (15) aircraft fuselage panels are fabricated in this manner with the rolling direction in the longitudinal direction.

Tensile specimen: These specimens were machined with nominal dimensions of 203.2 mm (8 in) x 50.8 mm (2 in) with a gauge section width of 25.4 mm (1 in). The grain direction was perpendicular to the loading direction. Figure 1 shows the specimens used to measure the tensile strength which conform to ASTM standard E8 (29) for tensile tests.

MT specimen. These specimens were slightly bigger than the tensile specimens. A total of five specimens were machined with nominal dimensions of 203.2 mm (8 in) in length x 76.2 mm (3 in) in width with grain direction perpendicular to loading direction. The gauge section width was 50.8 mm (2 in). After these specimens were cut, they were taken to the machine shop of Wright Laboratory (Bldg 5) so that a center cut could be made in the gauge section. The cut was made by a wire Electric Discharge Machine (EDM). This cut was 7.62 mm (0.3 in) in length with a notch root radius less than

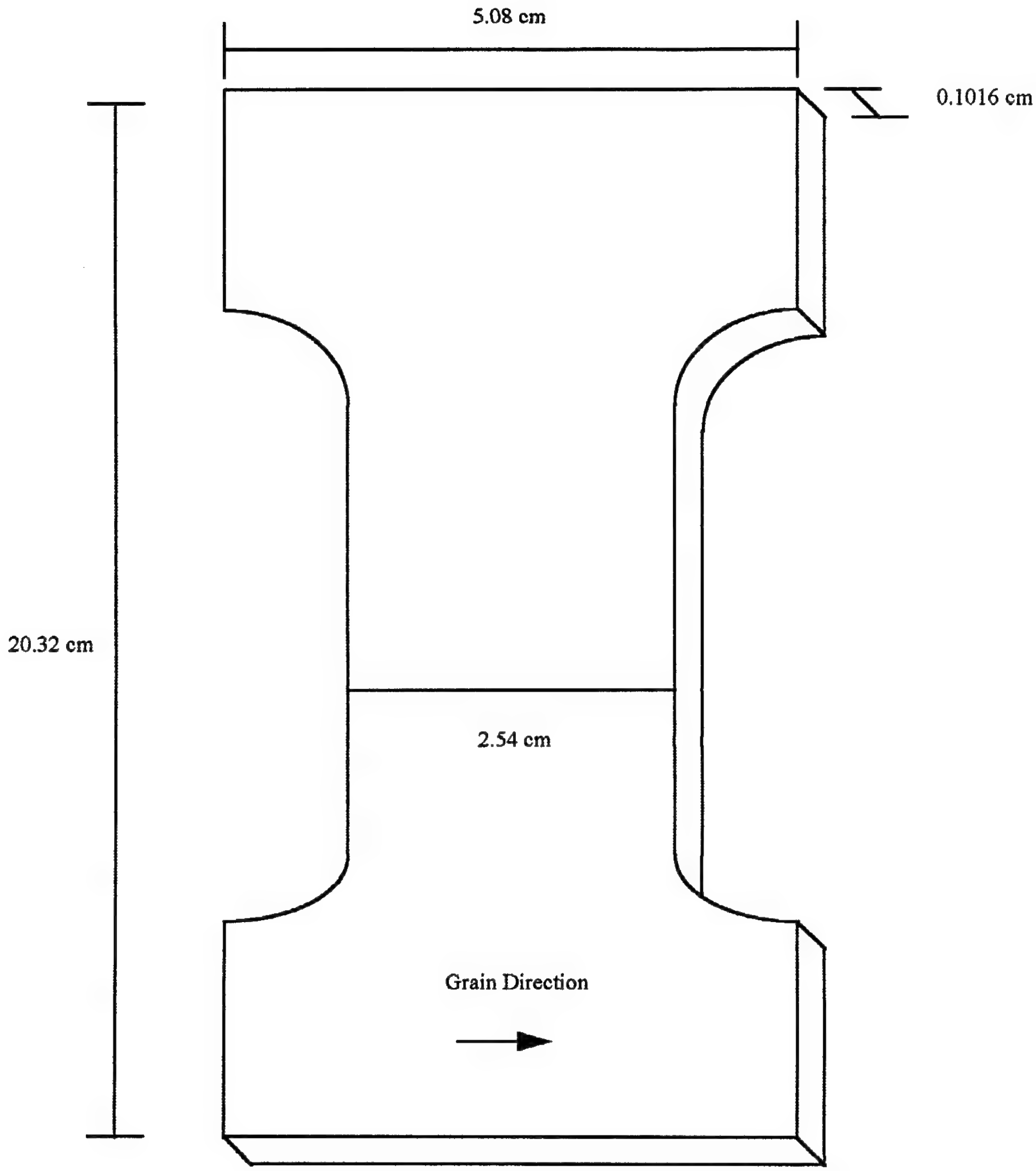

Figure 1. Tensile Test Specimen

0.075 mm (0.01 in). The specimens were then polished to a mirror like finish with semi-chrome polish so that crack length could be measured by an optical microscope having a resolution of +/- 0.0127 mm (0.0005 in). The MT specimens were then precracked at a stress of 40 MPa until cracks of 0.381 mm (0.015 in) emanated from both sides of the center cut. The MT specimens shown in Figure 2, conform to ASTM standard E647 (24).

RS specimen: The residual strength specimens were 1.016 m (40 in) x 0.609 m (24 in), with a 0.381 m (15 in) width across the gauge section as shown in Figure 3, with the grain direction perpendicular to the loading direction. After the initial dogbone shape was cut from the material lot, it was deburred, and bolt holes were punched into the gripping section of the specimens to allow them to be mounted into the testing machine. Holes of diameter 3.175 mm (0.125 in) were then drilled into the gauge section of the specimens conforming to the two configurations that were tested. The two different configurations used to measure the residual strength can be seen in Figure 4. Each configuration had two variations, lead cracks encompassed either five center holes, or seven center holes. Both configurations had a hole separation of 19.05 mm (0.75 in) measured from the hole centers. Configuration A was used to find the apparent stress intensity factor (K_{app}) for the material, and only had a central lead crack. Configuration B had a central lead crack and holes with MSD damage.

MSD damage involved two cracks emanating from all holes. These were prepared by precracking under fatigue loading conditions or machining by a fine saw. Specimens with fatigued precracks were initially drilled with holes 2.12 mm (0.0833 in) in diameter. These holes were then notched on both sides by a jewelers saw blade. The saw blade

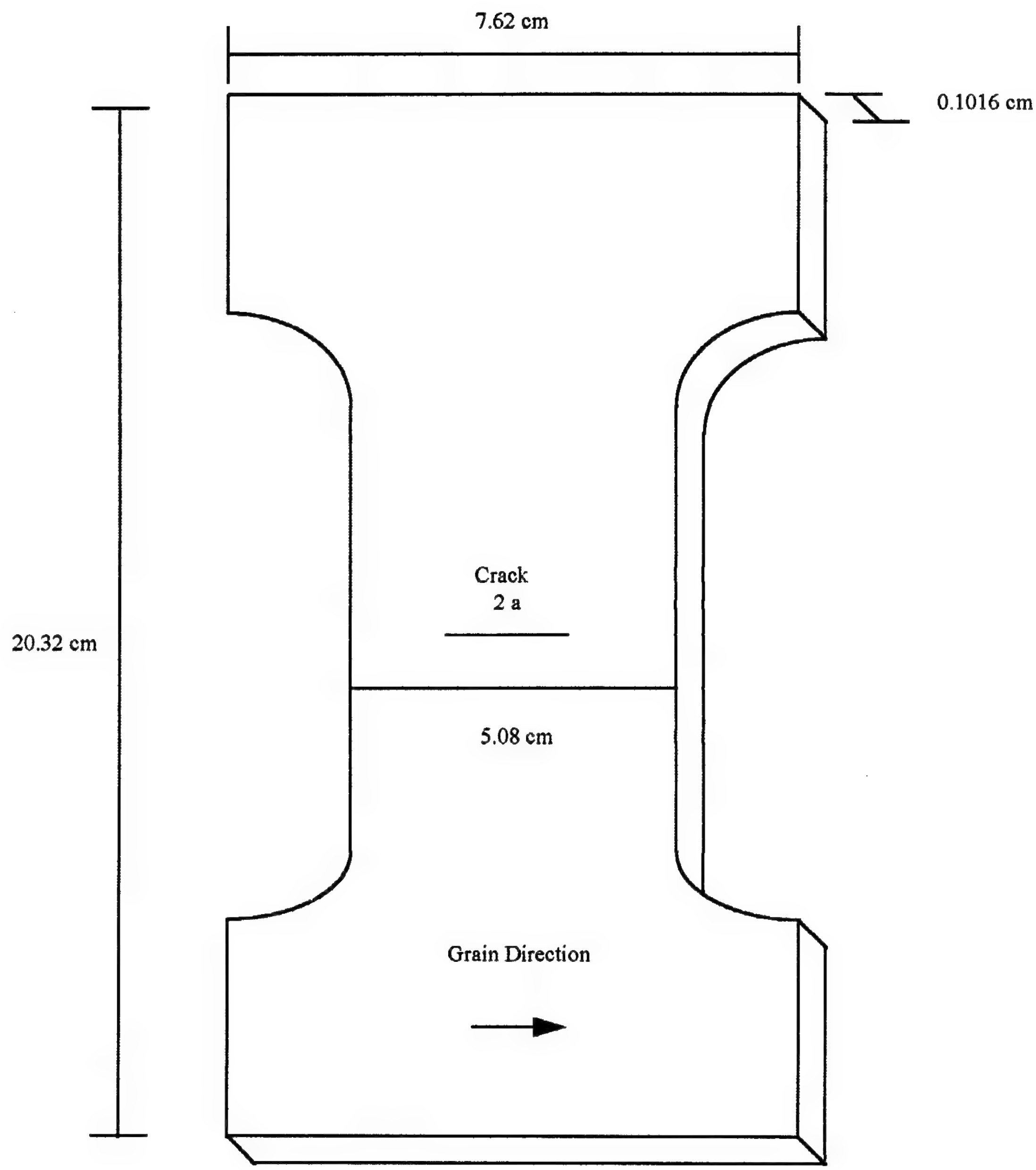

Figure 2. MT Specimen

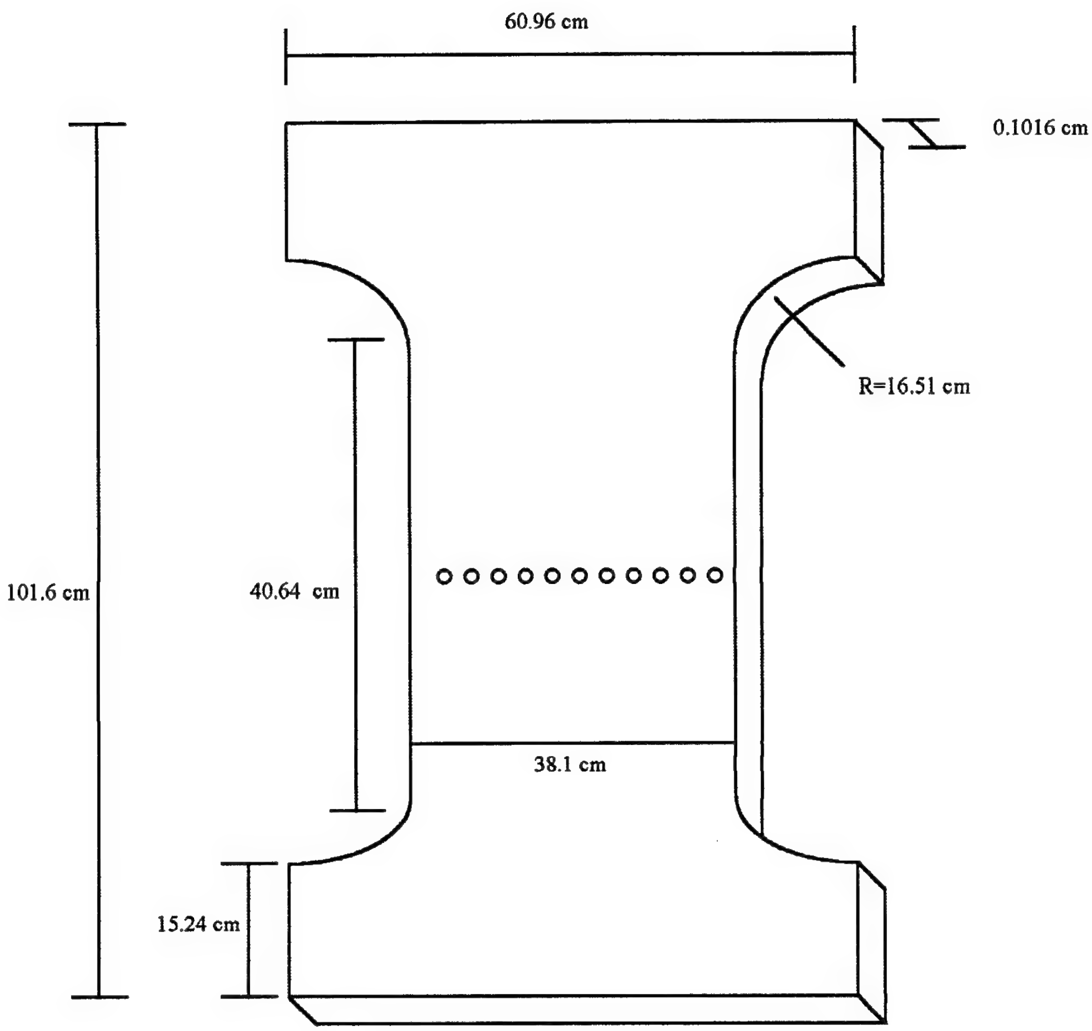

Figure 3. Residual Strength and Fatigue Specimens

Type A: Central Lead Crack only, No Holes or MSD (Lead Crack encompassed middle seven holes or middle five holes)

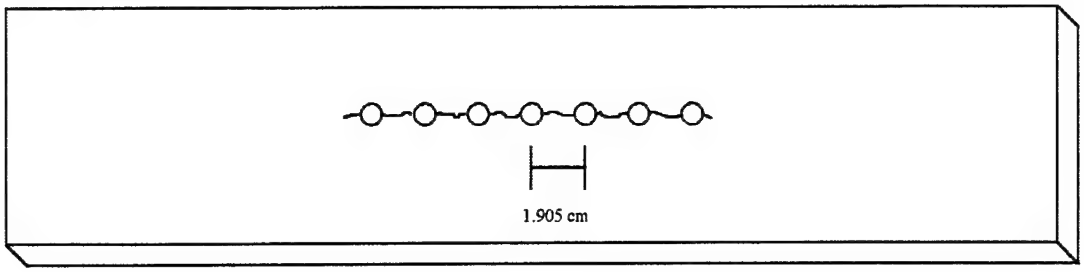

Type B: Central Lead Crack. MSD cracks at all Holes (Lead Crack encompassed middle seven holes or middle five holes)

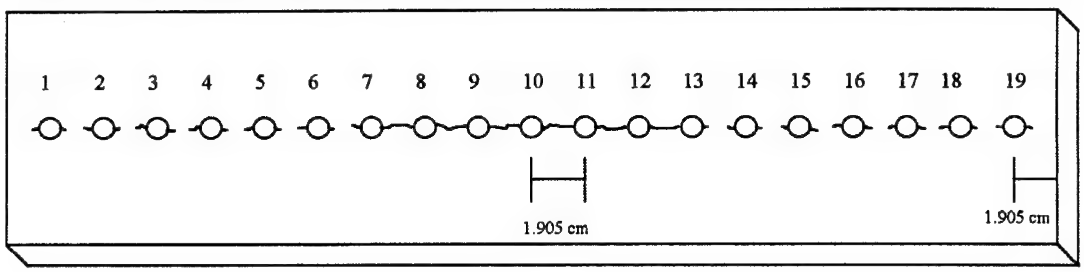

Figure 4. Residual Strength Specimen Configurations

had a thickness of 2.032 mm (0.08 in). These specimens were then fatigued under a constant amplitude cyclic condition at 75.8 MPa (11 ksi) stress level to force machined cracks to grow from the notched holes. After the cracks grew by at least 0.762 mm (0.03 in), the holes were then drilled to the 3.175 mm (0.125 in) diameter at which they were tested. This method gave real fatigue cracks emanating from the sides of holes.

Specimens with sawcuts substituting for fatigue cracks were drilled with holes of 3.175 mm diameter, and then notched with the jewelers saw. The central lead crack for all residual strength specimens was cut by a Ingersoll-Rand HS 3000 Water Jet Cutting System with an Alan Bradley 8400 CNC controller. Finally, two extensometer brackets were placed in the center of the specimen, above and below the lead crack. They were mounted with super glue, and taped down with electrical tape. The final length of all cracks at different holes along with the central lead cracks of these specimens are given in Table 1. The specimens with fatigued MSD cracks, RS 05B, and RS 06B, are given in boldface. The crack lengths given for each hole are measured from the hole edge.

Fatigue Specimen: The fatigue specimens were prepared in the same manner as the residual strength specimens. The initial holes of diameter 2.032 mm were notched with an EDM before they were precracked. These specimens were precracked at a 75.8 MPa stress level until 0.762 mm cracks grew from the notches. These holes were then drilled to their final diameter of 3.175 mm with fatigue cracks emanating from the sides after precracking. The three configurations used for the fatigue specimens can be seen in Figure 5. Like the residual strength specimens, all fatigue specimens had a hole separation of 3.175 mm. Configuration A consisted of holes with MSD and no central lead crack.

Table 1: **Crack Lengths (cm) of Residual Strength (RS) Specimens**

	SPECIMENS									
Hole	RS 1A	RS 2A	RS 3A	RS 4A	RS 1B	RS 2B	RS 3B	RS 4B	**RS 5B**	**RS 6B**
1L	---------	---------	---------	---------	0.0833	0.0888	0.0272	0.0329	**0.0193**	**0.1462**
1R	---------	---------	---------	---------	0.0526	0.0803	0.0326	0.0249	**0.0135**	**0.0464**
2L	---------	---------	---------	---------	0.0560	0.0850	0.0269	0.0265	**0.0114**	**0.2846**
2R	---------	---------	---------	---------	0.0744	0.1074	0.0211	0.0344	**0.0312**	**0.3137**
3L	---------	---------	---------	---------	0.0803	0.1043	0.0217	0.0347	**0.0060**	**0.3090**
3R	---------	---------	---------	---------	0.0818	0.1052	0.0271	0.0359	**0.0236**	**0.3000**
4L	---------	---------	---------	---------	0.0884	0.0649	0.0291	0.0298	**0.0033**	**0.1702**
4R	---------	---------	---------	---------	0.0842	0.0752	0.0298	0.0342	**0.0004**	**0.0061**
5L	---------	---------	---------	---------	0.0636	0.0862	0.0293	0.0357	**0.0144**	**0.2855**
5R	---------	---------	---------	---------	0.0936	0.0719	0.0312	0.0265	**0.0097**	**0.3059**
6L	---------	---------	---------	---------	0.0828	0.0779	0.0189	0.0254	**0.0720**	**0.1238**
6R	---------	---------	---------	---------	0.0855	0.0610	0.0301	0.0465	**0.0277**	**0.0775**
7L	*	*	---------	---------	0.0884	*	0.0368	*	**0.0572**	*
7R	*	*	---------	---------	0.1124	*	0.0400	*	**0.0396**	*
8L	*	*	*	*	*	*	*	*	*	*
8R	*	*	*	*	*	*	*	*	*	*
9L	*	*	*	*	*	*	*	*	*	*
9R	*	*	*	*	*	*	*	*	*	*
10L	*	*	*	*	*	*	*	*	*	*
10R	*	*	*	*	*	*	*	*	*	*
11L	*	*	*	*	*	*	*	*	*	*
11R	*	*	*	*	*	*	*	*	*	*
12L	*	*	*	*	*	*	*	*	*	*
12R	*	*	*	*	*	*	*	*	*	*
13L	*	*	---------	---------	0.0771	*	0.0136	*	**0.0119**	*
13R	*	*	---------	---------	0.0699	*	0.0324	*	**0.0213**	*
14L	---------	---------	---------	---------	0.1182	0.1006	0.0481	0.0287	**0.4408**	**0.1876**
14R	---------	---------	---------	---------	0.0892	0.0902	0.0302	0.0331	**0.4562**	**0.1858**
15L	---------	---------	---------	---------	0.0986	0.0814	0.0164	0.0331	**0.0702**	**0.0377**
15R	---------	---------	---------	---------	0.0799	0.0767	0.0234	0.0316	**0.2176**	**0.0418**
16L	---------	---------	---------	---------	0.0677	0.0771	0.0301	0.0340	**0.3656**	**0.0503**
16R	---------	---------	---------	---------	0.0823	0.0683	0.0240	0.0231	**0.3623**	**0.1146**
17L	---------	---------	---------	---------	0.0927	0.0872	0.0255	0.0377	**0.0244**	**0.0017**
17R	---------	---------	---------	---------	0.0922	0.0834	0.0259	0.0466	**0.2000**	**0.0058**
18L	---------	---------	---------	---------	0.0753	0.0889	0.0177	0.0302	**0.0145**	**0.0198**
18R	---------	---------	---------	---------	0.0686	0.0850	0.0273	0.0453	**0.0058**	**0.0231**
19L	---------	---------	---------	---------	0.0620	0.0827	0.0348	0.0260	**0.0809**	**0.0175**
19R	---------	---------	---------	---------	0.0733	0.1053	0.0357	0.0533	**0.1925**	**0.0603**
LEAD L	0.1588	0.1588	0.1588	0.3377	0.1391	0.1270	0.4849	0.5042	**0.1640**	**0.1768**
LEAD R	0.1588	0.1588	0.1588	0.3377	0.1675	0.1575	0.4679	0.5884	**0.1659**	**0.1471**
Lead Crack Length	12.065	12.065	8.255	8.6129	7.9266	11.7145	8.5728	12.5226	**7.9498**	**11.7539**

Note:

L = Left Side of Hole
R = Right Side of Hole
All crack lengths measured from hole edge
Bold face represent specimens with fatigued MSD cracks

Type A: No Lead Crack, MSD at all Holes

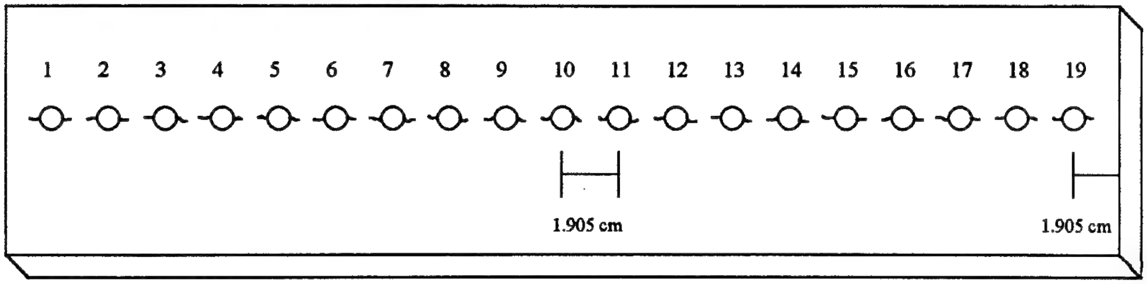

Type B: Lead Crack, Holes with No MSD (Lead crack encompassed middle seven holes or middle five holes)

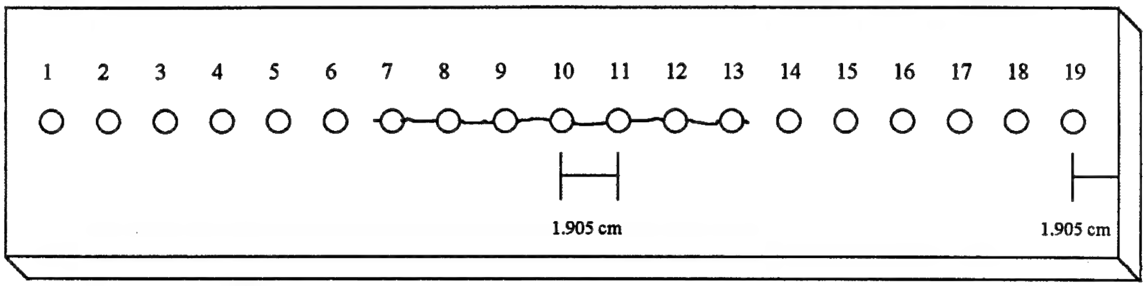

Type C: Lead Crack, MSD at all Holes (Lead crack encompassed middle seven holes or middle five holes)

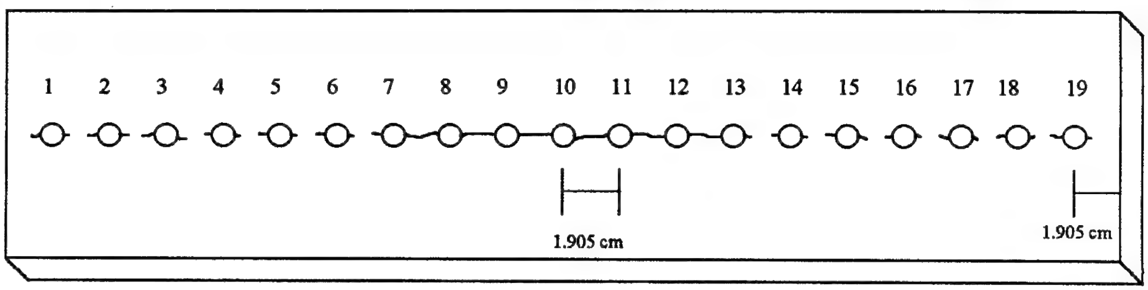

Figure 5. Fatigue Specimen Configurations

Configuration B had a central lead crack and holes without MSD. Configuration C had holes with MSD as well as a central lead crack. The final crack lengths for fatigued specimens are given in Table 2. As in the case of the residual strength specimens, these crack lengths were measured from the hole edge.

The grips used for this study were fabricated of A-36 Hot Roll Plate Steel by the AFIT model shop. Both the top and bottom pair of grips had two collinear rows of 1.27 cm (0.5 in) diameter holes. Each side of the grip had a total thickness of 1.27 cm. The top grip had a hole at its top which allowed it to be suspended from the test machine by a steel pin. This configuration enabled the top grip to swivel when a specimen was being loaded in the grip. The top grip was suspended by a 1.27 cm diameter steel pin that was connected to a steel block. The steel block, which was fabricated from the A-36 steel, was secured onto the testing machine. The steel bottom grip was placed directly in the bottom grip of the test machine, and was then hydraulically gripped. The dimensions of the grips can be seen in Figure 6. Both the fatigue, and residual strength specimens were loaded into the test machine with 1.27 cm (0.5 in) bolts torqued to 889.6 N (200 lbs).

Test Apparatus

MT specimens were tested on a servo-hydraulic test stand (Material Test System 808) equipped with a 2494.7 kg (5.5 kip) load cell. Crack growth was measured with a traveling optical microscope with a resolution of +/- 0.0127 mm (0.0005 in). The MT specimens were fatigued through a program called LOADTEST, developed by Sanders (23). The data required for the test to be conducted using this program included the

Table 2: **Crack Lengths (cm) of Fatigue Specimen**

	Specimens			
Hole	FAT 1A	FAT 1B	FAT 2B	FAT 1C
1L	0.0829	0	0	0.1488
1R	0.0593	0	0	0.1123
2L	0.1039	0	0	0.1186
2R	0.1139	0	0	0.0997
3L	0.1135	0	0	0.1300
3R	0.0847	0	0	0.0940
4L	0.0944	0	0	0.0879
4R	0.0870	0	0	0.1335
5L	0.1375	0	0	0.1179
5R	0.1293	0	0	0.0953
6L	0.0878	0	0	0.1623
6R	0.1420	0	0	0.1746
7L	0.1021	0.2818	0	0.0495
7R	0.0759	*	0	*
8L	0.1535	*	0.1816	*
8R	0.1021	*	*	*
9L	0.0949	*	*	*
9R	0.1871	*	*	*
10L	0.0565	*	*	*
10R	0.1245	*	*	*
11L	0.0605	*	*	*
11R	0.0533	*	*	*
12L	0.0512	*	*	*
12R	0.0757	*	0.1439	*
13L	0.0353	*	0	*
13R	0.0470	0.2544	0	0.0725
14L	0.1617	0	0	0.0776
14R	0.0801	0	0	0.1179
15L	0.1477	0	0	0.1243
15R	0.1655	0	0	0.0925
16L	0.1736	0	0	0.1212
16R	0.1205	0	0	0.1816
17L	0.1468	0	0	0.1077
17R	0.1222	0	0	0.0865
18L	0.0968	0	0	0.1527
18R	0.1156	0	0	0.0914
19L	0.0888	0	0	0.0903
19R	0.2438	0	0	0.0841
LEAD L	———	0.2818	0.1816	0.0495
LEAD R	———	0.2544	0.1439	0.0725
Lead Crack Length	———	11.9662	7.9455	11.5521

Note:

L = Left Side of Hole
R = Right Side of Hole

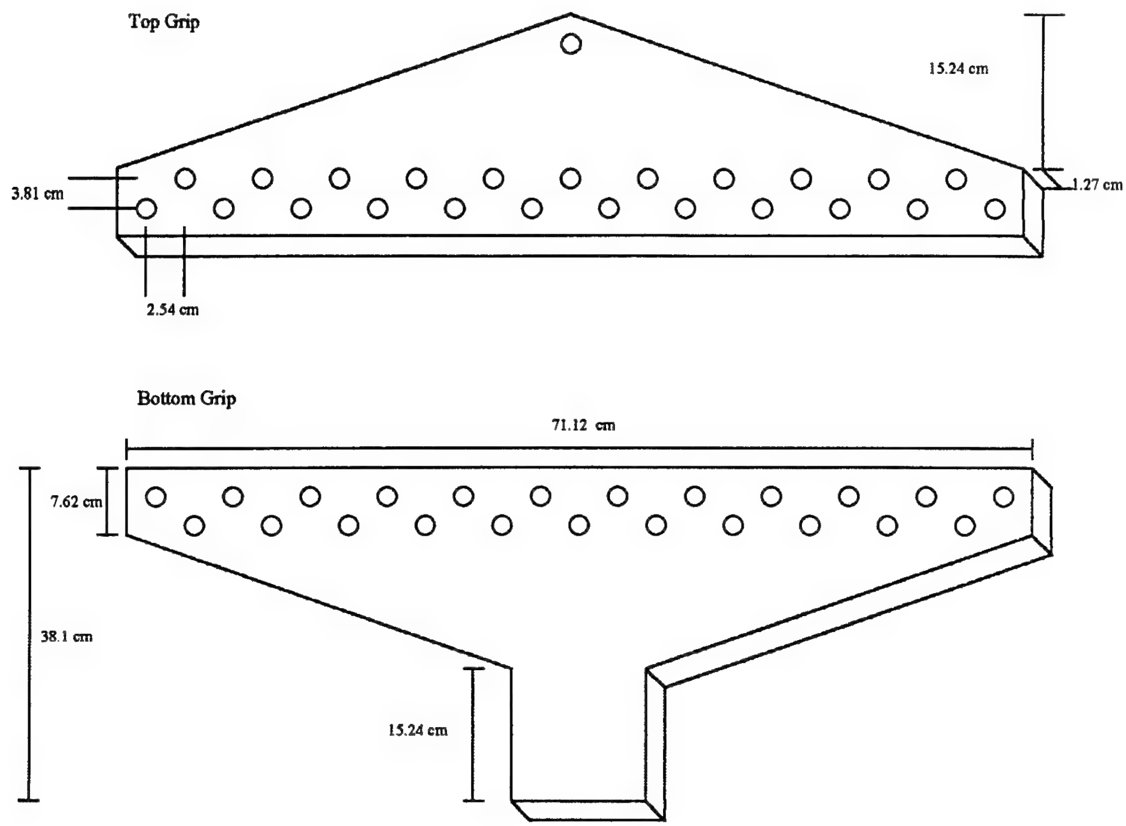

Figure 6. Top and Bottom Grips (each contained two pieces)

maximum stress to be reached during the test, the stress ratio, R, the maximum range of the load and strain, specimen area, and load frequency. These specifications were sent to the microprofiler which drove the load transducer.

Tensile specimens were tested with a MTS 810 equipped with a 9071.5 kg (20 kip) load cell. Strain data were obtained from a clip gauge MTS model 632.53E-04 1.27 cm (0.5 in) gage length. Tensile specimens were loaded to failure through a program called STATIC, developed by Derriso (8). The data required for the test to be conducted from this program included specimen area, maximum strain, gauge length of the extensometer, maximum load for the test, and data acquisition interval. The user also provided when the data acquisitions were to occur. The microprofiler on the test machine was used to drive the test. The STATIC program recorded the corresponding stress and strain for each tensile specimen.

Both residual strength specimens and fatigue specimens were tested using a Material Test System 810 with a 49890 kg (110 kip) load cell. Residual strength specimens were fixed with a clip gage extensometer (MTS model 632.03B-20) used to measure crack-mouth opening displacement as it was loaded. The STATIC program was used to record the crack mouth opening displacement as these specimens were loaded to failure. Electrical tape was used to help secure the extensometer in the brackets and keep it from slipping out as the specimen was loaded.

Crack growth in the fatigue specimen was measured via the traveling optical microscope. The microprofiler was programmed to drive both the residual strength and

fatigue tests. The testing apparatus for the residual strength and fatigue specimens can be seen in Figure 7.

Test Procedures

All tests were performed at room temperature using the servo-hydraulic test machines described previously for each type of specimen.

Tensile Specimens: Four tensile specimens were tested in accordance with ASTM E8 (29) in order to establish a stress strain relationship for the material used in this study. A uniaxial monotonic load was applied to the tensile specimens until failure occurred across the gauge section. The tensile specimens were loaded under strain control mode at a loading rate of 5.08 mm (0.2 in) per minute. The stress-strain data were acquired from a Zenith 486 computer through the STATIC program. These data were used to generate the stress/strain curves as presented in Chapter 4.

MT Specimens: These specimens were tested in accordance with ASTM E647 (24) in-order to establish a crack growth rate, da/dN data for the material. The five specimens were subjected to a constant amplitude cyclic stress of 40 MPa (5.8 ksi) at 5 hertz. The profile of cyclic loading was sinusoidal. The R ratio (minimum stress/maximum stress) was 0.2. The R ratio of 0.2 was used because the microprofiler used for the actual fatigue tests could only support a minimum ratio of 0.2. Crack growth was recorded at various intervals using a traveling optical microscope. The dimensions and loading conditions for these specimens are given in Table 3. Crack growth rate, da/dN was computed using the two point weighted average incremental slope approximation from the measured crack growth data for each test. The weighted average

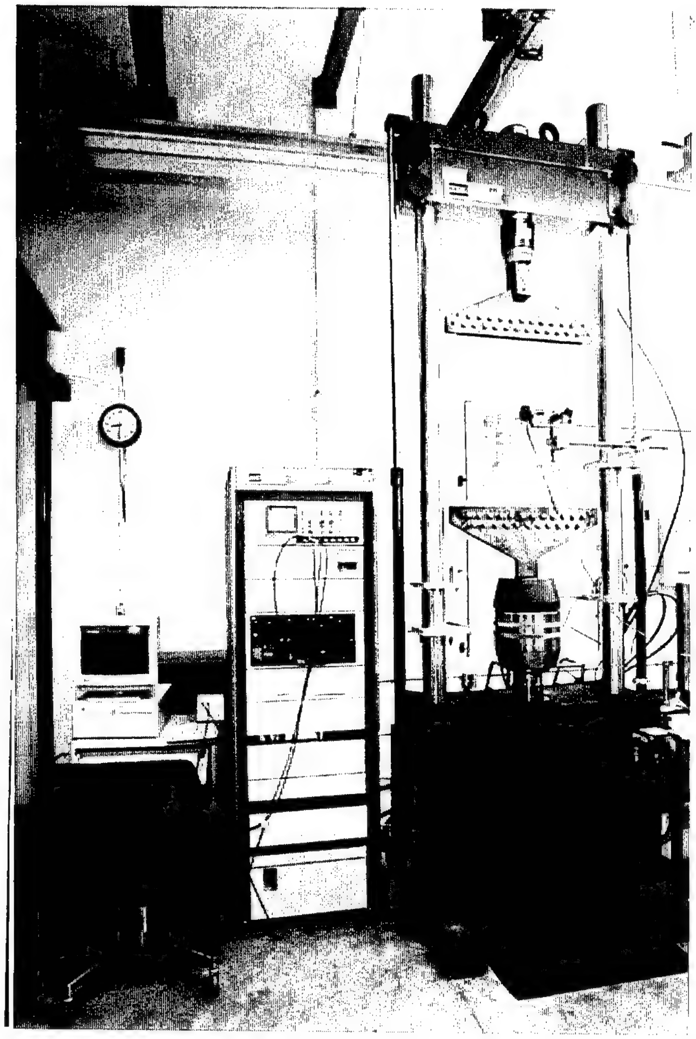

Figure 7. Test Apparatus

incremental slope approximation method is described in the material properties section of Chapter 4.

Table 3: **Dimensions and Loading Conditions for MT Specimens**

Specimen	Length (cm)	Width (cm)	Max Stress (MPa)	Min Stress (MPa)	Init. Crack length 2a (cm)
MT-1	19.05	5.08	40	8	1.3734
MT-2	19.05	5.08	40	8	0.9498
MT-3	19.05	5.08	40	8	0.8623
MT-4	19.05	5.08	40	8	0.8891
MT-5	19.05	5.08	40	8	0.8386

Residual Strength Specimens: Ten residual strength specimens were tested in the three configurations shown in Figure 5. These tests were performed to show the affects MSD cracks have on the residual strength of panels. Each residual strength specimen was placed in the test machine, and final adjustments were made to guard against bending effects. In order to minimize bending effects, the top and bottom grips were checked to ensure that they were aligned in the same plane. The bottom grips were then adjusted within the load cell to ensure that there was uniform tension across the span of the specimen. The specimens were subjected to a constantly increasing load at the rate of 4448.2 N (1000 lbs) /min until ultimate failure occurred across the center span. The residual strength of each specimen was compared to the analytical techniques discussed in Chapter 4. Stress and crack mouth opening displacement data were recorded for each specimen. The final fracture load for each specimen was also recorded.

Fatigue Specimens: These specimens were loaded into the test machine, and adjusted to minimize bending effects from the cyclic load. The tests grips were adjusted for each specimen to ensure uniform load across the entire mid-section. The four fatigue specimens were loaded at a constant amplitude load at 5 hertz. The R ratio was 0.2 matching that of the MT specimens. Table 4 lists the maximum and minimum remote stresses applied to each MSD fatigue specimen. Crack growth of the center crack was measured at varying intervals by the traveling optical microscope. The interval between measurements varied as the crack tips approached each other. Measurements were taken more often when rapid crack growth was observed. The tests concluded when the crack tips linked up, followed by failure of the specimens across the mid-section of the panel.

Table 4: **Hole and Crack Summary of Fatigue Specimens and Test Loads**

Specimen	Hole Spacing (cm)	Lead Crack 2a (cm)	Max Stress (MPa)	Min Stress (MPa)	Stress Range (MPa)
FAT-1A	1.905	None	75.8	17	58.9
FAT-1B	1.905	12.2837	74.9	17.9	57
FAT-2B	1.905	8.2630	76.2	16.8	59.4
FAT-1C	1.905	11.8696	74.7	17.8	56.9

Post-Failure Analysis

This analysis was accomplished to ensure that the tests performed were valid, and that their data could be included in the results and conclusions of this study. After the specimens failed, the fracture surface was examined. The MT specimens were examined to ensure that the crack angle from the initial crack tip did not vary more than +/- 20 degrees from the plane of symmetry over the distance of the fracture, conforming to ASTM standard E647 (24). The variance of the initial crack tips for MT specimens varied

a maximum of +/- 8 degrees. Residual strength specimens and fatigue specimens were checked for bending effects. Any specimens that had an excessive amount of bending were thrown out from the reported data. Bending effects were concluded to be present in the residual strength specimens if tearing was observed at the sides of the gauge section, as opposed to uniform fracture. Bending effects were concluded to be present within fatigue specimens if crack growth on the left and right sides of the gauge section, measured from the specimens center line, differed by more than 0.953 cm (0.375 in) conforming to ASTM E647(24).

Introduction

As mentioned previously, the objective of this investigation was to study the residual strength, and fatigue behavior of panels with MSD. For this purpose, fatigue tests, and residual strength tests were performed to determine if the available analytical techniques could adequately predict the response of these specimens. Some of the criteria used to predict failure relied on material properties for the 2024-T3 panels used in this study. This chapter outlines how various material properties were determined, and then explains the analytical methods used to predict failure and fatigue life with MSD.

Material Properties

The material properties for the 2024-T3 panels, tested in this study, were used to determine predicted fatigue life, and residual strength of the various configurations of MSD. Since a batch of material can differ somewhat from the reported material property values, tensile and crack growth tests were performed in this study.

The tensile specimens described in Chapter 3 were used to determine the yield strength (σ_{ys}) and ultimate strength (σ_{ult}) of the 2024-T3 panels tested in this study. The yield strength of a material is defined as the maximum stress that can be applied without exceeding a specified value of permanent strain upon unloading (25). The ultimate strength is simply the maximum stress the material will withstand (25). ASTM E8 (29) describes the 0.2% offset method as a viable way to determine a material's yield strength.

To determine yield strength by the 0.2% offset method, tension tests were performed to produce a plot of the stress vs. strain relationship. A line parallel to the linear portion of the stress strain relation was then placed on the plot. This line was set to intersect the x-axis at 0.2% of strain. The value of stress corresponding to the intersection of the offset line, and the stress strain plot was determined to be the materials yield strength. The σ_{ys} for this study was determined to be 290 MPa (42 ksi). The ultimate strength of the 2024-T3 aluminum was the stress corresponding to the highest point on the stress-strain plot for the tensile specimens. The σ_{ult} for this study was 400 MPa (58 ksi). The stress-strain plots for the four tensile specimens can be seen in Figure 8. The reported values for σ_{ys} and σ_{ult} taken from MIL-HDBK-5F are 290 MPa (42 ksi) and 434 MPa (63 ksi), respectively.

The MT specimens were used to determine the relationship between crack growth rate and the stress intensity factor range (da/dN and ΔK) for the 2024-T3 aluminum used in the study. The da/dN was determined by using the data from the MT tests, and the weighted average incremental slope approximation from MIL-HDBK-5F (17).

$$\left(\frac{da}{dn}\right) \approx \left(\frac{\Delta a}{\Delta N}\right)_{i-1} + \frac{N_i - N_{i-1}}{N_{i+1} - N_{i-1}}\left[\left(\frac{\Delta a}{\Delta N}\right)_i - \left(\frac{\Delta a}{\Delta N}\right)_{i-1}\right] \qquad (2)$$

for i = 2,..., n - 1

where: N = number of cycles
Δa = change in crack length
ΔN = change in number of cycles
n = number of data points (n - averaged 38 data points)

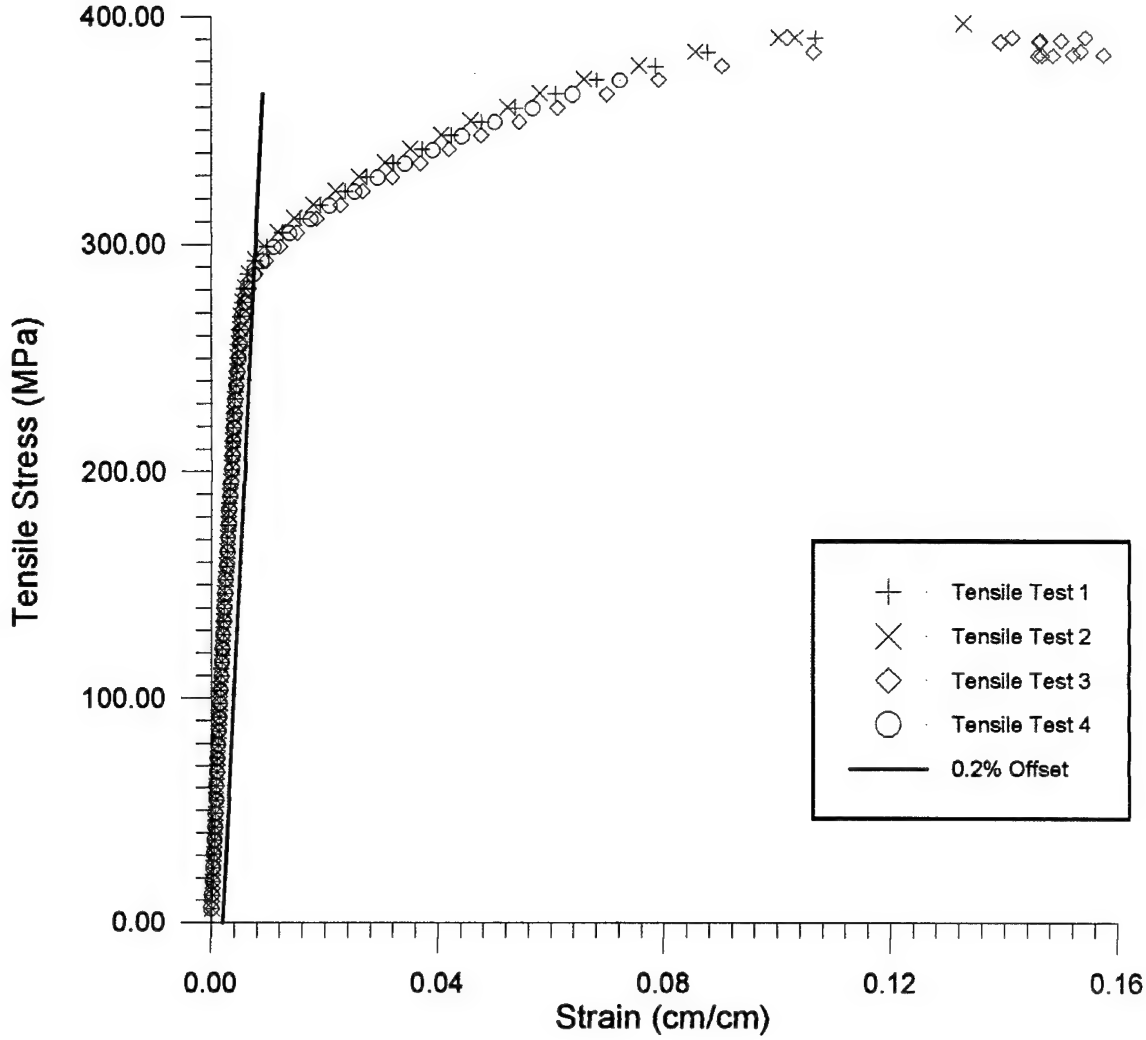

Figure 8. Tensile Test Results (Yield and Ultimate Strength Determination)

The stress intensity factor range ΔK corresponding to each da/dN was calculated using the following expression from ASTM E647 (24):

$$\Delta K = \frac{\Delta P}{B}\sqrt{\frac{\pi \cdot \alpha}{2W}\sec\left(\frac{\pi\alpha}{2}\right)} \qquad (3)$$

where: ΔK = change in stress intensity factor
ΔP = load range (Pmax - Pmin)
B = specimen thickness
W = width of the specimen
α = 2a/W
a = half the crack length

A log-log plot of da/dN as a function of ΔK was constructed using the data from the MT tests, and the above equations. Figure 9 shows the resultant plot of the MT tests. This plot was used to determine constants for the empirical crack growth law for the 2024-T3 panels. These constants were used to determine fatigue crack growth rates of specimens with MSD.

Residual Strength

The residual strength of a specimen is defined as the maximum stress a panel can withstand before failure occurs across its midspan. When MSD is present, the residual strength of panels can be greatly decreased below the failure load that would otherwise be expected from the material's properties. Their have been several analytical techniques proposed to predict failure of specimens subjected to a monotonically increasing load. As described in Chapter 3, RS specimens were tested to investigate the validity of these various analytical criteria to predict failure of the large panels. Failure loads were

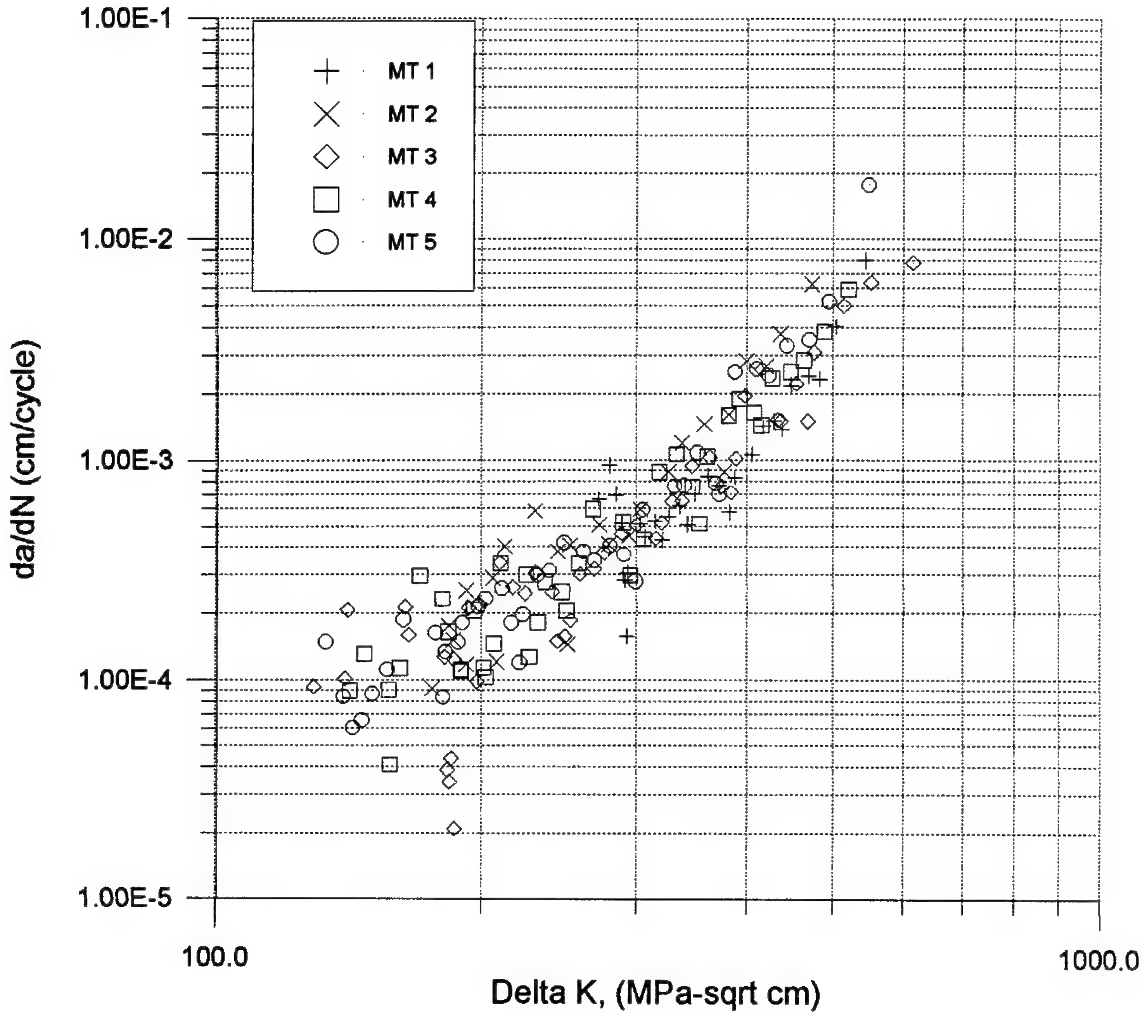

Figure 9. Fatigue Crack Growth Rate (da/dN vs ΔK) for 2024-T3 Aluminum

predicted based on the net loss of ligament method, the fracture mechanics method, a criterion proposed by Swift (28), and two criteria proposed by Jeong and Brewer (13). These criteria are described in this section. The predicted failure loads for each specimen will be presented in Chapter 5.

Net Ligament Loss Criterion [18]

The fracture strength of most of the aluminum alloys is limited to the typical net section yield strength. The net ligament loss method is derived from this basic engineering mechanics assumption. The criteria predicts failure based on the amount of material in the gauge section available to carry load. Consequently, the failure load is a function of the materials yield strength, and the number of flaw/inclusions in the gauge section. These inclusions include, the simulated rivet holes, the lead crack, and an average of the MSD crack length damage present in the specimen. The failure load P_{net} is the load that causes the net section stress to equal or exceed the material's yield strength.

$$P_{net} = \sigma_{ys} * \left(W - 2a_2 - n * d - 2n * L\right) * t \tag{4}$$

where: P_{net} = failure load based on the net ligament loss criterion
σ_{ys} = material's yield strength
W = width of gauge section
a_2 = half crack length of the central lead crack
n = number of holes
d = average diameter of the holes
L = average half crack length of the MSD cracks
t = panel thickness at the row of holes

These parameters of all RS specimens used to predict P_{net} are provided in Table 5.

Table 5. **Net Ligament Loss Criterion Parameters**

Specimen	W (cm)	a_2 (cm)	n	d (cm)	L (cm)	t (cm)
RS 01A	38.1	6.0325	0	0.3175	--------	0.1016
RS 02A	38.1	6.0325	0	0.3175	--------	0.1016
RS 03A	38.1	4.1275	0	0.3175	--------	0.1016
RS 04A	38.1	4.3064	0	0.3175	--------	0.1016
RS 01B	38.1	4.1220	14	0.3175	0.0812	0.1016
RS 02B	38.1	6.0160	12	0.3175	0.0848	0.1016
RS 03B	38.1	4.4451	14	0.3175	0.0281	0.1016
RS 04B	38.1	6.4200	12	0.3175	0.0338	0.1016
RS 05B	38.1	4.1337	14	0.3175	0.0931	0.1016
RS 06B	38.1	6.0357	12	0.3175	0.1086	0.1016

Fracture Mechanics Criterion [3]

Fracture mechanics method is based on the theory of linear elastic fracture mechanics. The primary assumption for this criterion is that there exists a critical stress intensity value K_c at a lead crack after which unstable fracture occurs when the specimens are subjected to an increasing load. This critical stress intensity value is difficult to calculate due to the rapid crack growth at the onset of a specimen's failure. For this reason, an approximation of the critical stress intensity was made using the Type A residual strength configuration, Figure 4.

The four Residual Strength Type A configuration specimens possessed a lead crack with no other holes or MSD. The stress intensity factor solution for a finite width panel with a central lead crack from Bannantine (3) is:

$$K = \sigma\sqrt{\pi \cdot a} * B_w \qquad (5)$$

where: K = stress intensity factor
σ = remote stress
W = specimens width

a = half lead crack length
B_w = secant width correction factor

$$B_w = \sqrt{\sec\left(\frac{\pi \cdot a}{W}\right)} \tag{5a}$$

In order to determine an approximate stress intensity factor to apply to the RS Type B specimens with MSD, an average of the stress intensity factors K_{app} from the type A specimens was calculated using Equation 5. The approximate stress intensity factor was assumed to be equal to the actual critical stress intensity factor K_c for the Type B specimens. The failure loads and calculated stress intensity factors for the Type A specimens can be seen in Chapter 5. The K_{app} used to calculate failure strength using the fracture mechanics method in the Type B specimens was 832 MPa-sqrt cm (75.7 ksi-sqrt in).

In order to determine the predicted failure load according to the fracture mechanics criteria for the Type B RS specimens, K_{app} is substituted into Equation 5.

$$P_{Kapp} = \frac{K_{app} * W * b}{\sqrt{\pi \cdot a} * B_w} \tag{6}$$

where: P_{Kapp} = failure load according to fracture mechanics criterion
W = specimen width
b = specimen thickness
a = half the lead crack length
B_w = secant width correction factor

The values of the parameters used to calculate P_{Kapp} for the residual strength specimens are listed in Table 6.

Table 6. **Fracture Mechanics Criterion Parameters**

Specimen	W (cm)	a (cm)	B_w	b (cm)
RS 01A	38.1	6.0325	1.0667	0.1016
RS 02A	38.1	6.0325	1.0667	0.1016
RS 03A	38.1	4.1275	1.0300	0.1016
RS 04A	38.1	4.3064	1.0327	0.1016
RS 01B	38.1	4.1220	1.0299	0.1016
RS 02B	38.1	6.0160	1.0663	0.1016
RS 03B	38.1	4.4451	1.0350	0.1016
RS 04B	38.1	6.4200	1.0764	0.1016
RS 05B	38.1	4.1337	1.0301	0.1016
RS 06B	38.1	6.0357	1.0668	0.1016

Swift Criterion

The net ligament loss method and fracture mechanics methods do not take into account the effect of plasticity at the tips of the cracks within the panel. The residual strength criterion proposed by Swift (27) employs a yield criterion to a linear elastic solution for the crack tip stress field. Swift has proposed a residual strength criteria based on the gross stress level which will cause the residual strength specimens' lead crack plastic zone to touch the MSD crack plastic zone. He postulates that failure is driven by the proximity of the plastic zone of the lead crack to the plastic zone of a MSD crack. He states that the material within the plastic zones of the cracks is unable to bear load when a perpendicular load is applied to the crack tip, and should not be included in determination of a panels strength. Swift estimates the size of the plastic zone as half the Irwin plastic zone size (4):

$$R = \frac{1}{2 \cdot \pi} * \left(\frac{K}{\sigma_{ys}} \right)^2 \tag{7}$$

where: R = radius of the plastic zone in front of the crack
K = stress intensity factor at the crack tip
σ_{ys} = yield strength of the material

As the remote stress level increases the plastic zone sizes of different cracks will increase and will eventually linkup. When the plastic zones of the lead crack meet the plastic zone from the nearest neighboring MSD crack, the ligament has effectively yielded. Therefore, the lead crack effectively extends to the far end of the MSD crack. Figure 10 shows a schematic of the Swift (27) linkup criteria. When the applied load reaches a level that causes the effective ligament to yield, the ligament will fail. The stress in the ligament to be used in the Swift criterion is not simply the material's yield strength based on the 0.2% offset method, but according to Swift (28) is equivalent to the material's flow strength.

$$\sigma_{fl} = \frac{\sigma_{ys} + \sigma_{ult}}{2} \tag{8}$$

where: σ_{fl} = material's flow strength
σ_{ys} = material's yield strength
σ_{ult} = material's ultimate strength

The flow strength for the material used in this study was 344.74 MPa (50 ksi). According to Swift, the predicted failure of a specimen with MSD is a function of the plastic zone size of the lead crack and its nearest neighboring MSD crack, the material's flow strength, and an interaction factor between the MSD crack, and the lead crack. The

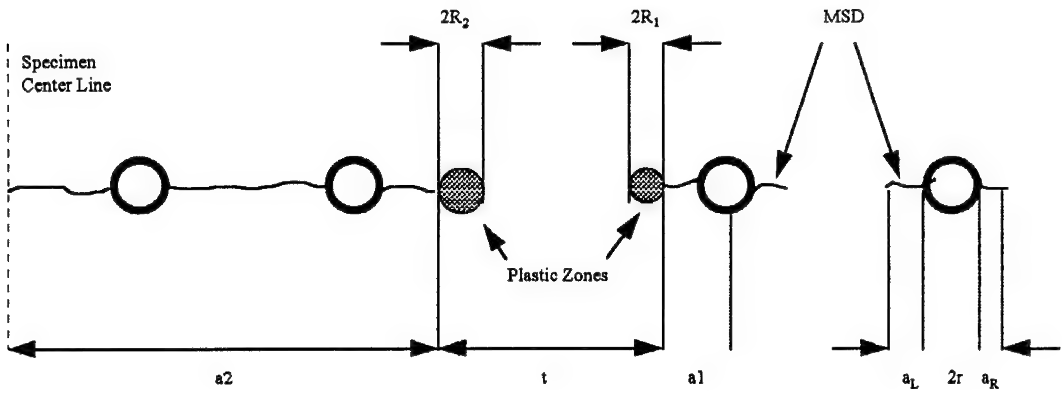

Note: a2 = half the lead crack length
a1 = the crack length of the largest MSD crack next to the lead crack
t = tip separation between MSD and lead crack
a_L = the measurement of the left side MSD crack
a_R = the measurement of the right side MSD crack
$2R_1$ = twice the Irwin plastic zone size of the MSD crack
$2R_2$ = twice the Irwin plastic zone size for the lead crack

Figure 10. Swift Residual Strength Schematic

interaction between the lead crack and its neighboring MSD crack can be determined from Rooke and Cartwright (22), or from Kamei and Yokobori (14). For this study, the Kamei and Yokobori criterion was used. Figure 11 shows a schematic, and equations used by Kamei and Yokobori to determine the stress intensity factors for unequal length cracks. The predicted failure load according to the Swift criterion, then, becomes:

$$P_{swift} = \sigma_{fl} * t * W_{net} * \sqrt{\frac{b}{\left(a_1 * B_{hs}{}^2 * B_{I\cdot 1}{}^2 + a_2 * B_{I\cdot 2}{}^2\right)}} \tag{9}$$

where: P_{swift} = failure load based on the Swift criterion
σ_{fl} = material's flow strength
t = specimen thickness
B_{I1} = Kamei and Yokobori interaction factor for MSD crack
B_{I2} = Kamei and Yokobori interaction factor for lead crack

b = crack tip separation

$$b = 3 * \delta - a_2 - a_1 - r \tag{9a}$$

where: δ = hole separation distance from center
a_2 = half the lead crack length
a_1 = largest MSD crack adjacent to lead crack, measured from hole center
r = radius of the holes

W_{net} = effective width of the gauge section

$$W_{net} = W - n * d - 2n * L \tag{9b}$$

where: W = width of the specimen
n = number of holes with MSD
d = average diameter of the holes with MSD
L = average MSD crack length from hole edge

B_{hs} = Bowie factor normalized for the a_1 crack measurement

$$B_{hs} = \sqrt{\frac{B_h{}^2 \cdot (a_1 - r)}{a_1}} \tag{9c}$$

where: B_{hs} = Bowie factor normalized to the a_1 measurement

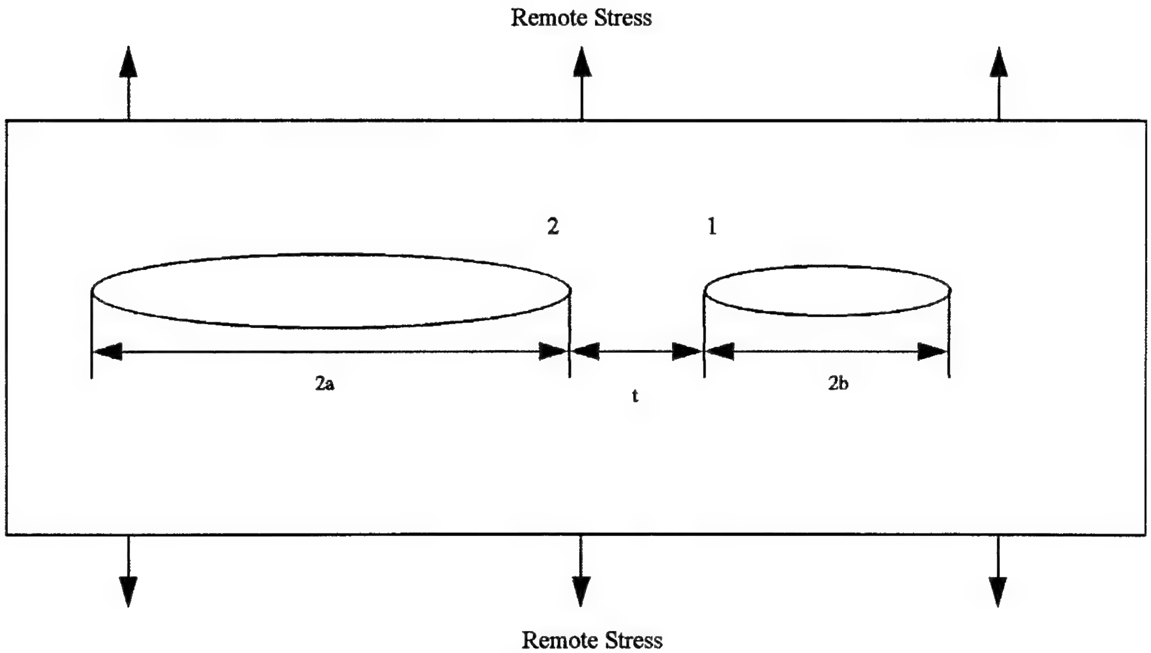

$$B_{I1} = \sigma \cdot \sqrt{\pi \cdot b} \cdot \sqrt{1 + \frac{2a}{t}} \cdot \left[1 - \left(1 + \frac{t}{2b} \right) \frac{K(k) - E(k)}{K(k)} \right]$$

$$B_{I2} = \sigma \cdot \sqrt{\pi \cdot a} \cdot \sqrt{1 + \frac{2b}{t}} \cdot \left[1 - \left(1 + \frac{t}{2a} \right) \frac{K(k) - E(k)}{K(k)} \right]$$

where K(k) = complete elliptic integral of the first kind
E(k) = complete elliptic integral of the second kind
t = crack tip separation
a = half the lead crack length
b = half the MSD crack length
σ = remote stress
k = geometry factor

$$k = 2 \cdot \sqrt{\frac{a \cdot b}{(2a + t)(2b + t)}}$$

Figure 11. Kamei and Yokobori Crack Interaction Factor

a_1 = largest MSD crack adjacent to lead crack, measured from hole center
r = radius of hole
B_h = Bowie factor

B_h = Bowie factor estimating equation

$$B_h = \left[\frac{F_1}{F_2 + \frac{a_b}{r}} + F_3 \right] \tag{9d}$$

where: a_b = MSD crack length measured from hole edge
r = radius of the hole
F_1, F_2, F_3 = hole configuration constants

for holes with cracks emanating from both sides:	for holes with only one side cracked:
F1 - 0.6865	F1 - 0.8733
F2 - 0.2772	F2 - 0.3245
F3 - 0.9439	F3 - 0.6762

Some of these parameters used for each residual strength specimen to determine failure load due to the Swift criterion are listed in Table 7.

Table 7. **Swift Criterion Parameters**

Specimen	a1 (cm)	B_{hs}	B_{l1}	B_{l2}	b (cm)	n	d (cm)	L (cm)
RS 01A	------	------	------	------	------	------	------	------
RS 02A	------	------	------	------	------	------	------	------
RS 03A	------	------	------	------	------	------	------	------
RS 04A	------	------	------	------	------	------	------	------
RS 01B	0.1068	0.8247	1.4920	1.0081	1.3218	14	0.3175	0.0812
RS 02B	0.1021	0.8114	1.8225	1.0228	1.3447	12	0.3175	0.0848
RS 03B	0.0783	0.6716	1.6464	1.0074	1.0711	14	0.3175	0.0281
RS 04B	0.0808	0.6975	1.9352	1.0076	0.9947	12	0.3175	0.0338
RS 05B	0.0781	0.6700	1.4804	1.0051	1.3837	14	0.3175	0.0931
RS 06B	0.1364	0.8753	1.7170	1.0134	1.2380	12	0.3175	0.1086

Average Displacement Criterion

According to Jeong and Brewer (13) the Swift criterion does not make provisions for the interaction of the stress fields produced at crack tips. Swift also does not account for the material surrounding the ligament to constrain plastic deformation, or the fact that the ligament fails rather than merely yields. Jeong and Brewer have proposed two different criteria for estimating the far field stress at which the average ligament stress would equal to the ultimate strength of the ligament between the crack tips.

The average displacement criterion proposed by Jeong and Brewer assumes that the stress across the ligament is uniformly equal to the material's ultimate strength. According to Jeong and Brewer, prior to a specimens failure, the displacement of the crack faces is assumed to be zero in the direction parallel to the crack. The situation where there is a single large lead crack surrounded by smaller MSD cracks was modeled as the superposition of two known crack face displacement cases. The two cases used were a single crack in an infinite medium subjected to remote tension, and a single crack subjected to pressure loading on its crack faces. A schematic of this superposition and crack face displacement equations can be seen in Figure 12. The locations of the crack tips used in the two criteria by Jeong and Brewer can be seen in Figure 13. Since the displacement of the crack faces is assumed to be zero in the crack direction, the sum of the two superposition equations becomes zero.

$$\int_a^b v_1(x)\cdot dx + \int_a^b v_2(x)\cdot dx = 0 \qquad (10)$$

where: $v_1(x)$ = displacement of the crack face (finite body uniform tension)
$v_2(x)$ = displacement of the crack face (infinite body pressure loading)

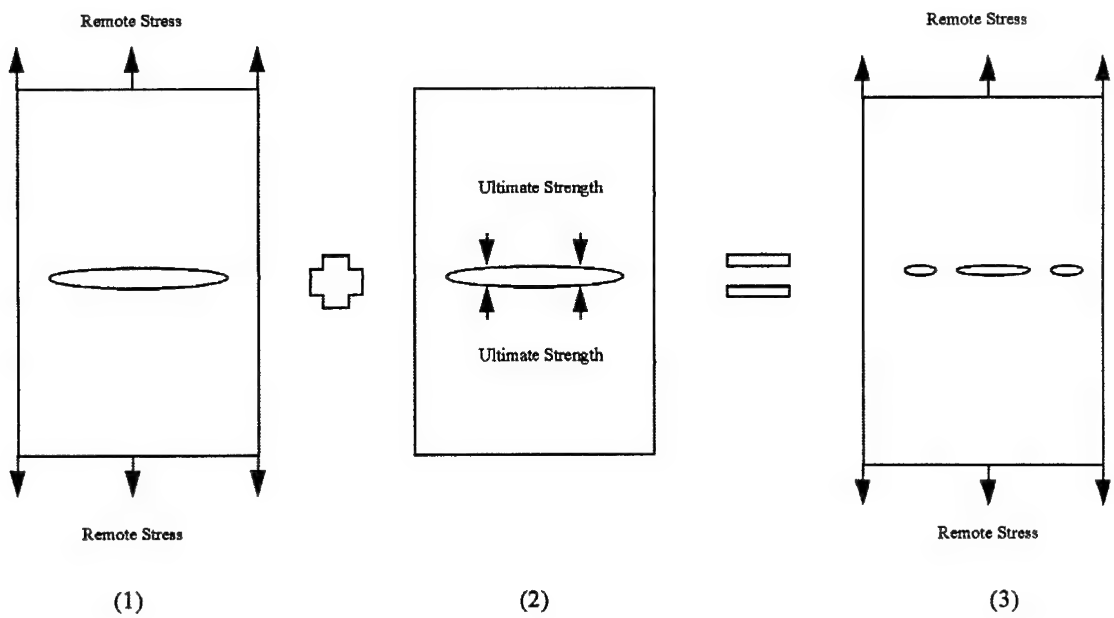

$$v_1(x) = \frac{2 \cdot \sigma_o}{E} \sqrt{c^2 - x^2}$$

$$v_2(x) = -\frac{2 \cdot \sigma_{ult}}{E \cdot \pi} \sqrt{c^2 - x^2} * \left[a\cos\left(\frac{b}{c}\right) - a\cos\left(\frac{a}{c}\right) \right] + (x+b) * \log\left[\frac{c * |x+b|}{c^2 + bx - \sqrt{c^2 - x^2} \cdot \sqrt{c^2 - b^2}} \right]$$

$$+(x-b) * \log\left[\frac{c * |x-b|}{c^2 - bx + \sqrt{c^2 - x^2} \cdot \sqrt{c^2 - b^2}} \right] - (x+a) * \log\left[\frac{c * |x+a|}{c^2 + ax - \sqrt{c^2 - x^2} \cdot \sqrt{c^2 - a^2}} \right]$$

$$-(x-a) * \log\left[\frac{c * |x-a|}{c^2 - ax - \sqrt{c^2 - x^2} \cdot \sqrt{c^2 - a^2}} \right]$$

Figure 12. Superposition and Displacement Equations used by Jeong and Brewer

Remote Stress

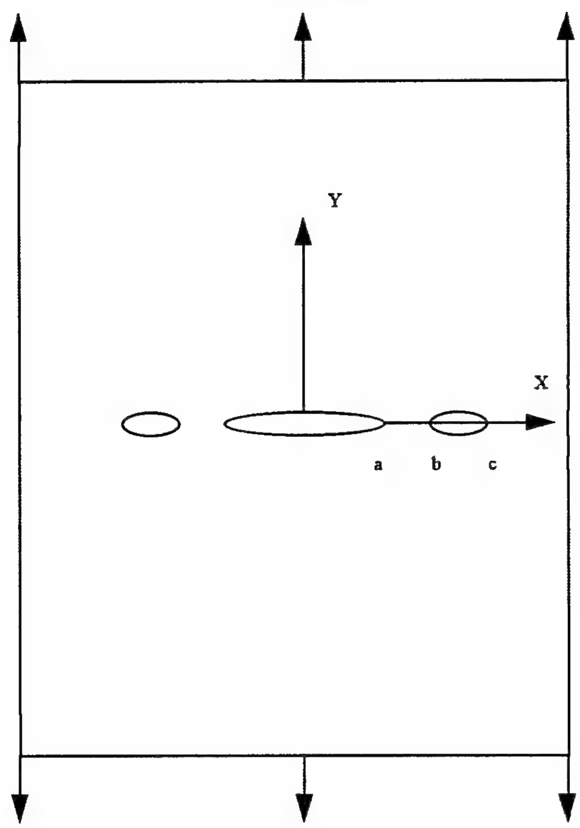

Remote Stress

Figure 13. Location of Crack Tip for Jeong and Brewer's Criterion

The predicted failure load of the panel according to the average displacement criterion becomes:

$$P_{avgd} = \frac{2\cdot\sigma_{ult}\cdot W\cdot t}{\pi}\cdot\frac{\int_a^b v_2(x)\cdot dx}{b\sqrt{c^2-b^2}-a\sqrt{c^2-a^2}+c^2\left[\sin^{-1}\left(\frac{b}{c}\right)-\sin^{-1}\left(\frac{a}{c}\right)\right]} \quad (11)$$

where: P_{avgd} = failure load according to the average displacement criterion
W = width of specimen
t = thickness of specimen
σ_{ult} = ultimate material strength
a,b,c = locations of the crack tips (see Figure 13)

The values used to determine the predicted failure load based on the average displacement criterion are listed in Table 8.

Average Stress Criterion

Jeong and Brewer (13) postulated that the stress in the ligament between the lead crack, and its nearest neighboring MSD crack is uniformly equal to the material's ultimate strength immediately prior to failure of the specimen. The average stress criterion models the various cracks individually and is based on the stress distribution between neighboring crack tips. The linkup between the two adjacent cracks is assumed to occur when the average stress in the ligament between the crack tips is equal to the ultimate tensile strength of the material. The criterion can be expressed as:

$$P_{avgst} = \sigma_{ult} * W * t\cdot\frac{b-a}{\int_a^b \frac{\left[\left(c^2-a^2\right)\cdot\frac{E(k)}{K(k)}+a^2\right]\cdot x - x^3}{\sqrt{\left(x^2-a^2\right)\left(b^2-x^2\right)\left(c^2-x^2\right)}}\cdot dx} \quad (12)$$

where: P_{avgst} = specimens failure load based on the average stress criterion
a,b,c = locations of the crack tips
E(k) = complete elliptic integral of the first kind
K(k) = complete elliptic integral of the second kind

W = specimen width
t = specimens thickness
k = geometry factor

$$k = \sqrt{\frac{c^2 - b^2}{c^2 - a^2}} \tag{12a}$$

The values for the parameters used in the calculation of the failure load based on the average stress criterion can be seen in Table 8.

Table 8. **Average Stress and Average Displacement Parameters**

Specimen	W (cm)	a (cm)	b (cm)	c (cm)	k	E(k)	K(k)	t (cm)
RS 01A	-------	-------	-------	-------	-------	-------	-------	-------
RS 02A	-------	-------	-------	-------	-------	-------	-------	-------
RS 03A	-------	-------	-------	-------	-------	-------	-------	-------
RS 04A	-------	-------	-------	-------	-------	-------	-------	-------
RS 01B	38.1	4.1220	5.4581	5.9764	0.5626	1.438	1.724	0.1016
RS 02B	38.1	6.0160	7.3454	7.8537	0.5505	1.444	1.716	0.1016
RS 03B	38.1	4.4451	5.5077	6.2621	0.6756	1.372	1.819	0.1016
RS 04B	38.1	6.4200	7.4569	7.8463	0.5412	1.449	1.71	0.1016
RS 05B	38.1	4.1337	5.5176	5.9319	0.5119	1.462	1.692	0.1016
RS 06B	38.1	6.0357	7.2885	7.9794	0.6223	1.405	1.769	0.1016

The criteria described in this section allowed comparisons to be made with the observed failure loads for the ten residual strength specimens. The Swift, Average Stress, and Average Displacement criteria assumed that a specimen possessed cracks adjacent to a lead crack within a specimen. Consequently, these criteria were only used to predict failure in the Type B specimens, which had a lead crack and smaller MSD cracks emanating from holes. The net ligament loss, and fracture mechanics criteria were only applicable to a lead crack within a specimen. These two criteria were used to predict

failure in all ten residual strength criteria. The results of the ten residual strength tests are provided in Chapter 5.

Fatigue Life

The fatigue life of a structure is defined as the maximum number of loading cycles that can be tolerated by the structure before failure occurs. This is important in aircraft because it determines the operational life of the aircraft, and the number of periodic inspections that must be accomplished to ensure safety. In this study the fatigue life of four 2024-T3 aluminum specimens in three configurations, Figure 5, were investigated. The predicted number of cycles to failure, or fatigue life, for the four specimens was determined using an iterative computer algorithm. This section describes the analytical methodology used to determine the expected fatigue life of the specimens.

Computer Algorithm

A computer algorithm was written to establish the predicted number of cycles until failure, or fatigue life, for each fatigue specimen. The algorithm, written in Turbo Pascal ©, used the material's fatigue growth rate relationship, da/dN vs ΔK, established by the MT specimens, to predict fatigue life. The computer algorithm used the specimen geometry, MSD configuration, and loading conditions to compute the stress intensity factor range ΔK for each crack within the specimen. The computer algorithm allowed crack interaction factors to be considered in the determination of the initial stress intensity factor range. Each crack's fatigue growth rate da/dN was then determined using the Paris Law equation (3):

$$da/dN = C(\Delta K)^m \tag{13}$$

where: da/dN = crack growth rate per unit cycle
C, m = material constants

The material constants used in the Paris Law equation were determined from data points on the da/dN vs ΔK plot in Figure 9.

The computer algorithm established a fatigue growth step size for each iteration by calculating a percentage of the smallest crack within the specimen. The program then determined the number of cycles necessary to grow the smallest crack within the specified percentage.

$$\Delta N = \frac{\Delta}{da/dN} \tag{14}$$

where: Δ = length corresponding to a percentage of the smallest crack
ΔN = number of cycles needed to grow the smallest crack Δ cm
da/dN = fatigue growth rate of smallest crack

The growth increments of the other cracks was then computed using the following relationship:

$$\Delta a = \Delta N * \left(da/dn\right) \tag{15}$$

where: Δa = crack growth increment
ΔN= number of cycles determined from the smallest crack
da/dn = fatigue growth rate of the crack of interest

The growth increments of each crack were added to its starting length to calculate a new length for the next iteration. The specimen's new crack geometry was then compared to failure criteria to determine if failure had occurred in the specimen. These steps were repeated until the failure of the panel was predicted. A flowchart of the algorithm developed for fatigue life prediction can be seen in Figure 14. The computer

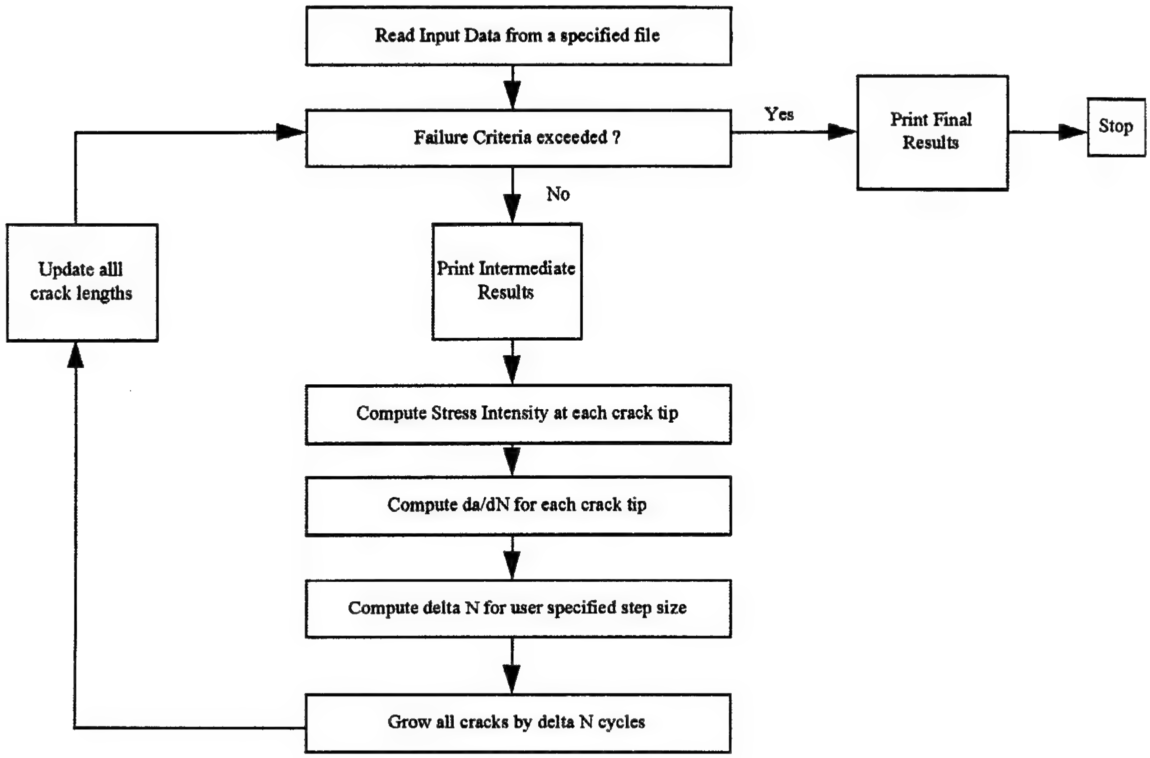

Figure 14. Flowchart of Computer Algorithm to Predict Fatigue Life

program is provided in Appendix A. A sample of the input and output for the program is provided in Appendix B.

Stress Intensity Factor Range

As mentioned previously the computer algorithm relied on an initial stress intensity range ΔK at each crack tip to determine the fatigue crack growth rate da/dN of each crack within the fatigue specimens. The stress intensity factor range of each crack tip was a function of the cracks length and proximity to other cracks. The initial ΔK was established for each crack tip based on the Bowie solution (9) or the center crack solution (9). If crack interaction effects were to be considered, the initial ΔK solution was then modified by an interaction factor to arrive at the stress intensity factor range for the crack tip. This method of determining ΔK is based on a form of the compounding method described in Chapter 2.

The initial stress intensity factor range was dependent on the length and location of each crack within the specimen. The Dowling transition crack length a_t was used to determine which solution method would be used to determine ΔK . The a_t for each crack was computed according to Equation 1. The transition length was then used to determine which solution method would be used to find ΔK for each crack.

If the cracks length was less than its transition crack length, then the Bowie solution was used to determine ΔK.

$$\Delta K = \Delta\sigma \cdot \sqrt{\pi \cdot a} \cdot B_h \qquad (16)$$

where: ΔK = stress intensity factor range
$\Delta\sigma$ = remote stress range
a = half crack length
a_t = Dowling Transition Crack Length, Equation 1

B_h = Bowie Correction factor, Equation 9c

If the cracks length was greater than or equal to the transition length, then the center crack solution was used to establish the stress intensity factor range.

$$\Delta K = \Delta\sigma \cdot \sqrt{\pi \cdot a} \cdot B_W \qquad (17)$$

where: ΔK = stress intensity factor range
$\Delta\sigma$ = remote stress range
a = half crack length
a_t = Dowling transition crack length
B_w = secant width correction factor, Equation 5a

The stress intensity factor ranges computed above do not account for the presence of surrounding cracks in the specimen. The computer program was written to allow the user to specify if interaction effects would be included in the fatigue life prediction of the specimens. If interaction effects were to be considered, the initial stress intensity factor ranges using the Bowie or center crack solutions were modified to determine the ΔK that would be used in the computer iterations. The crack interaction factor was based on the Kamei-Yokobori (14) interaction described in Figure 11. The final ΔK for each crack tip within the specimen was then computed using the following equation:

$$\Delta K = \Delta K_i * B_{\text{int}} \qquad (18)$$

where: ΔK = stress intensity factor range
ΔK_i = initial stress intensity factor range
B_{int} = Kamei-Yokobori interaction factor

Failure Criterion

When structures with MSD present are subjected to constant loading, the MSD cracks continue to grow until the structure fails. The computer algorithm in this study allowed three different failure criteria to be used to determine failure of the fatigued

specimens. The net ligament loss, fracture mechanics, and Swift criteria, described in the residual strength section, were used to predict failure of the four fatigue specimens. These criteria were used to establish a predicted failure load for each specimen.

As stated earlier, the computer algorithm incrementally grew the specimen's cracks under constant amplitude loading during each iteration. The failure criteria was set equal to the predicted failure load. The predicted failure load was computed according to one of the three criteria mentioned above based on the new specimen geometry established by the incremental crack growth within the specimen after each iteration. The maximum load used to cycle the specimens was compared to the predicted failure load after each iteration. If the maximum cyclic load met or exceeded the predicted failure load, the specimen was considered to have failed.

The computer algorithm described in this section established a predicted fatigue life of each specimen that was used to compare with experimental results. The three failure criteria coupled with the option of considering crack interaction effects, allowed several comparisons to be made with the measured fatigue life of each fatigue specimen. The results of this analysis are given in Chapter 5.

V. Results

Introduction

As mentioned previously, the objective of this investigation was to study the residual strength and fatigue behavior of large flat panels with MSD. This was accomplished by testing and applying various failure criteria to 381 mm (15 in) wide 2024-T3 aluminum specimens with MSD. These tests coupled with data from a previous study (18) sought to determine if width and thickness affect the validity of presently available analytical methods to predict residual strength and fatigue life. As a corollary, this study also investigated the effects of using sawcuts instead of cracks obtained by precracking to simulate fatigue cracks in the measurement of residual strength specimens with MSD.

This study was conducted in three different phases to characterize the behavior of large flat panels with MSD present. Tests were performed to determine the material properties of the same batch of aluminum used to fabricate the test specimens. This information was used in the analytical methods to predict residual strength, and also in the analysis that was used to predict fatigue life. Residual strength tests were then conducted using two different configurations to determine if available analytical theories are valid to predict failure in large flat panels. Finally, fatigue tests were conducted to determine if fatigue life could adequately be predicted.

This chapter outlines the results of the tests performed in this study. Outcomes are presented in both tabular and graphical format. An example of the computer run data from the fatigue life predictions are listed in Appendix B.

Material Properties

Several tests were conducted to investigate the material properties of the material used for the MSD specimens. Tests that were used to determine material properties for the aluminum batch, included tensile tests, and tests to characterize the fatigue crack growth rate of the 2024-T3 aluminum.

As seen in Figure 8, the tensile tests resulted in a yield stress σ_{ys} of 290 MPa (42 ksi), and an ultimate stress σ_{ult} of 400 MPa (58 ksi). The typical strengths for 2024-T3 aluminum sheets subjected to loading perpendicular to grain direction is 290 MPa for yield and 434 MPa as stated in MIL-HNDBK-5F (17). The experimentally measured strengths were incorporated into all failure theories that were used to predict fatigue life, and residual strength. The average stress, and average displacement criteria used the ultimate strength of the material, and the net ligament loss criterion relied on the materials yield strength. The Swift criterion required both the yield and ultimate strength to calculate the material's flow strength.

The MT tests were used to characterize the fatigue crack growth behavior for the batch of material used in this study. Figure 9 gives the relationship between crack growth and stress intensity factor range (da/dN and ΔK). This plot corresponds to Region II, or the linear portion, of reported values for da/dN vs. ΔK as stated in MIL-HNDBK-5F (17). Most of the current applications of linear elastic fracture mechanics concepts to describe crack growth behavior are associated with Region II (3). The data from this plot were used to determine crack growth rate in the fatigue life computer program developed for

this study. The crack growth rate for fatigue cracks was determined in the computer program using the Paris Law equation, Equation 13, and sampled points from the experimentally derived da/dN vs. ΔK plot. The computer program allowed the user to input sampled points corresponding to any crack growth rate plot. Therefore, material constants could be recomputed for different material batches. Typical points used in the computer algorithm for this study are listed in Table 9. The values for the material constants, C and m, were approximately 4.4 E -9 and 3, respectively. The material constants presented for the Paris Law equation conform with expected values (17).

Table 9. **Typical Points Used to Define Paris Law Segments**

delta K (MPa-sqrt cm)	da/dN (cm/cycle)
329.64	1.52E-02
262.18	3.68E-04
213.17	9.73E-05
78.13	4.01E-06

Residual Strength

The purpose of the residual strength tests was to demonstrate the validity of available analytical methods to predict the residual strength of specimens with MSD damage. The effects of sawcuts to simulate fatigue cracks were also investigated in these residual strength tests. Ten residual strength specimens were subjected to a monotonically increasing load until failure occurred across the gauge section of the specimens. During each test the load that caused failure across the midspan of the specimen was recorded. The failure loads were compared to the predicted residual strengths from five analytical criterion, as described in Chapter 4, to determine each criterion's validity.

Four Type A specimens, Figure 4, were tested to determine the apparent critical stress intensity factor, K_{app}, for the material. The K_{app} was used in the fracture mechanics criterion to predict the residual strength of Type B specimens as shown in Equation 6. Table 10 lists the stress intensity factors calculated from Equation 5 for the four Type A specimens using each specimens geometry, and the measured failure load. The specimen RS01A was not used in the calculation of the average value of K_{app}. The RS01A specimen slipped in its grips during testing, before fracture occurred. It was therefore removed from the determination of the average value of K_{app}. The average stress intensity factors for the three remaining Type A specimens were 832 MPa-sqrt cm (75.7 ksi-sqrt in). This value was used in the fracture mechanics criterion to predict failure in the Type B residual strength specimens with MSD.

Table 10. **Failure Loads and Stress Intensity for Type A RS Specimens**

Specimen	Failure Load (MPa)	K (MPa-sqrt cm)
RS 01A*	97.70	756.12
RS 02A	109.28	845.77
RS 03A	133.48	825.10
RS 04A	130.34	825.18
Average		832.02

Note: * RS01A not used to determine K_{app}

The Type B specimens with MSD, Figure 4, were tested in accordance with the procedure described in Chapter 3. The specimens were subjected to a monotonically increasing load until failure occurred across the midspan of the gauge section. Predicted failure loads were determined for each specimen based on five failure criteria described in

Chapter 4. These predicted failure loads were then compared to the experimentally measured failure loads for each specimen.

Jeong and Brewer (13) stated that the Swift criterion, as described in Chapter 4, failed to account for the fact that the ligaments between cracks fail instead of merely yielding. Therefore, the Swift criterion was employed using both the material's flow strength and ultimate strength. This was done to determine if the use of ultimate strength with the Swift criterion would provide better correlation with experimental failure loads.

The failure loads for all residual strength specimens are listed in Table 11. The failure loads obtained experimentally are compared with the predicted failure loads of each specimen according to the five failure criteria. The percentage error between the predicted loads and the actual loads are also listed in Table 11. The Swift, average displacement, and average stress criteria assume that MSD is present in the tested specimens. Consequently, predicted failure loads using these three criteria are only given for Type B specimens. The specimens that had fatigued MSD cracks instead of sawcuts are listed in boldface in Table 11. Figure 15 graphically presents the residual strength test results for the six Type B specimens with MSD. A 45 degree line in the figure represents 100% agreement between predicted and actual failure loads. The residual strength tests are discussed further in Chapter 6.

Table 11. **Predicted and Actual Failure Loads for RS Specimens**

Specimen	MSD/ Holes	Measured Load (kN)	CALCULATED *P_{kapp} (kN)	*P_{net} (kN)	*P_{swift} Ult St (kN)	*P_{swift} Flow St (kN)	*P_{avgst} (kN)	*P_{avgd} (kN)
RS 01A	No holes	63.03	69.35	76.60	-----	-----	-----	-----
RS 02A	No holes	70.50	69.35	76.60	-----	-----	-----	-----
RS 03A	No holes	86.12	86.83	87.81	-----	-----	-----	-----
RS 04A	No holes	84.12	84.78	86.74	-----	-----	-----	-----
RS 01B	MSD	67.08	86.87	68.06	68.37	58.94	52.18	26.87
RS 02B	MSD	53.91	69.48	59.52	54.49	46.97	44.75	18.77
RS 03B	MSD	61.61	83.27	70.55	58.49	50.44	43.37	22.69
RS 04B	MSD	49.86	66.59	60.72	47.37	40.83	37.85	12.41
RS 05B	**MSD**	**62.32**	**86.74**	**67.03**	**66.77**	**57.56**	**54.22**	**26.82**
RS 06B	**MSD**	**47.64**	**69.30**	**57.69**	**50.62**	**43.64**	**41.59**	**18.64**

Specimen	PERCENT ERROR** (%) P_{kapp}	P_{net}	P_{swift} Ult	P_{swift} Fl	P_{avgst}	P_{avgd}
RS 01A	10.02	21.52	-----	-----	-----	-----
RS 02A	-1.64	8.64	-----	-----	-----	-----
RS 03A	0.83	1.96	-----	-----	-----	-----
RS 04A	0.79	3.12	-----	-----	-----	-----
RS 01B	29.51	1.46	1.92	-12.14	-22.21	-59.95
RS 02B	28.88	10.40	1.07	-12.87	-17.00	-65.18
RS 03B	35.16	14.51	-5.05	-18.12	-29.60	-63.18
RS 04B	33.54	21.77	-5.00	-18.11	-24.09	-75.11
RS 05B	**39.19**	**7.57**	**7.14**	**-7.64**	**-12.99**	**-56.96**
RS 06B	**45.47**	**21.10**	**6.26**	**-8.40**	**-12.70**	**-60.88**
Average Error for Type B specimens	35.29	12.80	1.06	-12.88	-19.76	-63.54

Note: Boldface represent specimens with fatigued MSD
* Equations 4, 6, 9, 11, 12, used to calculate predicted failure load
** Error is calculated by subtracting actual load from predicted load and dividing by the actual load

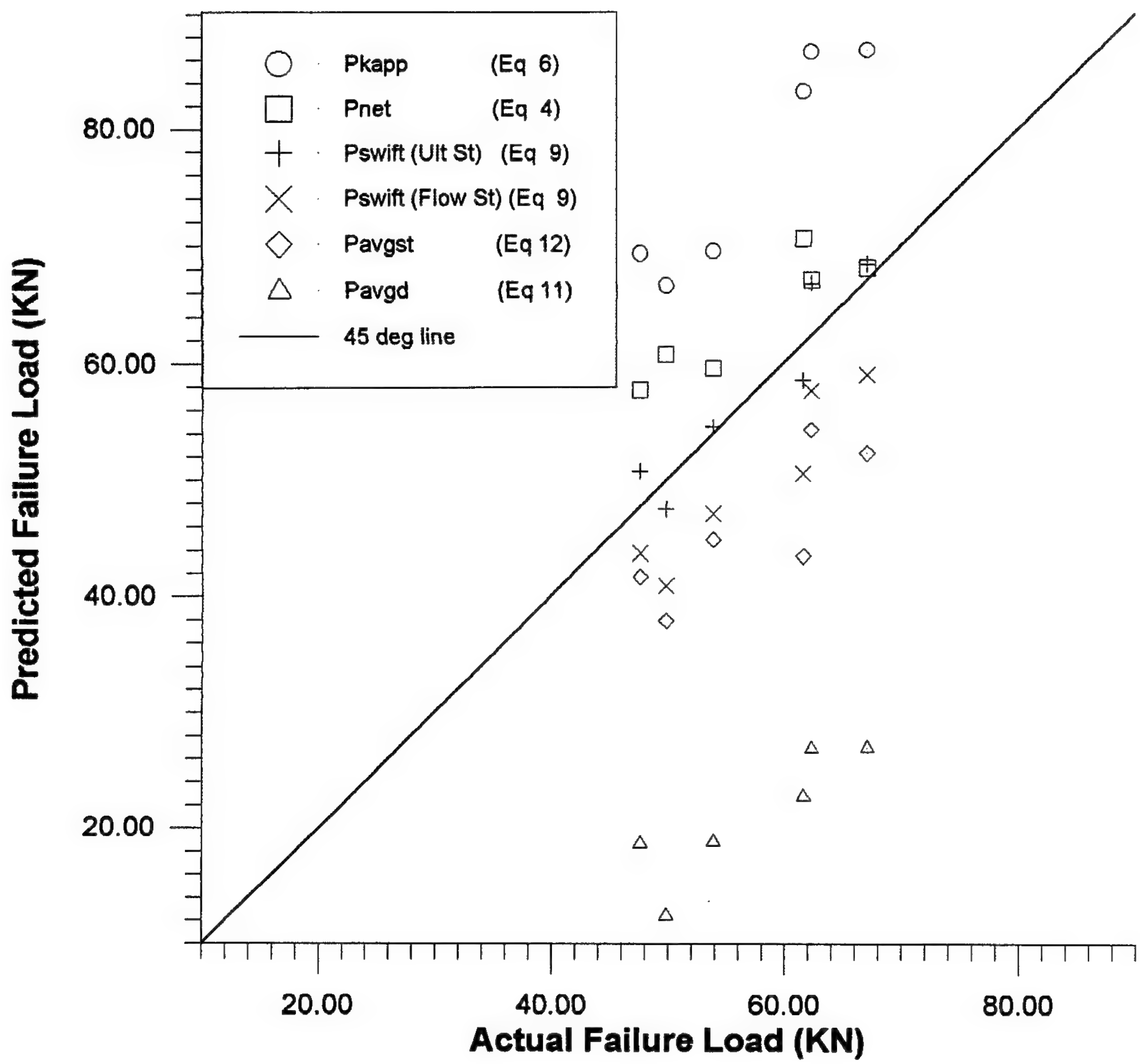

Figure 15. Comparison Between Actual and Predicted Failure Loads (Type B specimens)

The crack opening displacement of the central "lead crack" was measured throughout the residual strength testing. The crack opening measurements were plotted as a function of applied stress to show the behavior of the lead crack as the load was increased. Figure 16 and 17 present the crack opening displacement of the RS specimens for Type A and Type B specimens. These results show that the crack opening exhibits plasticity before specimen failure. Both the Type A, and Type B specimens exhibit this plasticity. The extensometer that was used to measure crack opening displacement fell from the clip fixtures before failure occurred in the RS specimens. The data reported in Figures 16, and 17 show the plasticity present during the testing of the residual strength specimens by the nonlinearity of the crack opening plot.

Fatigue Life

The purpose of the fatigue tests was to determine if analytical methods could be used to adequately predict the fatigue life of specimens with MSD. The fatigue life is defined as the number of cycles a specimen can withstand before failure occurs across the gauge section. The experimental results were compared with the predicted fatigue life from the three failure criteria used in the computer algorithm described in Chapter 4. The fracture mechanics, net ligament loss, and Swift criteria were used in the computer program to predict each specimen's fatigue life. The computer algorithm itself was validated by checking it by long hand calculations for the three failure criteria. The computer program was also run with a specimen from the study by Moukawsher (18) to

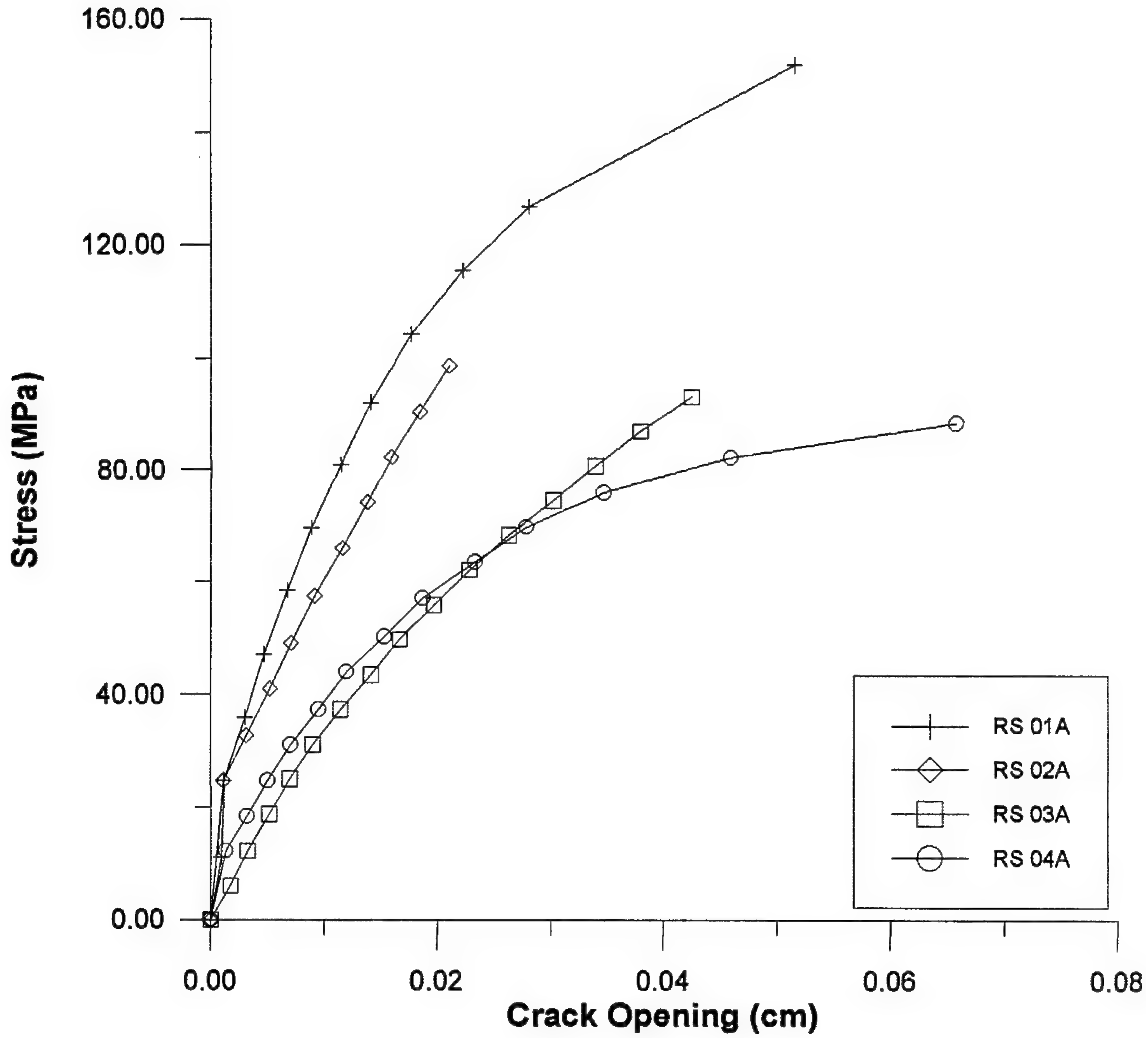

Figure 16. Crack Opening Displacement for Type A RS Specimens

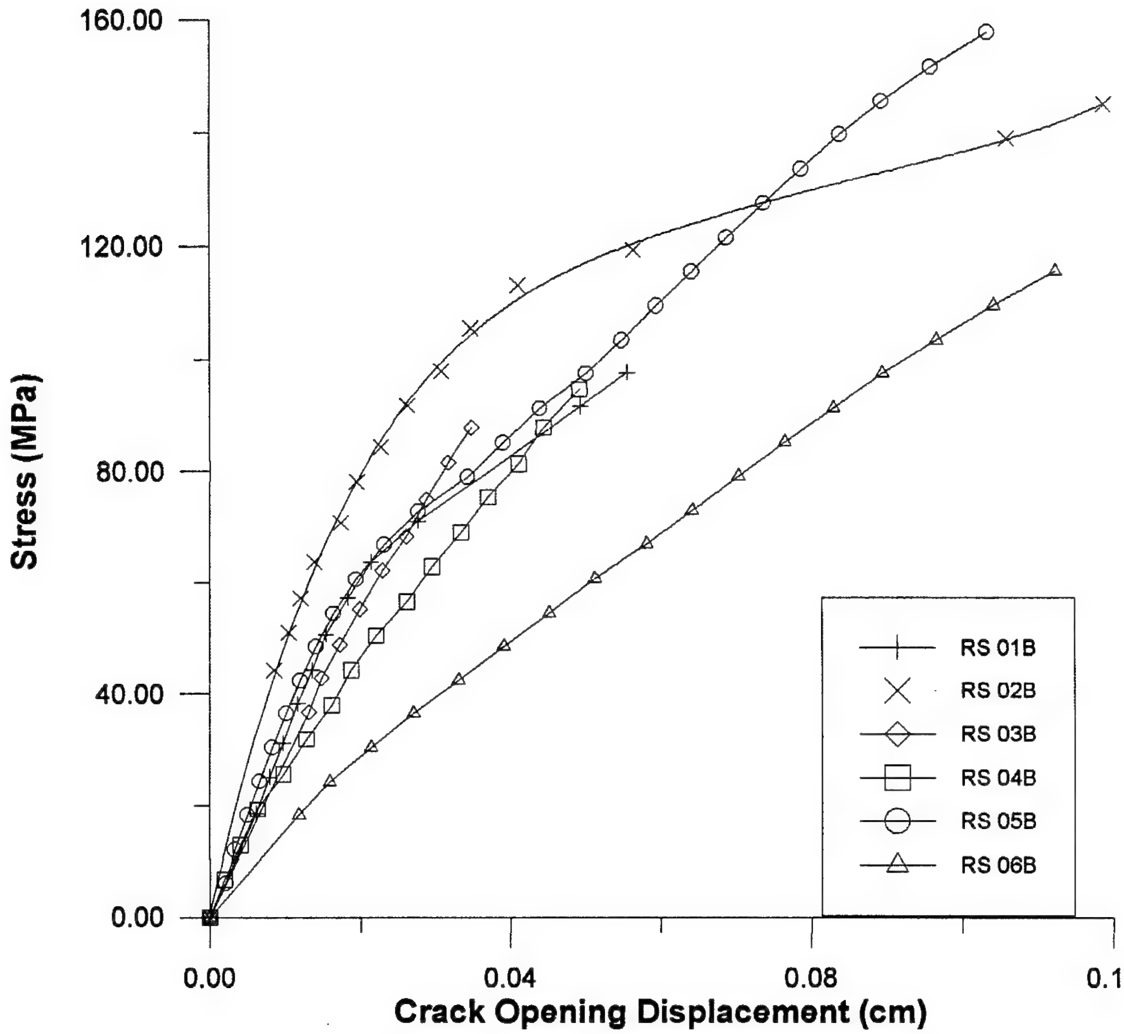

Figure 17. Crack Opening Displacement for Type B RS Specimens

ensure that the program produced similar results. A sample output from this program is provided in Appendix B.

The fatigue tests were conducted on four specimens in three different configurations, Figure 5. Some assumptions were made in the program to enable fatigue life to be predicted. The Type A configuration had holes with MSD spanning the gauge section, and no lead crack. When the Type A configuration was run in the computer algorithm the center MSD hole was assumed to be the lead crack for use with the three failure criteria. The fracture mechanics criterion could not predict fatigue life for the Type A specimen. The small lead crack caused the program to calculate an unattainable failure load using the fracture mechanics method. Only the Swift, and net ligament loss criteria were used with the Type A specimen. The Type B specimens had a central lead crack and holes without MSD. The program was run with the assumption that there were small cracks, 0.0003 cm (0.0001 in), at the side of each hole in the Type B specimens. This assumption enabled all failure criteria to be used. The Type C specimen had a central lead crack surrounded by holes with MSD. This specimen was identical to the Type B residual strength specimens. All three criteria were used to predict fatigue life for the Type C specimen.

A crack interaction procedure was used with the program, as described in Chapter 4, to account for the interaction effects the cracks have on one another. The Kamei-Yokobori Interaction factor was used to account for crack interaction as shown in Figure 11. Previous researcher has decreased the spacing between crack tips (t) by 60% when calculating the Kamei-Yokobori Interaction factor for use with fatigue life predictions

(18). This study evaluated the interaction effects on fatigue life using the crack tip spacing as shown in Figure 11, and also reducing the crack tip spacing by 60%.

The results from the fatigue tests without interaction effects are presented in Table 12. Table 13 shows the predicted fatigue lives of the fatigue specimens with crack interaction using the crack tip separation described by Kamei and Yokobori. Table 13 also lists the fatigue lives using 40% of the Kamei-Yokobori crack tip separation term (t). Figure 18 graphically presents the fatigue test results for the four specimens tested. A 45 degree line in the figure represents 100% agreement between predicted and actual failure loads. The fatigue data from the tests, and computer runs are presented in Appendix C. The fatigue tests are discussed further in Chapter 6.

Table 12. **Fatigue Test Results, No Crack Interaction Effects**

Specimen	Measured Fat Life (cycles)	Predicted Fatigue Life *Kapp (cycles)	*Net Loss (cycles)	*Swift (cycles)
FAT 01A	83336	------	158829	127545
FAT 01B	5850	19789	17841	4870
FAT 02B	12400	33283	30894	9597
FAT 01C	2245	21240	17115	4042

	PERCENT ERROR		
Specimen	Kapp	Net Loss	Swift
FAT 01A	------	90.59	53.05
FAT 01B	238.27	204.97	-16.75
FAT 02B	168.41	149.15	-22.60
FAT 01C	846.10	662.36	80.04
Average Error	417.60	276.77	23.43

Note: * Equations 4, 6, 9 used to calculate failure load
Swift Criterion computed with flow strength
dashed line represents conditions were the computer program could not determine fatigue life

Table 13. **Fatigue Test Results, Crack Interaction Effects Included**

Specimen	Measured Fat Life (cycles)	Predicted Fatigue Life *Kapp (t) (cycles)	*Kapp (40% t) (cycles)	*Net Loss (t) (cycles)	*Net Loss (40% t) (cycles)	*Swift (t) (cycles)	*Swift (40% t) (cycles)
FAT 01A	83336	------	------	265403	54494	268708	25787
FAT 01B	5850	18955	33982	13082	33982	11393	------
FAT 02B	12400	42955	78184	36608	45686	23168	14979
FAT 01C	2245	26491	21240	20899	15039	12264	4042

PERCENT ERROR

Specimen	Kapp (t)	Kapp (40% t)	Net Loss (t)	Net Loss (40% t)	Swift (t)	Swift (40% t)
FAT 01A	------	------	218.47	-34.61	222.44	-69.06
FAT 01B	224.02	480.89	123.62	480.89	94.75	------
FAT 02B	246.41	530.52	195.23	268.44	86.84	20.80
FAT 01C	1080.00	846.10	830.91	569.89	446.28	80.04
Average Error	516.81	619.17	342.06	321.15	212.58	10.60

Note: * Equations 4, 6, 9 used to calculate failure load
Swift Criterion computed with flow strength
dashed line represents conditions where the computer program could not determine fatigue life

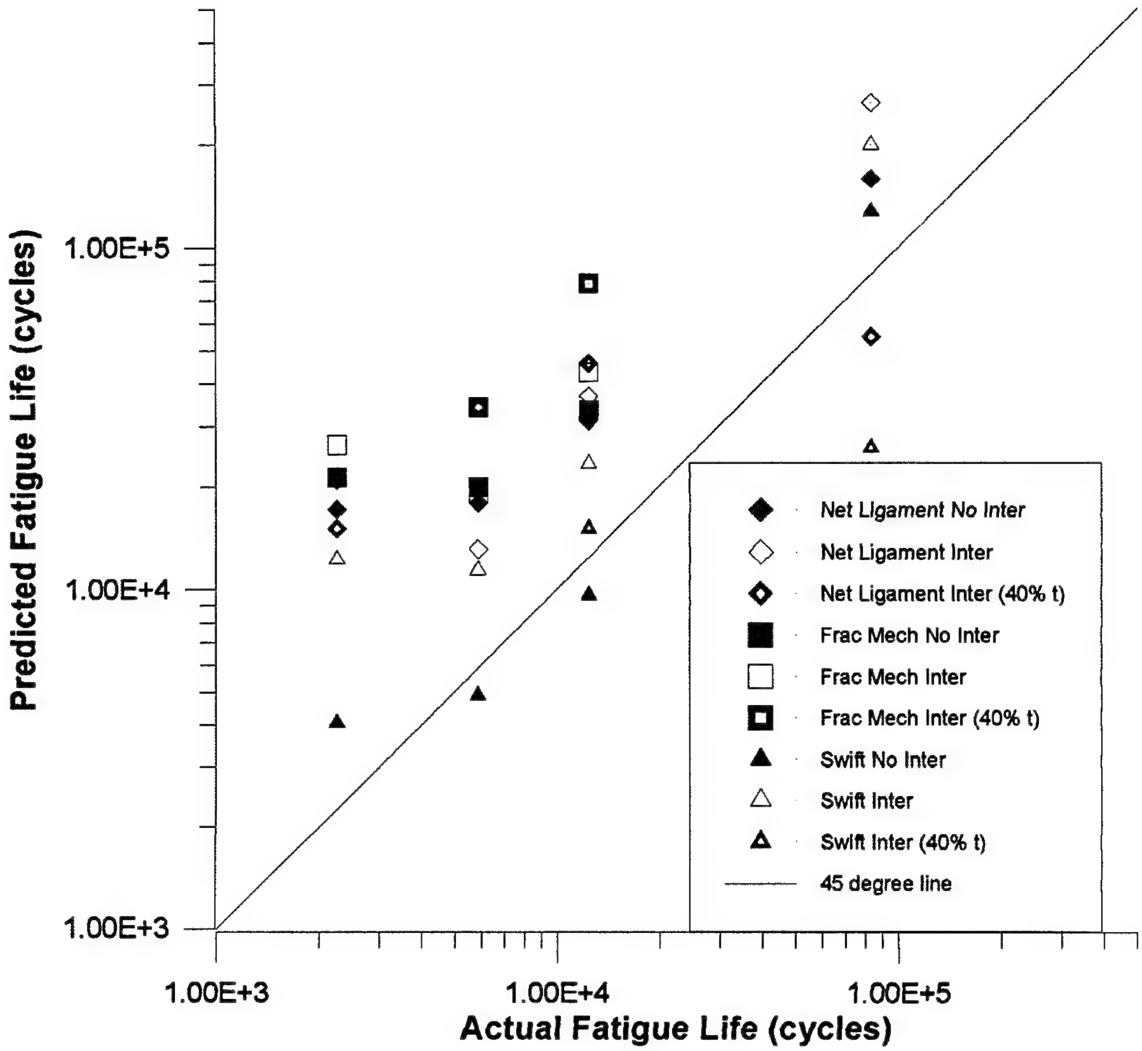

Figure 18. Comparison Between Actual and Predicted Fatigue Life

VI. Analysis and Discussion

Introduction

Residual strength and fatigue tests were conducted in this study to determine if available analytical methods can adequately predict fatigue life and residual strength of large specimens with multiple site damage. Ten residual strength tests, and four fatigue tests were conducted to determine an answer to this question. The previous chapter presented all the results from this effort. This chapter will focus on an analysis of the reported data, and their correlation with a previous study that investigated smaller test specimens. The results of the previous study are included in Appendix D.

The five analytical methods used to predict residual strength produced results ranging from unconservative to conservative failure estimates for specimens with MSD. The failure criteria based on a linear elastic fracture mechanics approach consistently overestimated the strength of specimens with MSD present. The three criteria which accounted for plasticity in the ligaments between cracked holes underestimated the specimens residual strength.

Analytical methods used to predict the fatigue life of specimens with MSD also produced a wide range of predicted fatigue lives. When crack interaction effects were considered in the specimens, the predicted fatigue life decreased in specimens with MSD. The Swift criterion using flow strength consistently provided better results when predicting fatigue life in the tested specimens.

Residual Strength

The residual strength tests were conducted to test the validity of the five failure criteria used in this study. The Type A specimens without MSD were only used to determine the apparent critical stress intensity factor to be used with the fracture mechanics criterion. The six Type B specimens had a lead crack, and holes with MSD. The effectiveness of the five failure criteria to predict residual strength are discussed in this section. In order to determine if the size and thickness of specimens affect residual strength predictions, the results of this study are compared to a study which tested the residual strength of smaller specimens. A study by Moukawsher (18) investigated the validity of three failure criteria, fracture mechanics, net ligament loss, and Swift to predict residual strength in specimens with MSD. The test specimens used by Moukawsher were relatively small, 22.86 cm (9 in) gauge section width, with a 0.229 cm (0.09 in) thickness. The results of Moukawsher's study may be seen in Appendix D.

Plots of crack opening displacement, Figures 16, and 17, showed that the residual strength specimens exhibited plasticity when subjected to a monotonically increasing load. Therefore, it was expected that failure criteria which accounted for plasticity would provide accurate prediction of residual strengths.

Fracture Mechanics

The fracture mechanics criterion, as described in Chapter 4, assumed that the specimens would fail when the critical stress intensity factor at the lead crack tip was reached. This criterion is similar to the failure criterion currently being used in the aircraft industry to predict failure of structures with a single crack.

The fracture mechanics criterion does not account for other structural details within the test panels. The number of holes or length of MSD cracks is not used in the prediction of failure load. The secant width correction factor is used to account for the effect of the central crack in a finite width specimen subjected to a tensile load. As expected, results show that this criterion consistently overestimates the residual strength of the Type B panels with MSD. The average error of residual strength prediction for the Type B specimens using this criterion was 35% as shown in Table 11. Moukawsher (18) found that the fracture mechanics method predicted failure of specimens with MSD with an average error of 28.8%.

The fracture mechanics criterion greatly overestimated the residual strength of panels with MSD. This unconservative method does not account for the holes or MSD cracks within the specimen, nor does it account for any plasticity effects. The use of this method will consistently overestimate residual strength of aircraft structures with MSD.

Net Ligament Loss

The net ligament loss criterion is based on a strength of material approach. Unlike the fracture mechanics method the criterion accounts for holes and MSD cracks within the test specimens. It relates the effective area of the specimen with the material's yield strength to arrive at a predicted residual strength.

Results show that the net ligament loss criterion does not provide accurate estimates for residual strength of specimens with MSD, Type B. Although it is more accurate than the fracture mechanics criterion, it remains unconservative. The net ligament loss criterion produced an average error of 12.8% when compared to actual

failure loads for the test specimens as seen in Table 11. The study on the smaller specimens by Moukawsher found that the net ligament loss method produced an average error of 22.4% when predicting residual strength of specimens with MSD.

The net ligament loss method does not take into account interaction of a lead crack with neighboring MSD cracks. For this reason, it was expected that the net ligament loss criterion would produce unconservative results. The net ligament loss method produced unconservative results in this study on large flat panels, as well as the study of smaller specimens by Moukawsher.

Swift

The Swift criterion (27) predicts failure using the plastic zone of the cracks within the specimen. This criterion assumes that failure occurs when the plastic zone in front of the lead crack comes in contact with the plastic zone of it's nearest neighboring MSD crack. This criterion accounts for the plasticity exhibited in the specimen when calculating residual strength.

The Swift criterion was used in this study with two different failure strengths. The flow strength of the material, as prescribed by Swift, and the ultimate strength of the material as postulated by Jeong and Brewer (13). Results show that when the ultimate strength is used with the Swift criterion, the residual strength of specimens with MSD is accurately predicted with an average error of only 1% as shown in Table 11. When the flow strength was used to predict failure according to the Swift criterion, the average error was 12% on the conservative side i.e. it underestimated the failure load by 12%.

Moukawsher used the Swift criterion to predict failure of specimens with MSD. He found that the Swift criteria using flow strength produced results with an average error of 9.6%. When the ultimate strength was used in Moukawsher's specimens to predict residual strength, the average error jumped up to 21%. It should be noted that Moukawsher used specimens with all MSD cracks fatigued instead of sawcut.

The Swift criterion produced relatively accurate results for predicting residual strength. The Swift criterion couples the loss in net section effectiveness due to holes and cracks in the specimens with the plasticity effects caused by crack propagation. Although the use of ultimate strength with the Swift criterion produced the most accurate results, the use of flow strength is probably better suited for prediction of residual strength in aircraft structures since the use of flow strength provides a good conservative estimate of the residual strength of panels with MSD.

Average Stress

The average stress criterion proposed by Jeong and Brewer (13) assumed that when the stress of the ligament between the lead crack and the MSD crack was equal to the ultimate strength of the material failure occurs. This failure prediction method accounts for interaction between the central lead crack, and its nearest neighboring MSD crack. It does not, however, account for the other flaw inclusions in the test specimen

The average stress criterion produced conservative residual strength estimates for the Type B, RS specimens. This study found that the average stress criterion predicted residual strength with an average error of -19.8% as shown in Table 11. The criterion consistently underestimated the residual strength of the tested specimens.

The average stress criterion was applied to the specimens and results of the study done by Moukawsher (18). It was found that the average stress criterion accurately predicted the residual strength of these small coupons with an average error of only -2 %. This finding is also supported by Jeong and Brewer (13) with their experimental results. They found that the use of this criteria produced linkup stresses which were accurate to an average error of -5.7%.

The average stress criterion produces conservative predictions of residual strength in specimens with MSD. The accuracy of this method is dependent on the size of the specimen. Both Jeong and Brewer, and Moukawsher tested specimens which were smaller than the specimens used in this study.

Average Displacement

The average displacement criterion proposed by Jeong and Brewer assumed that the displacement of the ligament between adjacent cracks in panels with MSD is zero. It also assumed that the stress across the ligament was uniformly equal to the material's ultimate strength. This criterion does not account for other cracks or holes within the tested panels. It relies on the assumption that the ligament will not displace until fracture occurs across the ligament.

Test results show that the average displacement criterion greatly underestimates the residual strength of panels with MSD. An average error of -63% (see Table 11) shows that the average displacement criterion is not accurate in predicting the residual strength of panels with MSD.

The average displacement criterion was also applied to the specimen geometry, and test results of the study accomplished by Moukawsher (18). It was found that the average displacement criterion still produced very conservative estimates for residual strength in the smaller specimens with an average error of -47%. Jeong and Brewer found in their experimental investigation that the average displacement criterion produced results that were accurate to an average error of -17.5%.

It is clear that the average displacement criterion produces the most conservative estimates of residual strength that would not provide much benefit to aircraft designers if they desire accurate estimate of the residual strength of aircraft structures with MSD.

Sawcut versus Fatigue Cracks

The corollary question in the residual strength tests was whether sawcut cracks could be used in place of fatigued cracks when MSD is simulated within test specimens. The time required to fabricate a residual strength test specimen could be greatly reduced if fatigue cracks were not necessary to simulate MSD. The saw blade used to make saw cuts at the specimen's holes was very thin 0.2 cm (0.08 in). It was assumed that the thin saw cuts used to simulate MSD cracks would produce test results commensurate with fatigued MSD cracks.

The RS05B and RS06B specimens were tested with fatigued MSD cracks instead of sawcut cracks. The use of most of the analytical methods to predict residual strength in these specimens resulted in error that was commensurate with the four Type B specimens with sawcut cracks with the following two exceptions. The error in the Swift and average stress criteria was reduced in the specimens with fatigued MSD. The RS05B and RS06B

specimens evaluated with the Swift criterion using flow strength had an average error of -8%. The sawcut specimens using the Swift criterion had an average error of -15.3%. Similarly, the error of the average stress criterion in the fatigued specimens was -12.8%, while the error in the four sawcut specimens was -23%.

Sawcuts should not be used in place of fatigued cracks in MSD specimens when either the Swift, or average stress criteria is used. When less accurate analytical methods are used to analyze specimens with MSD, sawcuts may be used in place of fatigued MSD cracks.

Summary

The residual strength tests were performed to test the validity of the available analytical methods to predict failure of specimens with MSD. The analytical methods used in this study provided the very unconservative failure predictions to very conservative failure predictions. The fracture mechanics method proved to be the most unconservative failure criteria, followed by the net ligament loss method. The Swift and average stress criteria produced the most accurate results, while remaining somewhat conservative. The average displacement criteria proved to be the most conservative criteria to predict residual strength in specimens with MSD. The average error of the five failure criteria with larger specimens and the previous study (18) with the smaller specimens are summarized in Figure 19.

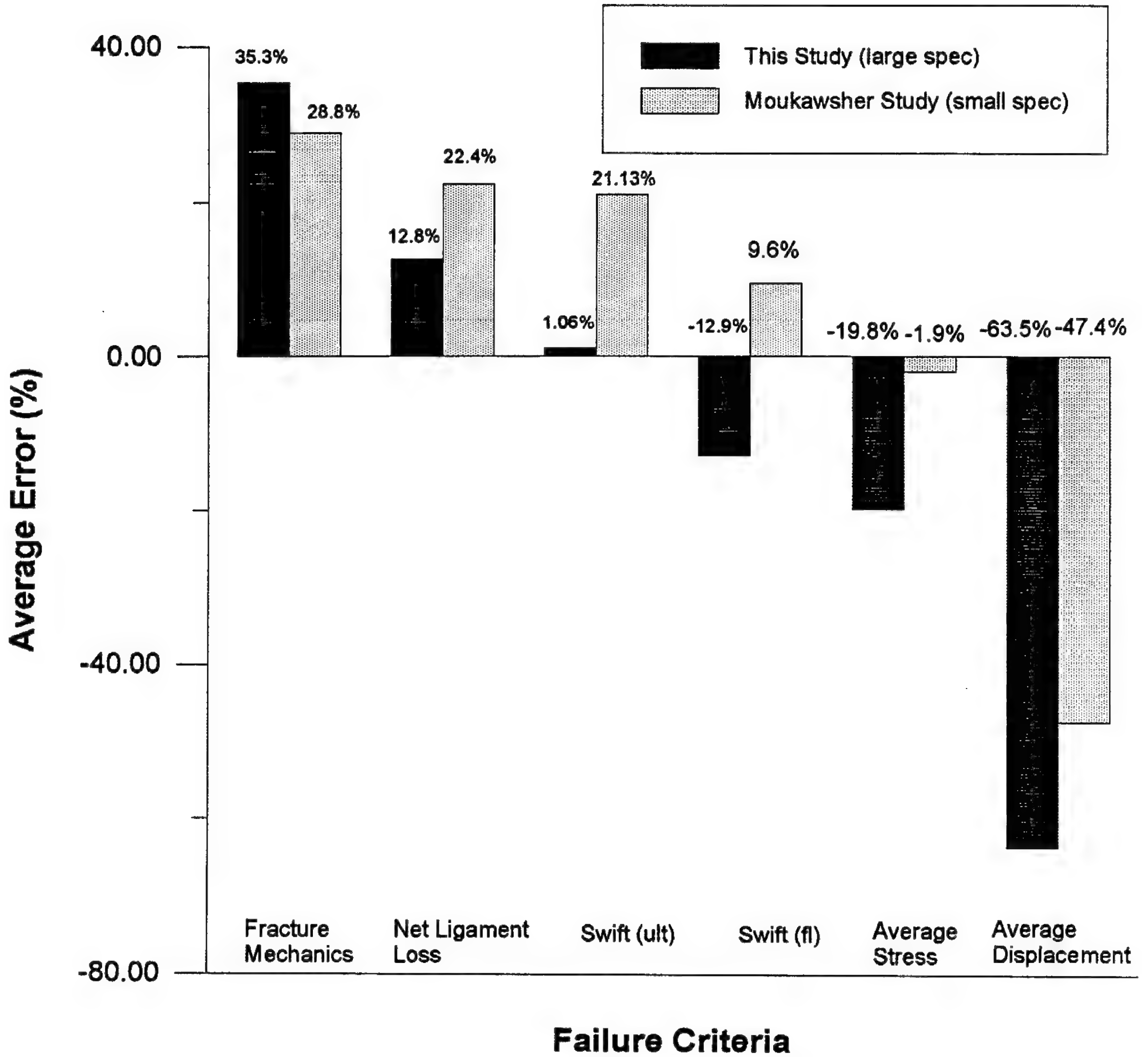

Figure 19. Comparison of Analytical Methods for Large and Small Specimens

The size of the specimens did not effect the validity of the five failure criterion. The fracture mechanics and net ligament loss criteria remained unconservative for both the larger specimens used in this study, and the smaller specimens studied by Moukawsher (18). The average displacement criterion produced very conservative residual strength predictions in both the large and small specimens. The Swift method and the average stress criterion produced the same trends but different accuracys when large and small specimens were considered. This can be attributed mostly to the fact that sawcuts were used on the majority of the large specimens considered in this study. Moukawsher (18) only used fatigued MSD cracks with small specimens.

Fatigue

The purpose of the fatigue tests of this study was to determine if the available methods could predict fatigue life of specimens with MSD. According to Broek (4) “fatigue crack propagation is affected by an endless number of parameters, and the circumstances during the test will seldom be the same as in service”. For this reason many researchers have found it difficult to adequately predict the fatigue life of aircraft structures. The computer algorithm used to predict fatigue life used three failure criteria for the four fatigue specimens tested in this study. The fracture mechanics, net ligament loss, and Swift criteria were used to predict fatigue life of the tested specimens. The average stress and average displacement criteria were not used in the computer program because they necessitated the evaluation of integrals which proved too difficult to program.

The specimens evaluated in this study included a specimen with MSD and no lead crack, FAT 01A. Two specimens with a lead crack and holes without MSD, FAT 01B and FAT 02B, were tested to evaluate the effect of MSD on the fatigue life of aluminum panels. Finally, a specimen with a central lead crack and MSD, FAT 01C was tested to determine if analytical methods could predict fatigue life with MSD present.

Fracture Mechanics

The fracture mechanics failure criterion, as stated previously, is derived from linear elastic fracture mechanics. This criterion proved to be unconservative in the prediction of residual strength in specimens with MSD. It was, therefore, expected that it would produce an unconservative estimate of fatigue life.

The fracture mechanics method was used on the three fatigue specimens with a long lead crack, FAT 01B, FAT 02B, and FAT 01C. The specimen with no lead crack could not be evaluated with this criteria. Results show that this method produced an average error of 417% in relation to the measured fatigue life as shown in Table 12. When crack interaction effects were included, the average error was still over 500%. The use of 40% of the tip separation in the Kamei-Yokobori (14) interaction method did not produce results that were better than the evaluation of fatigue life without crack interaction (Table 13).

As expected the fracture mechanics method produced the unconservative fatigue life prediction. The use of the Kamei-Yokobori crack interaction factor with this method produced results that deviated further from measured fatigue life than without interaction being included.

Net Ligament Loss

The net ligament loss criteria produced residual strength predictions that were more conservative than the fracture mechanics method, but less conservative than the Swift criteria. It was expected that the net ligament loss method would provide fatigue life results that would be closer to measured values than the fracture mechanics criteria.

The net ligament loss method produced fatigue life results which had an average error of 277% when crack interaction effects were not used (see Table 13). When crack interaction effects were considered the net ligament loss method still produced a high error. However, when the interaction effects were considered using 40% of the crack tip separation as described by Kamei and Yokobori, for the specimens with MSD, FAT 01A, and FAT 01C better results were obtained. The consideration of interaction produced results that were closer to measured fatigue life.

When the net ligament loss criterion is used to predict fatigue life, the predicted results remain unconservative . However, crack interaction effects using 40% of the crack tip separation produced better prediction in fatigue life.

Swift

The Swift residual strength criterion produced the most accurate results for predicting residual strength of specimens with MSD. It was, therefore, expected that this criterion would also be able to accurately predict fatigue life. The computer program used the Swift method with the flow strength of the material as opposed to the material's ultimate strength.

The Swift method produced fatigue life predictions which were accurate with an average error of 23.4% when crack interaction effects were not considered. The Swift method is derived with crack interaction effects included. Therefore it is expected that the use of the crack interaction procedure within the computer algorithm with the Swift method would produce less accurate results. Results show that when crack interaction is considered using the Kamei-Yokobori crack interaction procedure, less accurate fatigue lives are predicted. However, when the interaction procedure is coupled with a crack tip separation of 40% of (t) as described by Moukawsher (18), more accurate results occur. The Swift method was not able to produce results while using the 40% of (t) method for FAT 01B. The small MSD crack size coupled with the long lead crack produced a singularity within the program.

The Swift criterion produced the most accurate results for predicted fatigue life in specimens with and without MSD damage. The crack interaction effects using the full crack tip separation (t) produce inaccurate results when coupled with the Swift criteria. Interaction effects employing 40% of the crack tip separation (t), produces the most accurate results using this method.

Summary

The computer algorithm, that was employed to predict fatigue life, was validated using the results from Moukawsher's study (18). Moukawsher only used the net ligament loss and Swift failure criteria to predict fatigue life. The fatigue lives of specimens in that study were predicted with an average error of 40% using interaction effects with a crack tip separation of 40% (t). Without interaction effects the Moukawsher could only predict

fatigue life within 275%. It was found that the large flat panels in this study produced similar results. An average fatigue life error of 10.6% using the Swift method with 40% (t) crack interaction, and a 276% error using the net ligament loss criterion with no crack interaction considered. This study supports the use of the 40% (t) crack tip separation method in fatigue life prediction using the Kamei-Yokobori interaction factor as proposed by Moukawsher (18). Without this transformation of (t), less conservative results were predicted. Figure 20 shows a comparison of the error between the measured fatigue life and the fatigue life predicted by the Swift method without crack interaction for this study and Moukawsher's study (18) for similar configurations.

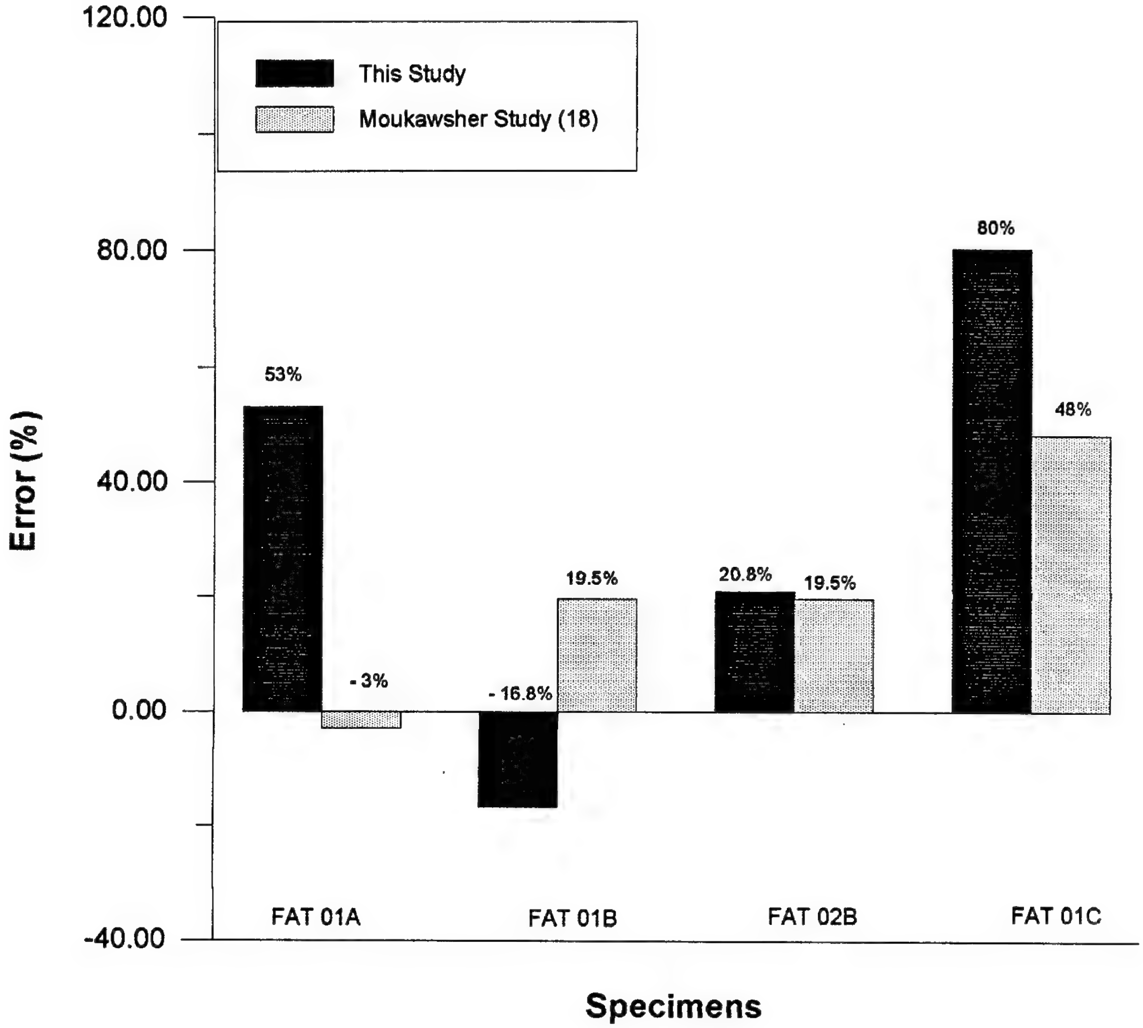

Figure 20. Comparison of Fatigue Life in Small and Large Panels

VII. Conclusions and Recommendations

The purpose of this study was to determine if the available analytical methods could be used to predict residual strength and fatigue life of unstiffined specimens with multiple site damage (MSD). The present study also sought to determine if their was a significant effect of the size of tested specimens on fatigue life and residual strength by making comparisons of results of this study with large specimens with a previous study with small specimens (18).

The available failure criteria produced a wide range of residual strength predictions of large panels with MSD. The fracture mechanics approach produced the most unconservative results followed by the net ligament loss criterion. The Swift failure criterion incorporating the material's ultimate strength produced the most accurate residual strength predictions in this study. When the Swift method was used with the material's flow strength, slightly less accurate conservative results were obtained. The average stress criterion produced consistently conservative predictions of residual strength. Finally, the average displacement criterion produced the most inaccurate and conservative residual strength prediction. The range of the five failure criteria from unconservative residual strength predictions to conservative residual strength predictions can be seen in Figure 21.

The Swift and average stress criterion produced the most accurate results for both small and large specimens with MSD. The Swift method should be used with the materials flow strength when this criterion is used to predict residual strength for design

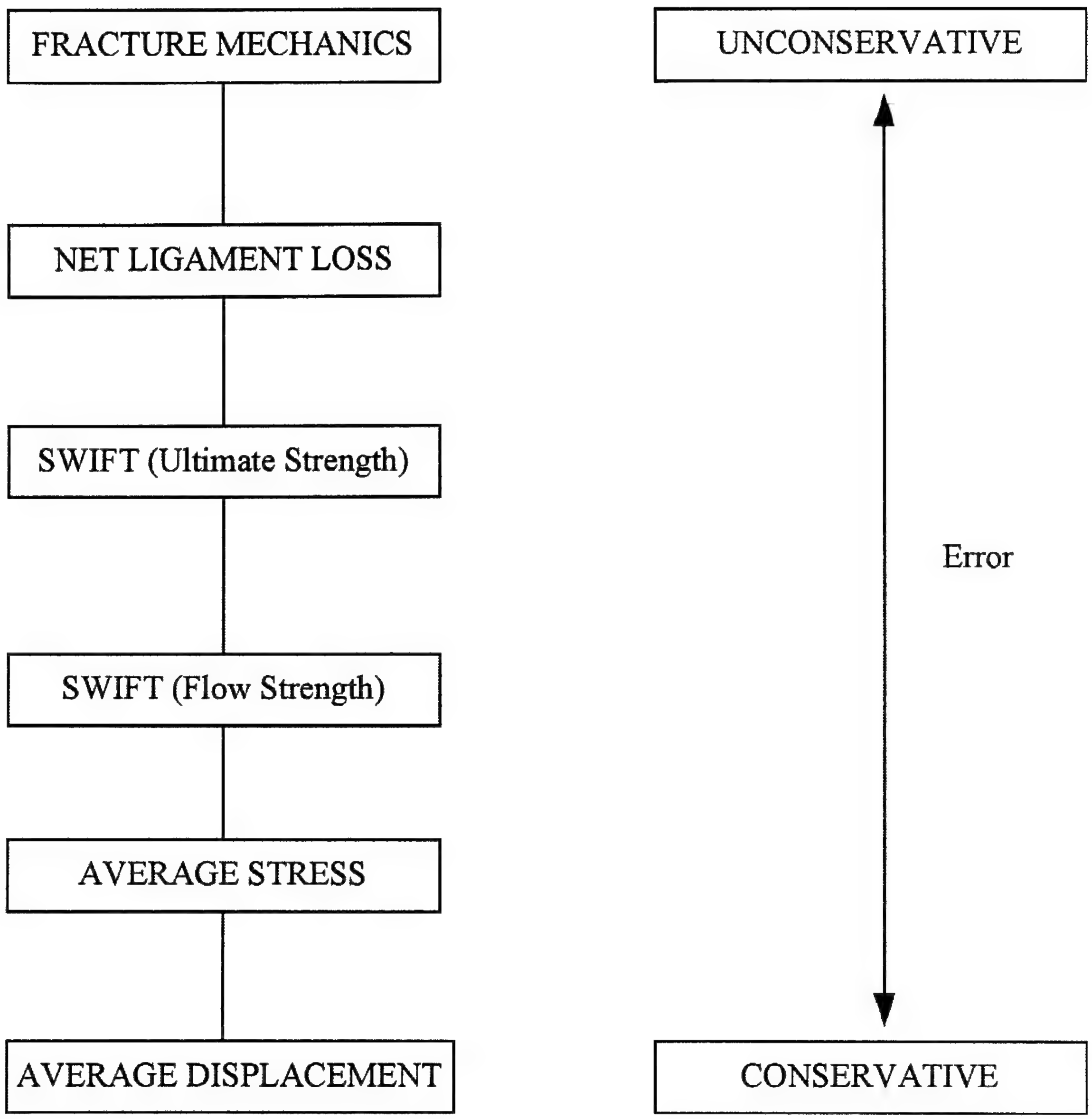

Figure 21. Range of Error from Five Analytical Criteria

purposes since it provides accurate as well as conservative residual strength predictions.

The larger size of the specimens used in this study produced results similar to a previous study with smaller specimens. The trends of unconservative to conservative residual strength and fatigue life predictions remained the same for the five failure criteria between these two sizes. The most accurate residual strength prediction changed from the Swift method using ultimate strength to the Swift method using flow strength and the average stress criterion when large and small specimens are compared.

A small difference was noticed when sawcut cracks were substituted for fatigue cracks in large thin panels. The residual strength of fatigued MSD cracks is more accurately predicted using the Swift and average stress criteria. The fatigued cracks should be used to test specimens for residual strength since they are closer to actual aircraft conditions.

Fatigue life of structures with MSD was predicted with reasonable accuracy with the Swift failure criterion along with the Paris crack growth law. The fracture mechanics and net ligament loss methods in conjunction with the Paris crack growth law did not predict accurate fatigue life of structures with MSD. The Kamei-Yokobori crack interaction equations should be modified to use 40% of the calculated crack tip separation, when the fatigue lives of specimens with MSD are predicted. This modification produces more accurate results in both large and small specimens.

The investigation of the effects of MSD on aircraft structures is an important research area. This study fills the need for characterization of MSD in large flat unstiffened panels. Much more research is required to obtain a complete picture of how

MSD effects aircraft structures. The effects of stiffeners on MSD in large flat panels remains to be investigated. The average stress and average displacement criterion should be incorporated in a computer program to determine if they are more accurate in predicting fatigue life of structures with MSD. The outcome of this study provides a clearer picture of how MSD affects aircraft structures. The full characterization of the effects of multiple site damage on aircraft structures remains incomplete. As aircraft inventories around the world age, a complete understanding of the affects of MSD becomes more and more vital.

Appendix A: Fatigue Life Algorithm

The following is the computer code, written in Turbo Pascal© , that was used to predict fatigue life of the four specimens tested. Given an input file that described a specimens geometric configuration, material properties, and loading condition, the program computed the specimens fatigue life. The program used one of three failure criteria; net ligament loss, fracture mechanics, or Swift, to compute the predicted failure load for each program iteration. The predicted failure load was compared with the maximum cyclic load to determine if failure had occurred in the specimen. A sample input and output file is listed in Appendix B.

```
(****************************************************************************)
(*  Capt Mark C. Cherry      19 December 1995                               *)
(*                                                                          *)
(*  Program Fatigue Calculation                                             *)
(*                                                                          *)
(*  This program was developed for use in a Masters Thesis to predict      *)
(*  fatigue life of aircraft structures with Multiple Site Damage (MSD)    *)
(*  This computer program predicts the fatigue life of specimens           *)
(*  subjected to a cyclic load.  The program uses material property        *)
(*  values and calculates the expected fatigue life, expressed as          *)
(*  cycles to failure, for specimens with MSD damage.                      *)
(****************************************************************************)
Program Fatigue (input,output,infile,outfile);

uses winCRT;
Type
 answer = array [1..19,1..2] of char;
 matrix2 = array [1..19,1..2] of real;
 side = array [1..2] of real;

Var
 infile:text;
 outfile:text;
 (* infile - data file program reads from *)
 (* outfile - data file program prints output to *)
 filename:string[25];
 (* filename - used to specify what the output file will be *)
 E,W,th,del,yst,ust,fst,d,r,Kapp,delh: real;
 minst,maxst,delst,Pmax,Pmin,delP,C,a2,a1,Percent: real;
 Kta2,ata2,Kta1,ata1,cycle,delcycle: real;
 M,Nmsd,Interact,mode: integer;
 Hole,Kt,crack,at,delKi,delKf,Bint,dadn,da: matrix2;
 ans1: answer;
 a2d,dKia2,dKfa2,Binta2,dadna2,daa2: side;
 dKia1,dKfa1,Binta1,dadna1,daa1: real;
 fail: integer;
 chold,thresh,Z: real;

Function Power (X: real; Q: integer): real;
(* This function is used to take a number to a power  *)

Var Product: real;
  I: integer;

begin
 if Q>= 0 then
 begin
  Product:= 1;
  for I:= 1 to Q do
   Product:= X*Product;
   Power:= Product
```

```
  end
  else Power:= 1/Power(x,-Q)
end;


Procedure Getinfo;
(* This procedure gets information from an input file designated in MAIN for
the program to use to calculate fatigue life of specimens with MSD.*)

Var
  da1,da2,dK1,dK2,exp,temp,per: real;
  x,hol: integer;
  ans2: char;

Begin
  fail:= 2;
  cycle:= 0;
  chold:= 0;
  z:= 0.4;
  thresh:= 5000;
  Writeln ('This program calculates the number of cycles to failure ');
  Writeln ('for a specimen with MSD damage');
  Writeln ('MSD is assumed to exist on both sides of holes');
  Writeln ('First the material properties will be inputed.');
  Writeln ('What is the materials modulus of elasticity in ksi?');
  Writeln (outfile,'What is the materials modulus of elasticity in ksi?');
  Readln (infile,E);
  Writeln (outfile,E:10:2);
  Writeln (E);
  Writeln ('Enter the specimens width (in)');
  Writeln (outfile,'Enter the specimens width (in)');
  Readln (infile,W);
  Writeln (W);
  Writeln (outfile,W:8:2);
  Writeln ('Enter the specimens thickness (in)');
  Writeln (outfile,'Enter the specimens thickness (in)');
  Readln (infile,th);
  Writeln (th);
  Writeln (outfile,th:8:2);
  Writeln ('Enter the spacing between holes from center to center (in)');
  Writeln (outfile,'Enter the spacing between holes from center to center (in)');
  Readln (infile,del);
  Writeln (del);
  Writeln (outfile,del:8:2);
  Writeln ('Enter the materials yield stress (ksi)');
  Writeln (outfile,'Enter the materials yield stress (ksi)');
  Readln (infile,yst);
  Writeln (yst);
  Writeln (outfile,yst:8:2);
  Writeln ('Enter the materials ultimate stress (ksi)');
  Writeln (outfile,'Enter the materials ultimate stress (ksi)');
  Readln (infile,ust);
  Writeln (ust);
  Writeln (outfile,ust:8:2);
```

```
fst:= (ust+yst)/2;
Writeln ('Enter the materials approximate stress concentration factor (ksi sqrt in)');
Writeln (outfile,'Enter the materials approximate stress concentration factor (ksi sqrt in)');
Readln (infile,Kapp);
Writeln (Kapp);
Writeln (outfile,Kapp:8:2);
Writeln ('Enter the diameter of the holes used in the specimens (in)');
Writeln (outfile,'Enter the diameter of the holes used in the specimens (in)');
Readln (infile,d);
Writeln (d);
Writeln (outfile,d:8:4);
r:= d/2;
Writeln ('Enter the maximum remote stress used to cycle the specimens (ksi)');
Writeln (outfile,'Enter the maximum remote stress used to cycle the specimens (ksi)');
Readln (infile,maxst);
Writeln (maxst);
Writeln (outfile,maxst:8:2);
Writeln ('Enter the minimum remote stress used to cycle the specimens (ksi)');
Writeln (outfile,'Enter the minimum remote stress used to cycle the specimens (ksi)');
Readln (infile,minst);
Writeln (minst);
Writeln (outfile,minst:8:2);
Pmax:= maxst*W*th;
Pmin:= minst*W*th;
delst:= maxst-minst;
delP:= Pmax-Pmin;
Writeln ('Enter the first da/dn point used to determine Paris Law Coeffs');
Writeln (outfile,'Enter the first da/dn point used to determine Paris Law Coeffs');
Readln (infile,da1);
Writeln (da1);
Writeln (outfile,da1:10:8);
Writeln ('Enter the delta K corresponding to the first point');
Writeln (outfile,'Enter the delta K corresponding to the first point ');
Readln (infile,dK1);
Writeln (dK1);
Writeln (outfile,dK1:8:2);
Writeln ('Enter the second da/dn point used to determine Paris Law Coeffs');
Writeln (outfile,'Enter the second da/dn point used to determine Paris Law Coeffs');
Readln (infile,da2);
Writeln (da2);
Writeln (outfile,da2:10:8);
Writeln ('Enter the delta K corresponding to the second point');
Writeln (outfile,'Enter the delta K corresponding to the second point ');
Readln (infile,dK2);
Writeln (dK2);
Writeln (outfile,dK2:8:2);
exp:= (ln(da1)-ln(da2))/(ln(dK1)-ln(dK2));
M:= round(exp);
C:= da1/Power(dK1,M);
Writeln ('Enter the number of holes with MSD');
Writeln (outfile,'Enter the number of holes with MSD');
Readln (infile,Nmsd);
Writeln (Nmsd);
Writeln (outfile,Nmsd);
```

```
Writeln ('Enter the half crack length of the lead crack');
Writeln (outfile,'Enter the half crack length of the lead crack');
Readln (infile,a2);
Writeln (a2);
Writeln (outfile,a2:8:4);
a2d[1]:= a2;
a2d[2]:= a2;
Writeln ('Enter the number of holes the lead crack encompasses ');
Writeln (outfile,'Enter the number of holes the lead crack encompasses ');
Readln (infile,hol);
Writeln (hol);
Writeln (outfile,hol);
If Odd(hol) Then
begin
  delh:= del + del * ((hol-1)/2);
end
Else
begin
  delh:= del + del/2 + (del*((hol/2)-1));
end;
For x:= 1 to Nmsd do
begin
  Writeln ('Enter the crack length of the left ',x,' hole crack');
  Writeln (outfile,'Enter the crack length of the left ',x,' hole crack');
  Writeln ('measured from the hole edge (in) hole numbers progress');
  Writeln ('from the left side of the panel to the right side');
  Writeln (outfile,'measured from the hole edge (in) hole numbers progress ');
  Writeln (outfile,'from the left side of the panel to the right side');
  Readln (infile,crack[x,1]);
  Writeln (crack[x,1]);
  Writeln (outfile,crack[x,1]:8:4);
  Writeln ('Is this crack adjacent to the lead crack y or n ?');
  Writeln (outfile,'Is this crack adjacent to the lead crack y or n ?');
  Readln (infile,ans1[x,1]);
  Writeln (outfile,ans1[x,1]);
  If ans1[x,1]=  'y' then
  begin
    Writeln ('Is this the largest crack adjacent to the lead crack?');
    Writeln (outfile,'Is this the largest adjacent crack to the lead crack?');
    Readln (infile,ans2);
    writeln (outfile,ans2);
    If ans2= 'y' then
    begin
      a1:= crack[x,1]+r;
    end;
  end;
  Writeln ('Enter the crack length of the right ',x,' hole crack');
  Writeln (outfile,'Enter the crack length of the right ',x,' hole crack');
  Writeln ('measured from the hole edge (in)');
  Writeln (outfile,'measured from the hole edge (in)');
  Readln (infile,crack[x,2]);
  Writeln (crack[x,2]);
  Writeln (outfile,crack[x,2]:8:4);
  Writeln ('Is this crack adjacent to the lead crack y or n ?');
```

```
  Writeln (outfile,'Is this crack adjacent to the lead crack y or n ?');
  Readln (infile,ans1[x,2]);
  Writeln (outfile,ans1[x,2]);
  If ans1[x,2]= 'y' then
  begin
    Writeln ('Is this the largest crack adjacent to the lead crack?');
    Writeln (outfile,'Is this the largest adjacent crack to the lead crack?');
    Readln (infile,ans2);
    Writeln (outfile,ans2);
    If ans2= 'y' then
    begin
      a1:= crack[x,2]+r;
    end;
  end;
  Hole[x,1]:= crack[x,1]+r;
  Hole[x,2]:= crack[x,2]+r;
 end;
 Writeln ('Enter the percentage of the length of the smallest hole with MSD');
 Writeln (outfile,'Enter the percentage of the length of the smallest hole with MSD');
 Writeln ('you want to grow the cracks in the panel(used as a stepsize).');
 Writeln (outfile,'you want to grow the cracks in the panel (used as a stepsize).');
 Writeln ('Use 10 for 10%');
 Writeln (outfile,'Use 10 for 10%');
 Readln (infile,per);
 Writeln (per);
 Writeln (outfile,per:8:2);
 Percent:= per/100;
 Writeln ('Enter the failure criteria to be used in the analysis ');
 Writeln (outfile,'Enter the failure criteria to be used in the analysis');
 Writeln ('1 - Net Ligament Loss  2 - Fracture mechanics  3 - Swift');
 Writeln (outfile,'1 - Net Ligament Loss  2 - Fracture mechanics 3 - Swift');
 Readln (infile,mode);
 Writeln (mode);
 Writeln (outfile,mode);
 Writeln ('Do you want crack interaction factors to be considered ?');
 Writeln (outfile,'Do you want crack interaction factors to be considered ?');
 Writeln ('Enter 1 - for yes and 2 - for no');
 Writeln (outfile,'Enter 1 - for yes and 2 - for no');
 Readln (infile,Interact);
 Writeln (Interact);
 Writeln (outfile,Interact);
End;

Function cel(qqc,pp,aa,bb: real): real;
(* Returns the general complete elliptic integral cel(kc,p,a,b) with
qqc = kc, pp = p, aa= a, and bb = b; (From Numerical Recipes in Pascal
by Press, Flannery, Teukolsky, and Vetterling) *)

LABEL 99;
CONST
   ca = 0.0003;
   pio2 = 1.5707963268;
VAR
  a,b,e,f,g: real;
```

```
  em,p,q,qc: real;
BEGIN
   If qqc = 0.0 THEN BEGIN
     writeln('pause in routine CEL');
     readln
   END;
   qc:= abs(qqc);
   a:= aa;
   b:= bb;
   p:= pp;
   e:= qc;
   em:= 1.0;
   IF p > 0.0 THEN BEGIN
     p:= sqrt(p);
     b:= b/p
   END
   ELSE BEGIN
      f:= qc*qc;
      q:= 1.0-f;
      g:= 1.0-p;
      f:= f-p;
      q:= q*(b-a*p);
      p:= sqrt(f/g);
      a:= (a-b)/g;
      b:= -q/(g*g*p)+a*p
   END;
   WHILE true DO BEGIN
      f:= a;
      a:= a+b/p;
      g:= e/p;
      b:= b+f*g;
      b:= b+b;
      p:= g+p;
      g:= em;
      em:= qc+em;
      IF abs(g-qc)<= g*ca THEN GOTO 99;
      qc:= sqrt(e);
      qc:= qc+qc;
      e:= qc*em
   END;
99:
  cel:= pio2*(b+a*em)/(em*(em+p))
END;


Procedure Intfactor;
(* This procedure is used to add a crack interaction factor
  to the calculated stress intensity factor *)
var
 x,y:integer;
 a,b,t,kfac,temp,fac:real;

begin
 Bint[1,1]:= 1;
```

```
Bint[Nmsd,2]:= 1;
For x:= 2 to Nmsd Do
begin
 If ans1[x,1]= 'n' then
 begin
  a:= Hole[x-1,2];
  b:= Hole[x,1];
  t:= Z*del-Hole[x-1,2]-Hole[x,1];
  If t>0 then
  begin
   temp:= (a*b)/(((2*a)+t)*((2*b)+t));
   kfac:= 2*sqrt(temp);
   fac:= (cel(kfac,1,1,1)-cel(kfac,1,1,kfac*kfac))/cel(kfac,1,1,1);
   Bint[x,1]:= sqrt(1+(2*a/t))*(1-(1+t/(2*b))*fac);
   Bint[x,1]:= abs(Bint[x,1]);
  end
  else
   Bint[x,1]:= 1;
 end;
 If ans1[x,1]= 'y' then
 begin
  a:= a2;
  b:= Hole[x,1];
  t:= Z*delh-a2-Hole[x,1];
  If t>0 then
  begin
   temp:= (a*b)/(((2*a)+t)*((2*b)+t));
   kfac:= 2*sqrt(temp);
   fac:= (cel(kfac,1,1,1)-cel(kfac,1,1,kfac*kfac))/cel(kfac,1,1,1);
   Bint[x,1]:= sqrt(1+(2*a/t))*(1-(1+t/(2*b))*fac);
   Binta2[2]:= sqrt(1+(2*b/t))*(1-(1+t/(2*a))*fac);
   Bint[x,1]:= abs(Bint[x,1]);
   Binta2[2]:= abs(Binta2[2]);
  end
  else
  begin
   Bint[x,1]:= 1;
   Binta2[2]:= 1;
  end;
 end;
end;
For x:= 1 to Nmsd-1 Do
begin
 If ans1[x,2]= 'n' then
 begin
  a:= Hole[x+1,1];
  b:= Hole[x,2];
  t:= Z*del-Hole[x+1,1]-Hole[x,2];
  If t>0 then
  begin
   temp:= (a*b)/(((2*a)+t)*((2*b)+t));
   kfac:= 2*sqrt(temp);
   fac:= (cel(kfac,1,1,1)-cel(kfac,1,1,kfac*kfac))/cel(kfac,1,1,1);
   Bint[x,2]:= sqrt(1+(2*a/t))*(1-(1+t/(2*b))*fac);
```

```
      Bint[x,2]:= abs(Bint[x,2]);
    end
    else
      Bint[x,2]:= 1;
  end;
  If ans1[x,2]= 'y' then
  begin
    a:= a2;
    b:= Hole[x,2];
    t:= Z*delh-a2-Hole[x,2];
    If t>0 then
    begin
      temp:= (a*b)/(((2*a)+t)*((2*b)+t));
      kfac:= 2*sqrt(temp);
      fac:= (cel(kfac,1,1,1)-cel(kfac,1,1,kfac*kfac))/cel(kfac,1,1,1);
      Bint[x,2]:= sqrt(1+(2*a/t))*(1-(1+t/(2*b))*fac);
      Binta2[1]:= sqrt(1+(2*b/t))*(1-(1+t/(2*a))*fac);
      Bint[x,2]:= abs(Bint[x,2]);
      Binta2[1]:= abs(Binta2[1]);
    end
    else
    begin
      Bint[x,2]:= 1;
      Binta2[1]:= 1;
    end;
  end;
end;
For x:= 1 to Nmsd Do
begin
  For y:= 1 to 2 Do
  begin
    delKf[x,y]:= delKi[x,y]*Bint[x,y];
  end;
end;
For x:= 1 to 2 Do
begin
  dKfa2[x]:=dKia2[x]*Binta2[x];
end;
a:= a2;
b:= a1;
t:= Z*delh-a2-a1;
If t>0 then
begin
  temp:= (a*b)/(((2*a)+t)*((2*b)+t));
  kfac:= 2*sqrt(temp);
  fac:= (cel(kfac,1,1,1)-cel(kfac,1,1,kfac*kfac))/cel(kfac,1,1,1);
  Binta1:= sqrt(1+(2*a/t))*(1-(1+t/(2*b))*fac);
  Binta1:= abs(Binta1);
  dKfa1:= dKia1*Binta1;
end
else
  Binta1:= 1;
End;
```

```
Procedure InitK;
(* This procedure computes an initial stress intensity factor
   for each MSD crack, and the lead crack  if crack interaction
   is not considered the stress intensity computed in this
   procedure is carried to the following procedures     *)

Var
  x,y:integer;
  temp,temp2,temp3,temp4:real;

Begin
  For x:= 1 to Nmsd do
  begin
    temp:= cos(pi*Hole[x,1]/W);
    temp2:= abs(temp);
    temp3:= cos(pi*Hole[x,2]/W);
    temp4:= abs(temp3);
    If temp2>0 then
      Kt[x,1]:= maxst*sqrt(pi*Hole[x,1])*sqrt(1/temp2)
    else
      Kt[x,1]:= maxst*sqrt(pi*Hole[x,1]);
    If temp4>0 then
      Kt[x,2]:= maxst*sqrt(pi*Hole[x,2])*sqrt(1/temp4)
    else
      Kt[x,2]:= maxst*sqrt(pi*Hole[x,2]);
  end;
  For x:= 1 to Nmsd do
  begin
    For y:= 1 to 2 do
    begin
      at[x,y]:= r/(Power(1.12*Kt[x,y],2)-1);
      If Hole[x,y]>=at[x,y] then
      begin
        temp:= cos(pi*Hole[x,y]/W);
        temp2:= abs(temp);
        If temp2>0 then
          delKi[x,y]:= delst*sqrt(pi*Hole[x,y])*sqrt(1/temp2)
        else
          delKi[x,y]:= delst*sqrt(pi*Hole[x,y]);
      end;
      If Hole[x,y]<at[x,y] then
      begin
        delKi[x,y]:= delst*sqrt(pi*Hole[x,y])*((0.6865/(0.2772+(Hole[x,y]-r)/r))+0.9439);
      end;
    end;
  end;
  temp:= cos(pi*a2/W);
  temp2:= abs(temp);
  If temp2>0 then
    Kta2:= maxst*sqrt(pi*a2)*sqrt(1/temp2)
  else
    Kta2:= maxst*sqrt(pi*a2);
  ata2:= r/(Power(1.12*Kta2,2)-1);
```

```
temp:= cos(pi*a1/W);
temp2:= abs(temp);
If temp2>0 then
 Kta1:= maxst*sqrt(pi*a1)*sqrt(1/temp2)
else
 Kta1:= maxst*sqrt(pi*a1);
ata1:= r/(Power(1.12*Kta1,2)-1);
If a2>=ata2 then
begin
 For y:= 1 to 2 do
 begin
  temp:= cos(pi*a2d[y]/W);
  temp2:= abs(temp);
  If temp2>0 then
   dKia2[y]:= delst*sqrt(pi*a2d[y])*sqrt(1/temp2)
  else
   dKia2[y]:= delst*sqrt(pi*a2d[y]);
 end;
end;
If a2<ata2 then
begin
 For y:= 1 to 2 do
 begin
  dKia2[y]:= delst*sqrt(pi*a2d[y])*((0.6865/(0.2772+(a2d[y]-(delh-del)-r)/r))+0.9439);
 end;
end;
If a1>=ata1 then
begin
 temp:= cos(pi*a1/W);
 temp2:= abs(temp);
 If temp2>0 then
  dKia1:= delst*sqrt(pi*a1)*sqrt(1/temp2)
 else
  dKia1:= delst*sqrt(pi*a1);
end;
If a1<ata1 then
begin
 dKia1:= delst*sqrt(pi*a1)*((0.6865/(0.2772+(a1-r)/r))+0.9439);
end;
If Interact = 1 then
begin
 Intfactor;
end;
If Interact = 2 then
begin
 For x:= 1 to Nmsd Do
 begin
  For y:= 1 to 2 Do
  begin
   delKf[x,y]:= delKi[x,y];
  end;
 end;
 For y:= 1 to 2 Do
 begin
```

```
      dKfa2[y]:= dKia2[y];
    end;
    dKfa1:= dKia1;
  end;
End;


Procedure CalcdadN;
(* This procedure uses the Paris Law to calculate a da/dN ratio
   for each crack tip in the specimen. The da/dN ratio is based
   on the computed stress intensity factor and the Paris Law
   material constants                              *)

Var
  x,y: integer;

Begin
  For x:= 1 to Nmsd Do
  begin
    For y:= 1 to 2 Do
    begin
      dadn[x,y]:= C*Power(delKf[x,y],M);
    end;
  end;
  For x:= 1 to 2 Do
  begin
    dadna2[y]:= C*Power(dKfa2[y],M);
  end;
  dadna1:=C*Power(dKfa1,M);
End;



Procedure Growcracks;
(* This procedure grows a designated number of cycles based on
   a percentage of the smallest crack within the specimen     *)

Var
  x,y: integer;
  grow,small,dadnsm: real;

Begin
  small:= 10;
  For x:= 1 to Nmsd Do
  begin
    For y:= 1 to 2 Do
    begin
      If small>= Hole[x,y] Then
      begin
        small:= Hole[x,y];
        dadnsm:= dadn[x,y];
      end;
    end;
  end;
```

```
  grow:= percent*small;
  delcycle:= grow/dadnsm;
  cycle:= cycle+delcycle;
  For x:= 1 to Nmsd Do
  begin
    For y:= 1 to 2 Do
    begin
      da[x,y]:= dadn[x,y]*delcycle;
      Hole[x,y]:= Hole[x,y]+da[x,y];
      crack[x,y]:= crack[x,y]+da[x,y];
    end;
  end;
  For x:= 1 to 2 Do
  begin
    daa2[x]:= dadna2[x]*delcycle;
    a2d[x]:= a2d[x]+daa2[x];
    a2:= a2d[x];
  end;
  daa1:= dadna1*delcycle;
  a1:= a1+daa1;
End;

Procedure Print;
(* This procedure is used to print intermediate results of the
   fatigue life of the specimen.  It is also used to print the
   final results after failure has occured in the specimen     *)

Var
  x,y: integer;
  nst,nstsi,sum: real;
  Icycle,Fcycle: real;

Begin
  If fail = 1 Then (*True *)
  begin
    Fcycle:= cycle;
    Writeln;
    Writeln;
    Writeln;
    Writeln('************************************************************');
    Writeln;
    Writeln('              FINAL DATA FOR EACH HOLE                   ');
    Writeln;
    Writeln ('Failure of this specimen occured after ', Fcycle:8:0, ' cycles');
    Writeln;
    Writeln;
    Writeln (' MSD Hole Number     Left Side     Right Side ');
    For x:= 1 to Nmsd Do
    begin
      Writeln ('       ',x,'          ', crack[x,1]:8:4,'      ',crack[x,2]:8:4);
    end;
    Writeln;
    Writeln ('The lead crack length at fracture was (in) ', a2:4:4);
    Writeln(outfile);
```

```
 Writeln(outfile);
 Writeln(outfile);
 Writeln(outfile,'**********************************************************');
 Writeln(outfile);
 Writeln(outfile,'          FINAL DATA FOR EACH HOLE              ');
 Writeln(outfile);
 Writeln(outfile,'Failure of this specimen occured after ', Fcycle:8:0, ' cycles');
 Writeln(outfile);
 Writeln(outfile);
 Writeln (outfile,' MSD Hole Number    Left Side    Right Side ');
 For x:= 1 to Nmsd Do
 begin
  Writeln (outfile,'      ',x,'          ', crack[x,1]:8:4,'     ',crack[x,2]:8:4);
 end;
 Writeln(outfile);
 Writeln (outfile,'The lead crack length at fracture was  ', a2:4:4);
end;
If fail = 2 Then  (* False *)
begin
 If (chold + thresh) <= cycle Then
 begin
  chold:= cycle;
  Icycle:= cycle;
  sum:= 0;
  For x:= 1 to Nmsd Do
  begin
   For y:= 1 to 2 Do
   begin
   sum:= sum+crack[x,y];
   end;
  end;
  nst:= Pmax/((W-sum-2*a2-d*Nmsd)*th);
  nstsi:= nst* 6.8947;
  Writeln;
  Writeln;
  Writeln;
  Writeln ('This intermediate output occured at ', Icycle:8:0, ' cycles');
  Writeln;
  Writeln ('The net section stress is now ', nst:8:3,' (ksi) or ', nstsi:8:3,' MPa ');
  Writeln;
  Writeln (' MSD Hole Number    Left Side    Right Side ');
  For x:= 1 to Nmsd Do
  begin
   Writeln ('      ',x,'          ', crack[x,1]:8:4,'     ',crack[x,2]:8:4);
  end;
  Writeln;
  Writeln ('The half lead crack length is now (in) ', a2:4:4);
  Writeln(outfile);
  Writeln(outfile);
  Writeln(outfile);
  Writeln (outfile,'This intermediate output occured at ', Icycle:8:0, ' cycles');
  Writeln(outfile);
  Writeln (outfile,'The net section stress is now ', nst:8:3,' (ksi) or ', nstsi:8:3,' MPa ');
  Writeln(outfile);
```

```
    Writeln (outfile,' MSD Hole Number     Left Side     Right Side ');
    For x:= 1 to Nmsd Do
    begin
      Writeln (outfile,'      ',x,'          ', crack[x,1]:8:4,'     ',crack[x,2]:8:4);
    end;
    Writeln(outfile);
    Writeln (outfile,'The half lead crack length is now  ', a2:4:4);
   end;
  end;
End;

Procedure NetLig;
(* This procedure is used to compute a predicted failure load based
   on the net ligament loss criterion. It compares the max cyclic
   load with the predicted failure load to determine if the specimen
   has failed *)

Var
  x,y:integer;
  Pnet,length,L: real;

Begin
  length:= 0;
  For x:= 1 to Nmsd Do
  begin
   For y:= 1 to 2 Do
   begin
     length:= length + crack[x,y];
   end;
  end;
  L:= length/(2*Nmsd);
  Pnet:= yst*(W-2*a2-Nmsd*d-2*Nmsd*L)*th;
  If Pmax>= Pnet Then
  begin
   fail:= 1;
  end;
  Print;
End;


Procedure FracMech;
(* This procedure is used to compute a predicted failure load based
   on the fracture mechanics criterion. It compares the max cyclic
   load with the predicted failure load to determine if the specimen
   has failed *)

Var
  x:integer;
  Pkapp: real;
  temp,temp2,temp3: real;

Begin
  temp:= pi*a2/W;
  temp2:= cos(temp);
```

```
 temp3:= abs(temp2);
 Pkapp:= (Kapp*W*th)/((sqrt(pi*a2))*(sqrt(1/temp3)));
 If Pmax>= Pkapp Then
 begin
  fail:= 1;
 end;
 Print;
End;



Procedure Swift;
(* This procedure is used to compute a predicted failure load based
   on the Swift criterion.  It compares the max cyclic
   load with the predicted failure load to determine if the specimen
   has failed *)

Var
 x,y: integer;
 Pswift,g,Wnet,Bh,Bhs,Btemp,Bi1,Bi2,length,L: real;
 a,b,t,temp,kfac,fac: real;

Begin
 length:= 0;
 For x:= 1 to Nmsd Do
 begin
  For y:= 1 to 2 Do
  begin
   length:= length + crack[x,y];
  end;
 end;
 L:= length/(2*Nmsd);
 Wnet:= W-Nmsd*d-2*Nmsd*L;
 g:= delh-a2-a1;
 Bh:= (0.6865/(0.2772+(a1-r)/r))+0.9439;
 Btemp:= Power(Bh,2);
 Bhs:= sqrt(Btemp*(a1-r)/a1);
 a:= a2;
 b:= a1;
 t:= delh-a2-a1;
 If t>0 then
 begin
  temp:= (a*b)/(((2*a)+t)*((2*b)+t));
  kfac:= 2*sqrt(temp);
  fac:= (cel(kfac,1,1,1)-cel(kfac,1,1,kfac*kfac))/cel(kfac,1,1,1);
  Bi1:= sqrt(1+(2*a/t))*(1-(1+t/(2*b))*fac);
  Bi2:= sqrt(1+(2*b/t))*(1-(1+t/(2*a))*fac);
  Bi1:= abs(Bi1);
  Bi2:= abs(Bi2);
 end
 else
 begin
  Bi1:= 1;
```

```
  Bi2:= 1;
 end;
 Pswift:=yst*th*Wnet*sqrt(g/(a1*Power(Bhs,2)*Power(Bi1,2)+a2*Power(Bi2,2)));
 If Pmax>= Pswift Then
 begin
  fail:= 1;
 end;
 Print;
End;

BEGIN (*Main, this executes the program*)
 Writeln('Enter filename:');
 readln(filename);
 assign(outfile, 'c:\data\mark\'+filename+'.dat');
 rewrite(outfile);
 assign (infile, 'c:\data\mark\fat1c.dat');
 reset (infile);
 Getinfo;
 If mode= 1 Then
 Begin
  Repeat
   NetLig;
   If fail = 2 then
   begin
    InitK;
    CalcdadN;
    Growcracks;
   end;
  Until fail = 1;
 End;
 If mode= 2 Then
 Begin
  Repeat
   FracMech;
   If fail = 2 then
   begin
    InitK;
    CalcdadN;
    Growcracks;
   end;
  Until fail = 1;
 End;
 If mode= 3 Then
 Begin
  Repeat
   Swift;
   If fail = 2 then
   begin
    InitK;
    CalcdadN;
    Growcracks;
   end;
  Until fail = 1;
 End;
```

```
  Close(outfile);
  Close(infile);
END. (*Main*)
```

Appendix B: FAT 01C Input/ Output File

The following is an example input and output file used for the FAT 01C specimen which had a lead crack with MSD. This file uses the Swift criterion with no crack interaction to predict fatigue life.

What is the materials modulus of elasticity in ksi?
10000.00
Enter the specimens width (in)
15.00
Enter the specimens thickness (in)
0.04
Enter the spacing between holes from center to center (in)
0.75
Enter the materials yield stress (ksi)
42.00
Enter the materials ultimate stress (ksi)
58.00
Enter the materials approximate stress concentration factor (ksi sqrt in)
75.72
Enter the diameter of the holes used in the specimens (in)
0.1250
Enter the maximum remote stress used to cycle the specimens (ksi)
10.83
Enter the minimum remote stress used to cycle the specimens (ksi)
2.58
Enter the first da/dn point used to determine Paris Law Coeffs
0.00000158
Enter the delta K corresponding to the first point
7.11
Enter the second da/dn point used to determine Paris Law Coeffs
0.00003830
Enter the delta K corresponding to the second point
19.40
Enter the number of holes with MSD
12
Enter the half crack length of the lead crack
2.3365
Enter the number of holes the lead crack encompasses
7
Enter the crack length of the left 1 hole crack
measured from the hole edge (in) hole numbers progress
from the left side of the panel to the right side
0.0586
Is this crack adjacent to the lead crack y or n ?
n
Enter the crack length of the right 1 hole crack
measured from the hole edge (in)
0.0442
Is this crack adjacent to the lead crack y or n ?
n
Enter the crack length of the left 2 hole crack
measured from the hole edge (in) hole numbers progress
from the left side of the panel to the right side
0.0467
Is this crack adjacent to the lead crack y or n ?
n
Enter the crack length of the right 2 hole crack
measured from the hole edge (in)
0.0392

Is this crack adjacent to the lead crack y or n ?
n
Enter the crack length of the left 3 hole crack
measured from the hole edge (in) hole numbers progress
from the left side of the panel to the right side
0.0512
Is this crack adjacent to the lead crack y or n ?
n
Enter the crack length of the right 3 hole crack
measured from the hole edge (in)
0.0370
Is this crack adjacent to the lead crack y or n ?
n
Enter the crack length of the left 4 hole crack
measured from the hole edge (in) hole numbers progress
from the left side of the panel to the right side
0.0346
Is this crack adjacent to the lead crack y or n ?
n
Enter the crack length of the right 4 hole crack
measured from the hole edge (in)
0.0525
Is this crack adjacent to the lead crack y or n ?
n
Enter the crack length of the left 5 hole crack
measured from the hole edge (in) hole numbers progress
from the left side of the panel to the right side
0.0464
Is this crack adjacent to the lead crack y or n ?
n
Enter the crack length of the right 5 hole crack
measured from the hole edge (in)
0.0375
Is this crack adjacent to the lead crack y or n ?
n
Enter the crack length of the left 6 hole crack
measured from the hole edge (in) hole numbers progress
from the left side of the panel to the right side
0.0639
Is this crack adjacent to the lead crack y or n ?
n
Enter the crack length of the right 6 hole crack
measured from the hole edge (in)
0.0688
Is this crack adjacent to the lead crack y or n ?
y
Is this the largest adjacent crack to the lead crack?
y
Enter the crack length of the left 7 hole crack
measured from the hole edge (in) hole numbers progress
from the left side of the panel to the right side
0.0306
Is this crack adjacent to the lead crack y or n ?
y

Is this the largest adjacent crack to the lead crack?
n
Enter the crack length of the right 7 hole crack
measured from the hole edge (in)
0.0464
Is this crack adjacent to the lead crack y or n ?
n
Enter the crack length of the left 8 hole crack
measured from the hole edge (in) hole numbers progress
from the left side of the panel to the right side
0.0489
Is this crack adjacent to the lead crack y or n ?
n
Enter the crack length of the right 8 hole crack
measured from the hole edge (in)
0.0364
Is this crack adjacent to the lead crack y or n ?
n
Enter the crack length of the left 9 hole crack
measured from the hole edge (in) hole numbers progress
from the left side of the panel to the right side
0.0477
Is this crack adjacent to the lead crack y or n ?
n
Enter the crack length of the right 9 hole crack
measured from the hole edge (in)
0.0715
Is this crack adjacent to the lead crack y or n ?
n
Enter the crack length of the left 10 hole crack
measured from the hole edge (in) hole numbers progress
from the left side of the panel to the right side
0.0424
Is this crack adjacent to the lead crack y or n ?
n
Enter the crack length of the right 10 hole crack
measured from the hole edge (in)
0.0340
Is this crack adjacent to the lead crack y or n ?
n
Enter the crack length of the left 11 hole crack
measured from the hole edge (in) hole numbers progress
from the left side of the panel to the right side
0.0601
Is this crack adjacent to the lead crack y or n ?
n
Enter the crack length of the right 11 hole crack
measured from the hole edge (in)
0.0360
Is this crack adjacent to the lead crack y or n ?
n
Enter the crack length of the left 12 hole crack
measured from the hole edge (in) hole numbers progress
from the left side of the panel to the right side

0.0356
Is this crack adjacent to the lead crack y or n ?
n
Enter the crack length of the right 12 hole crack
measured from the hole edge (in)
0.0331
Is this crack adjacent to the lead crack y or n ?
n
Enter the percentage of the length of the smallest hole with MSD
you want to grow the cracks in the panel (used as a stepsize).
Use 10 for 10%
0.10
Enter the failure criteria to be used in the analysis
1 - Net Ligament Loss 2 - Fracture mechanics 3 - Swift
3
Do you want crack interaction factors to be considered ?
Enter 1 - for yes and 2 - for no
2

This intermediate output occured at 1192 cycles

The net section stress is now 21.473 (ksi) or 148.053 MPa

MSD Hole Number	Left Side	Right Side
1	0.0593	0.0448
2	0.0473	0.0398
3	0.0518	0.0375
4	0.0351	0.0532
5	0.0470	0.0380
6	0.0646	0.0695
7	0.0310	0.0470
8	0.0496	0.0369
9	0.0483	0.0723
10	0.0430	0.0345
11	0.0608	0.0365
12	0.0361	0.0336

The half lead crack length is now 2.4087

This intermediate output occured at 2382 cycles

The net section stress is now 21.958 (ksi) or 151.393 MPa

MSD Hole Number	Left Side	Right Side
1	0.0600	0.0453
2	0.0479	0.0403
3	0.0525	0.0380
4	0.0356	0.0538
5	0.0476	0.0385
6	0.0654	0.0703

7	0.0315	0.0476
8	0.0502	0.0374
9	0.0489	0.0731
10	0.0435	0.0350
11	0.0615	0.0370
12	0.0366	0.0341

The half lead crack length is now 2.4850

This intermediate output occured at 3568 cycles

The net section stress is now 22.494 (ksi) or 155.088 MPa

MSD Hole Number	Left Side	Right Side
1	0.0607	0.0459
2	0.0485	0.0409
3	0.0531	0.0386
4	0.0361	0.0545
5	0.0482	0.0391
6	0.0661	0.0711
7	0.0320	0.0482
8	0.0508	0.0379
9	0.0495	0.0739
10	0.0441	0.0355
11	0.0622	0.0375
12	0.0371	0.0346

The half lead crack length is now 2.5660

****

FINAL DATA FOR EACH HOLE

Failure of this specimen occured after 4042 cycles

MSD Hole Number	Left Side	Right Side
1	0.0610	0.0462
2	0.0487	0.0411
3	0.0534	0.0388
4	0.0363	0.0547
5	0.0484	0.0393
6	0.0664	0.0714
7	0.0321	0.0484
8	0.0510	0.0381
9	0.0498	0.0743
10	0.0443	0.0357
11	0.0625	0.0377
12	0.0373	0.0348

The lead crack length at fracture was 2.5998

Appendix C: Fatigue Life Data

The following are plots of results of fatigue life experiments performed in this study. Plots including measured and predicted fatigue life are presented for the four fatigue specimens tested in this study.

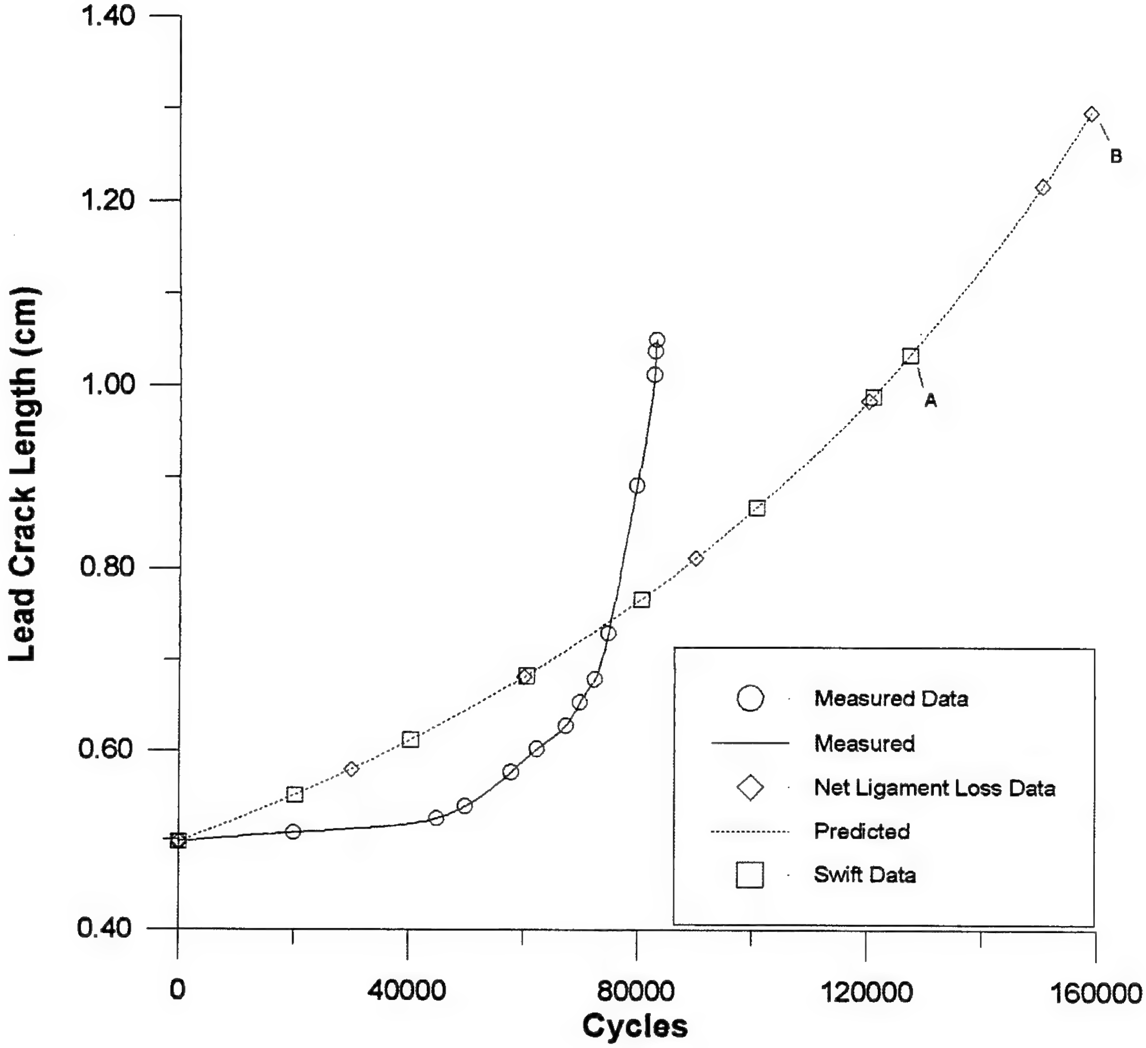

Note: A - maximum predicted fatigue life with Swift criterion
B - maximum predicted fatigue life with Net Ligament Loss criterion

Figure 22. **Specimen FAT 01A**: Fatigue Life Results, No Crack Interaction Effects

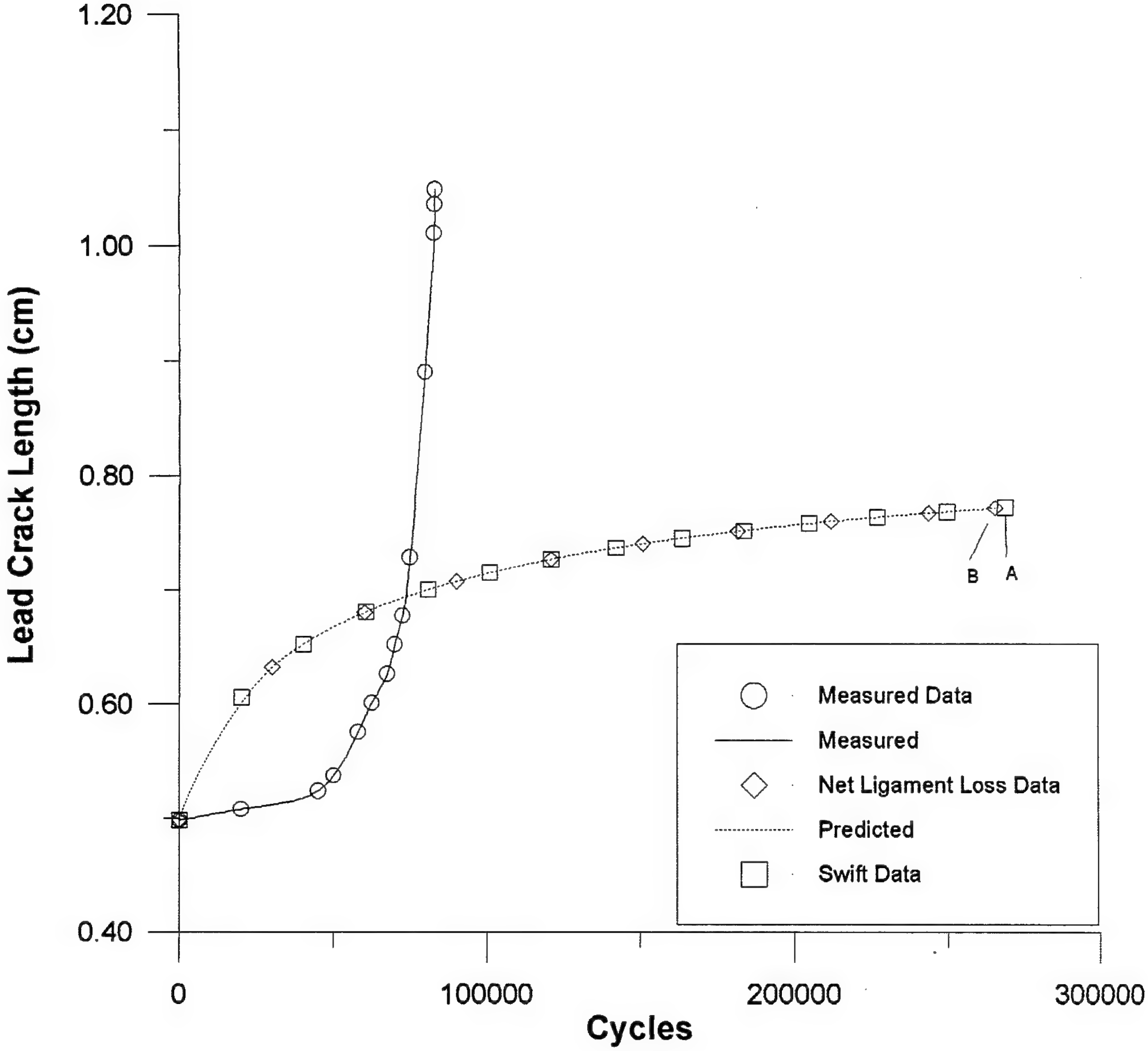

Note: A - maximum predicted fatigue life with Swift criterion
B - maximum predicted fatigue life with Net Ligament Loss criterion

Figure 23. **Specimen FAT 01A**: Fatigue Life Results, With Crack Interaction Effects

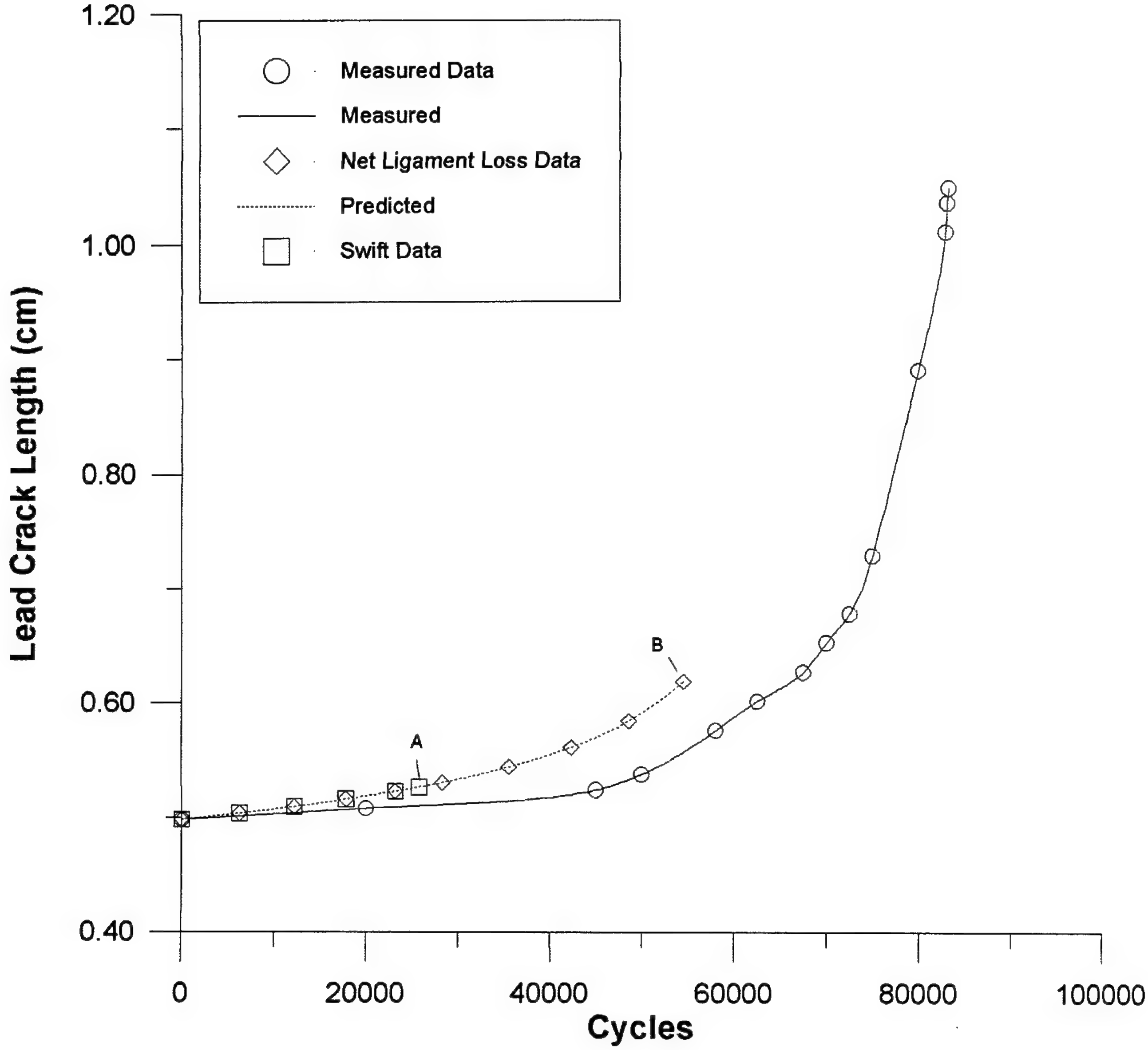

Note: A - maximum predicted fatigue life with Swift criterion
B - maximum predicted fatigue life with Net Ligament Loss criterion

Figure 24. **Specimen FAT 01A**: Fatigue Life Results, With Interaction Effects 40% (t)

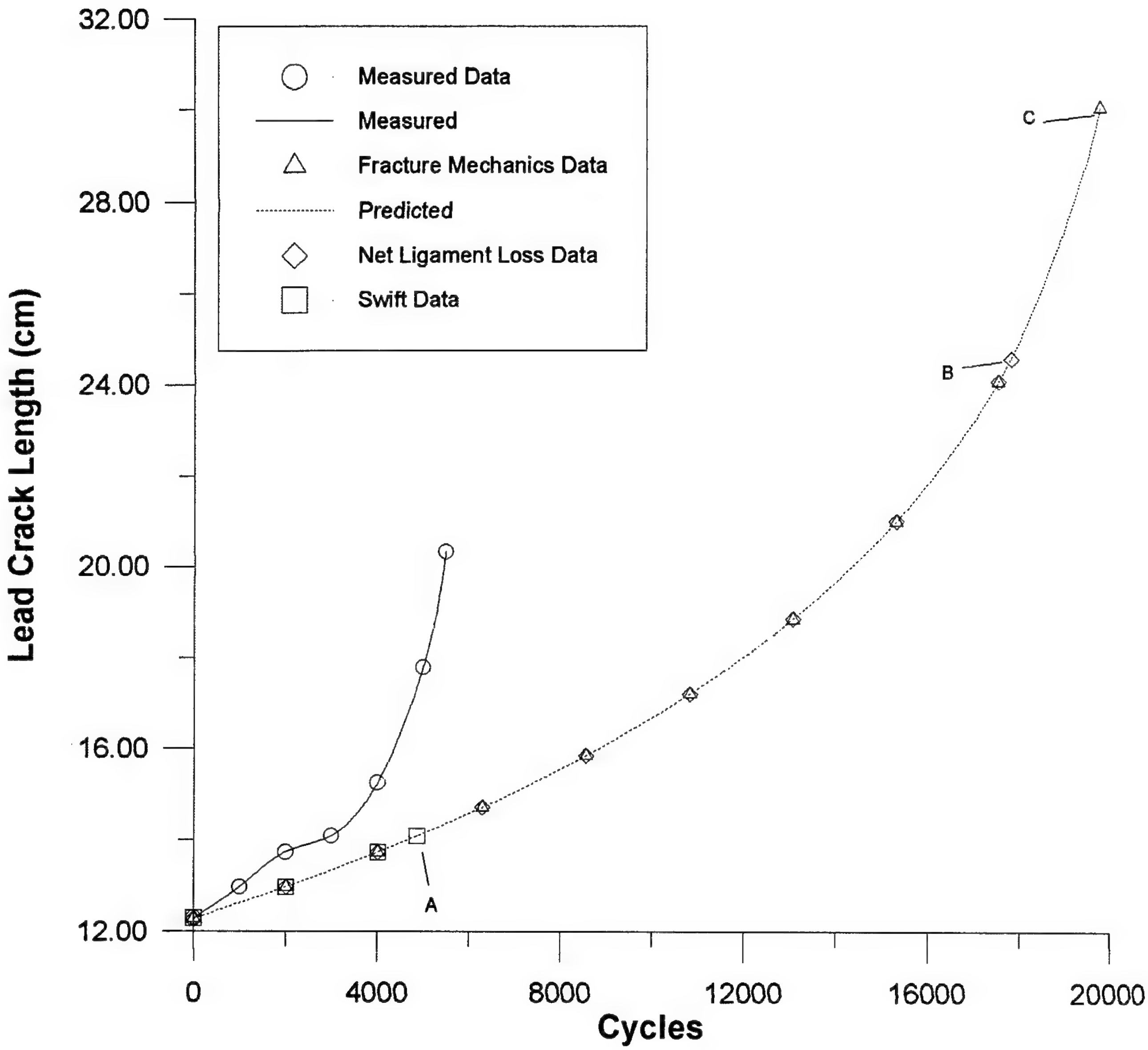

Note: A - maximum predicted fatigue life with Swift criterion
B - maximum predicted fatigue life with Net Ligament Loss criterion
C - maximum predicted fatigue life with Fracture Mechanics criterion

Figure 25. **Specimen FAT 01B**: Fatigue Life Results, No Crack Interaction Effects

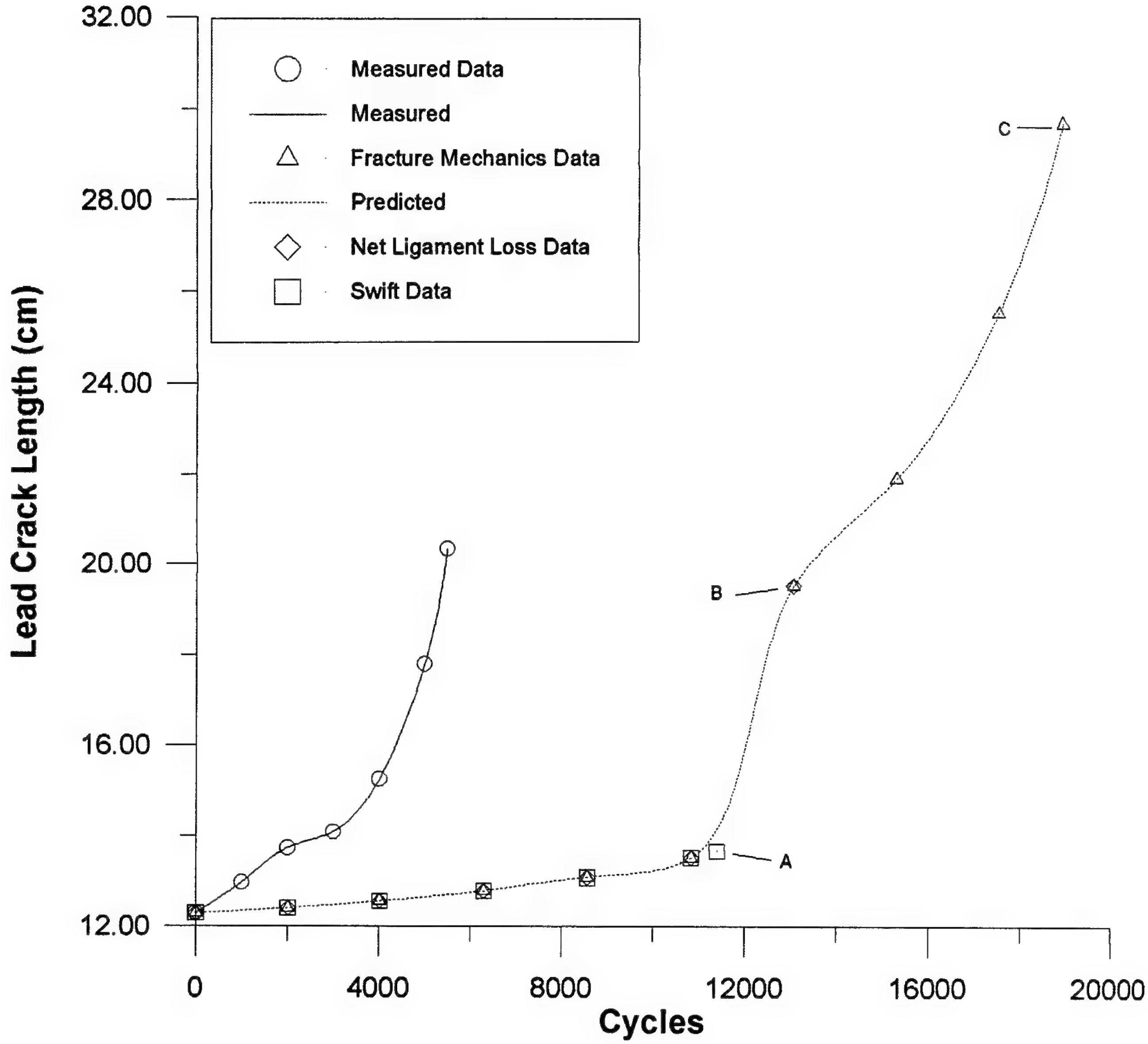

Note: A - maximum predicted fatigue life with Swift criterion
B - maximum predicted fatigue life with Net Ligament Loss criterion
C - maximum predicted fatigue life with Fracture Mechanics criterion

Figure 26. **Specimen FAT 01B**: Fatigue Life Results, With Crack Interaction Effects

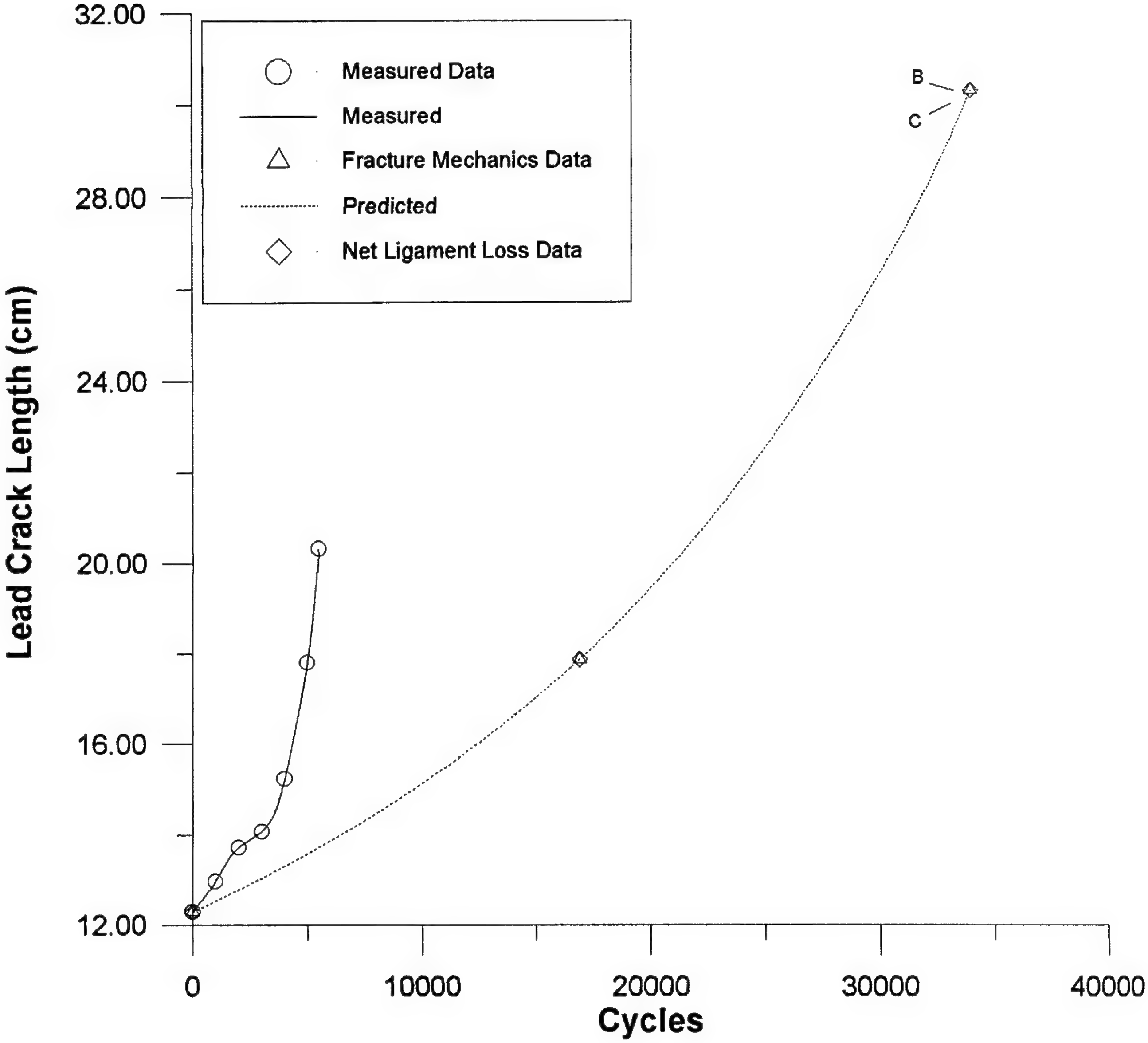

Note: B - maximum predicted fatigue life with Net Ligament Loss criterion
C - maximum predicted fatigue life with Fracture Mechanics criterion

Figure 27. **Specimen FAT 01B**: Fatigue Life Results, With Interaction Effects 40% (t)

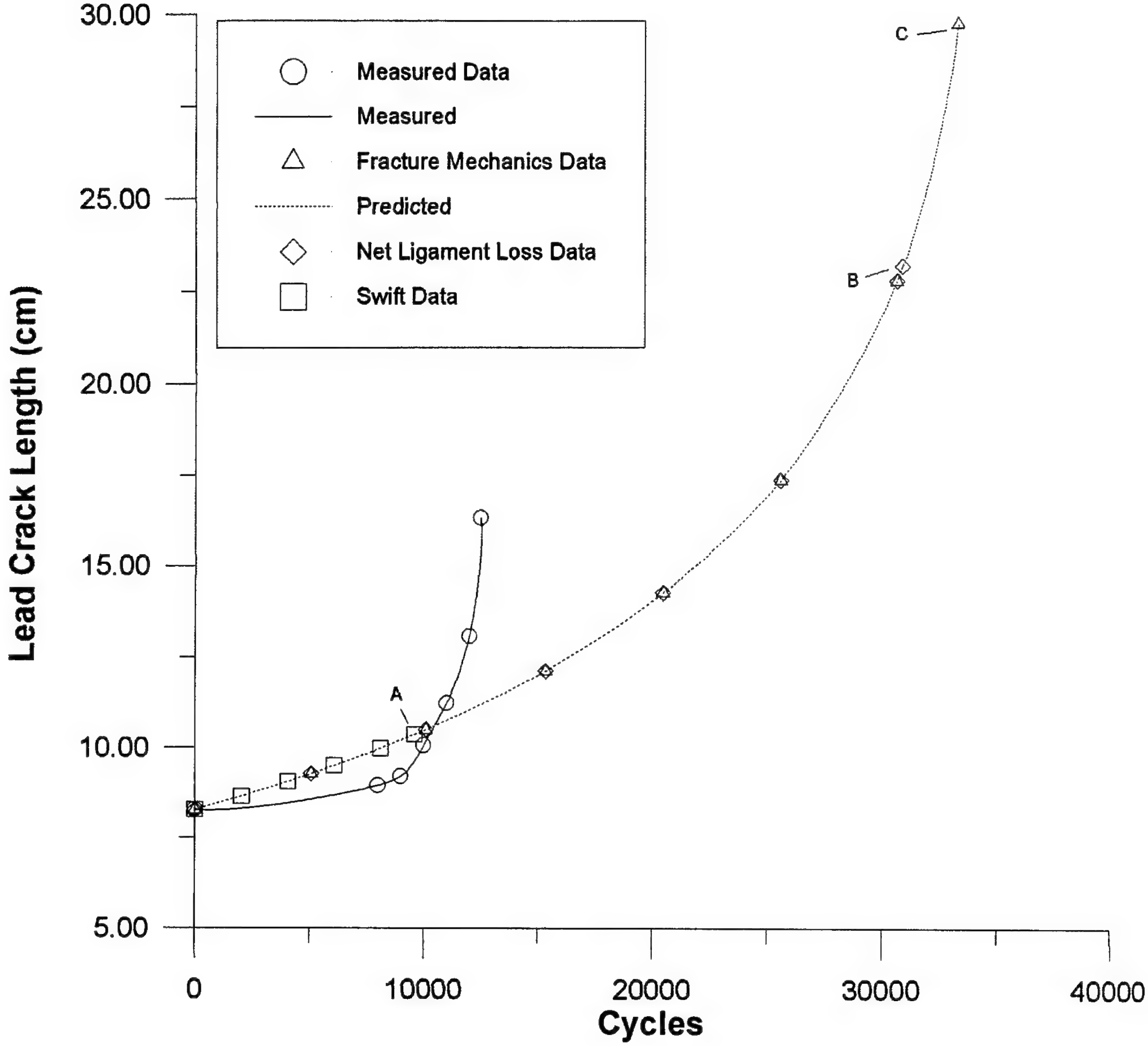

Note: A - maximum predicted fatigue life with Swift criterion
B - maximum predicted fatigue life with Net Ligament Loss criterion
C - maximum predicted fatigue life with Fracture Mechanics criterion

Figure 28. **Specimen FAT 02B**: Fatigue Life Results, No Crack Interaction Effects

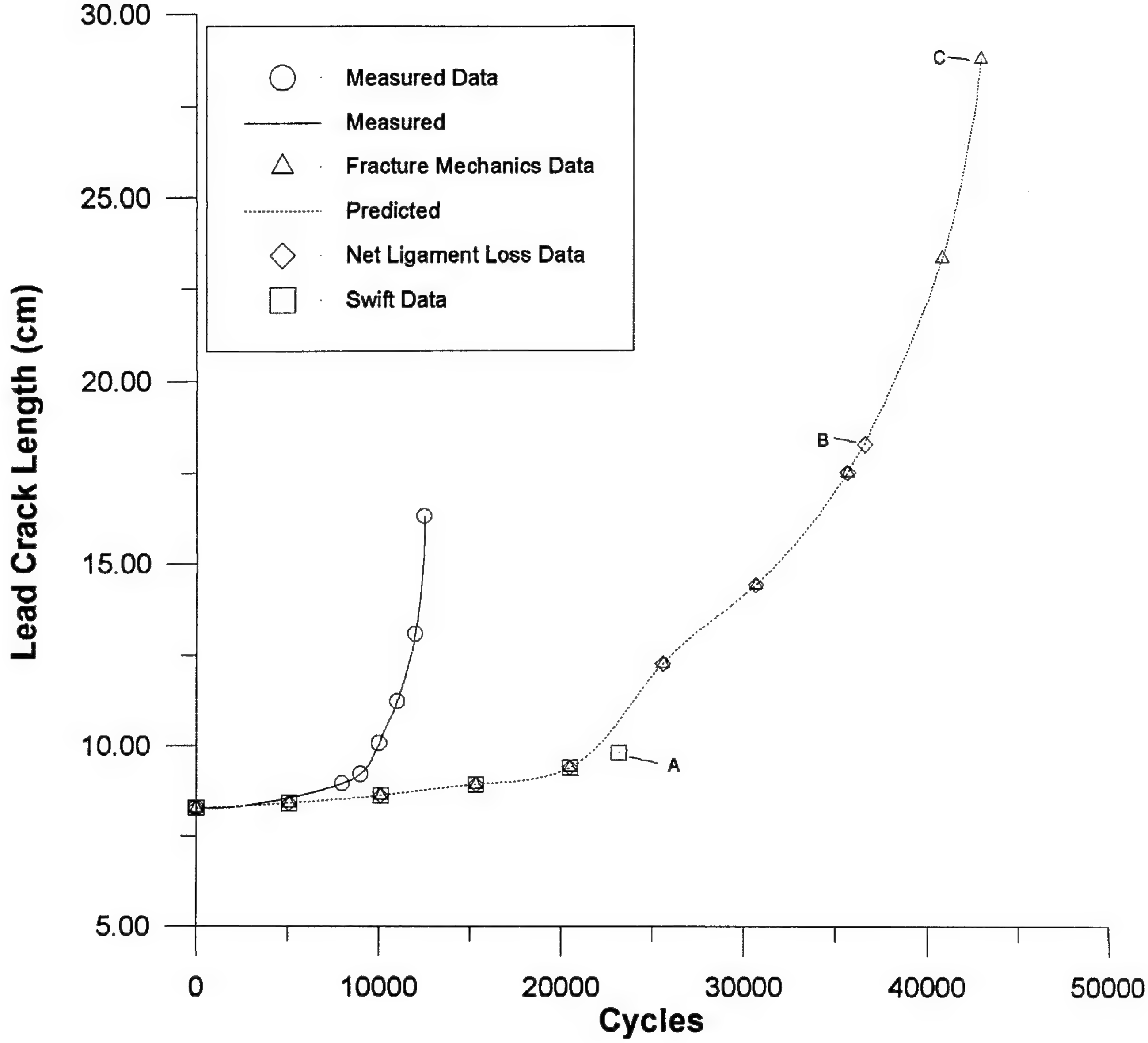

Note: A - maximum predicted fatigue life with Swift criterion
B - maximum predicted fatigue life with Net Ligament Loss criterion
C - maximum predicted fatigue life with Fracture Mechanics criterion

Figure 29. **Specimen FAT 02B**: Fatigue Life Results, With Crack Interaction Effects

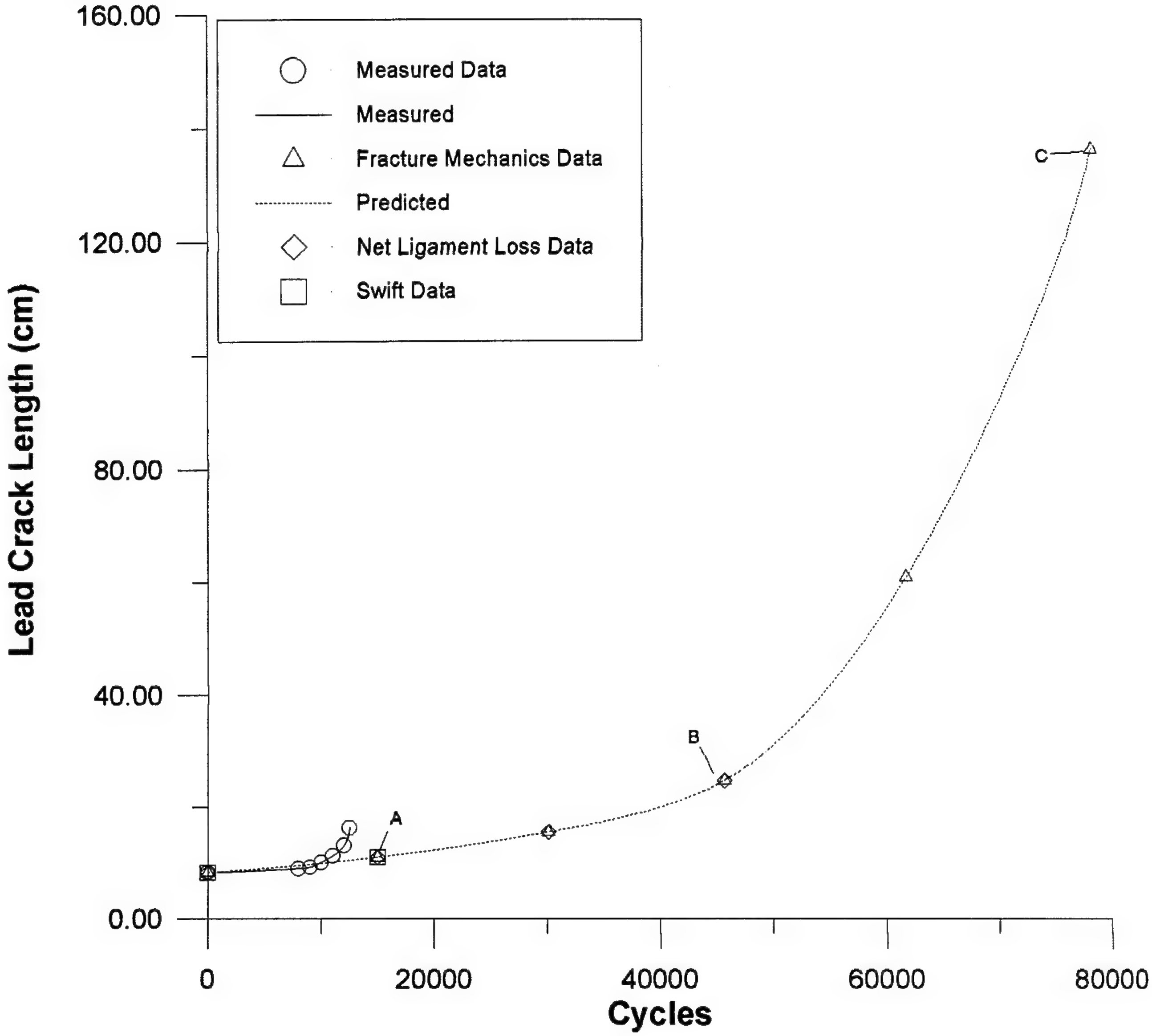

Note: A - maximum predicted fatigue life with Swift criterion
B - maximum predicted fatigue life with Net Ligament Loss criterion
C - maximum predicted fatigue life with Fracture Mechanics criterion

Figure 30. **Specimen FAT 02B**: Fatigue Life Results, With Interaction Effects 40% (t)

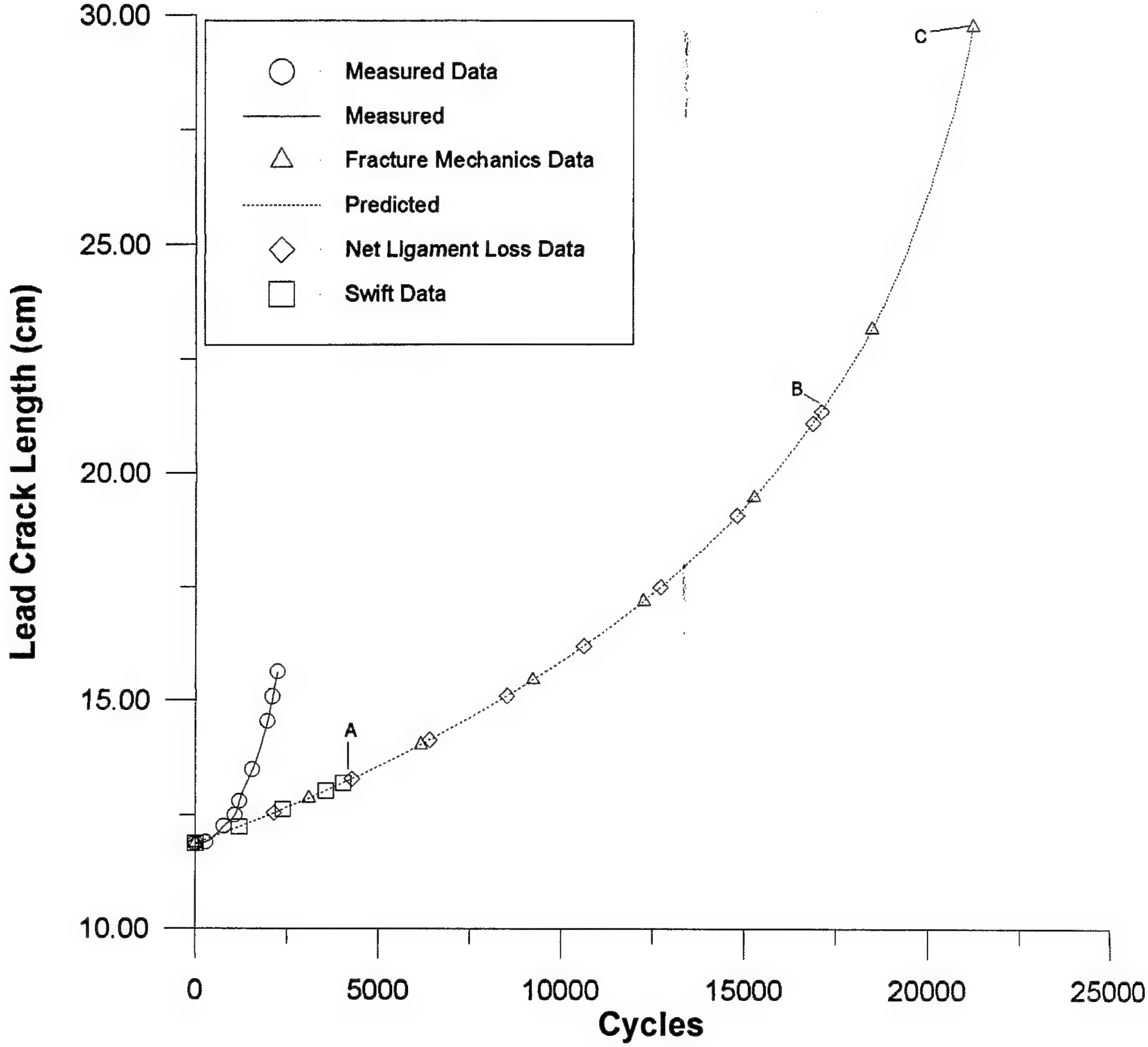

Note: A - maximum predicted fatigue life with Swift criterion
B - maximum predicted fatigue life with Net Ligament Loss criterion
C - maximum predicted fatigue life with Fracture Mechanics criterion

Figure 31. **Specimen FAT 01C**: Fatigue Life Results, No Crack Interaction Effects

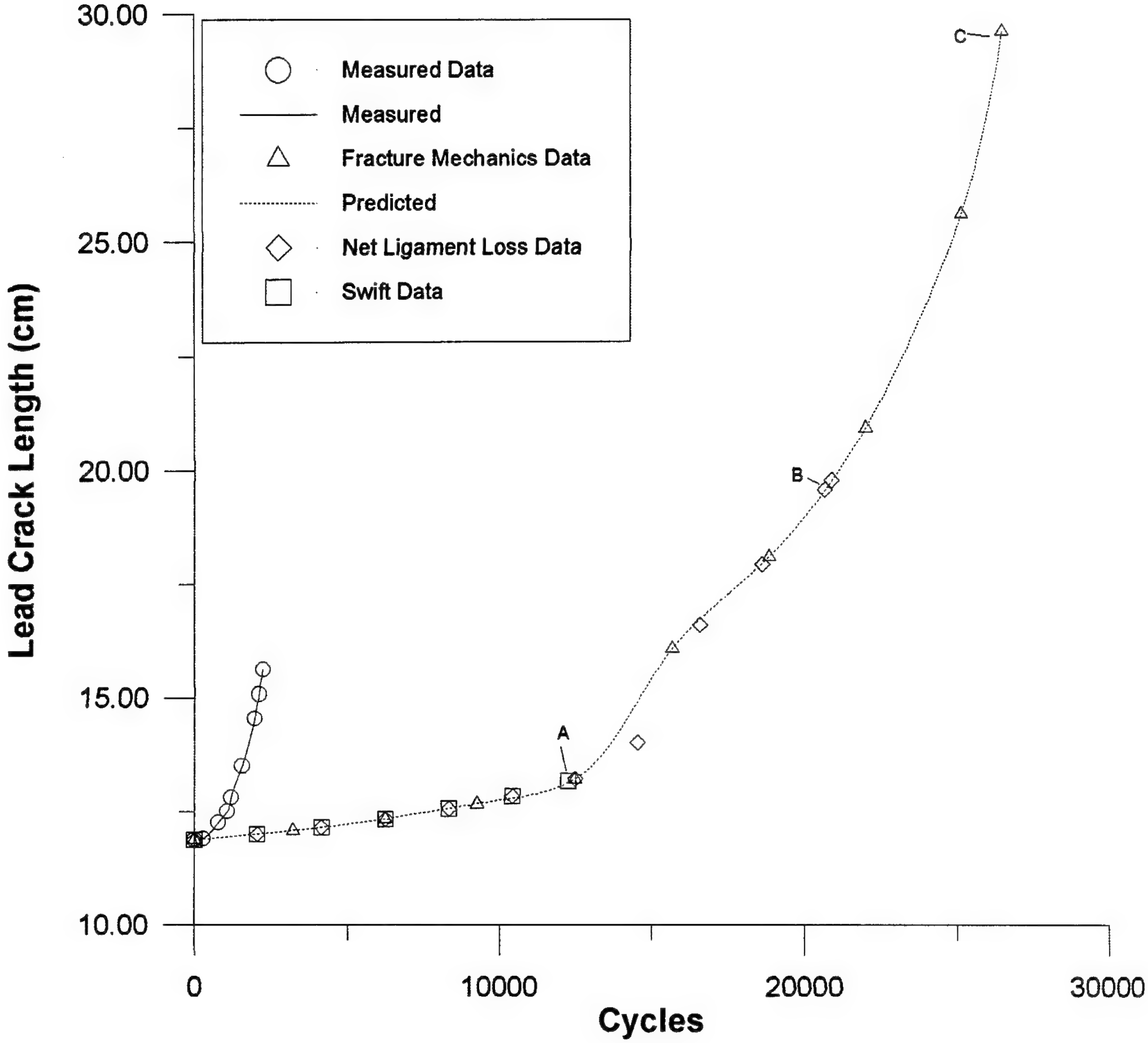

Note: A - maximum predicted fatigue life with Swift criterion
B - maximum predicted fatigue life with Net Ligament Loss criterion
C - maximum predicted fatigue life with Fracture Mechanics criterion

Figure 32. **Specimen FAT 01C**: Fatigue Life Results, With Crack Interaction Effects

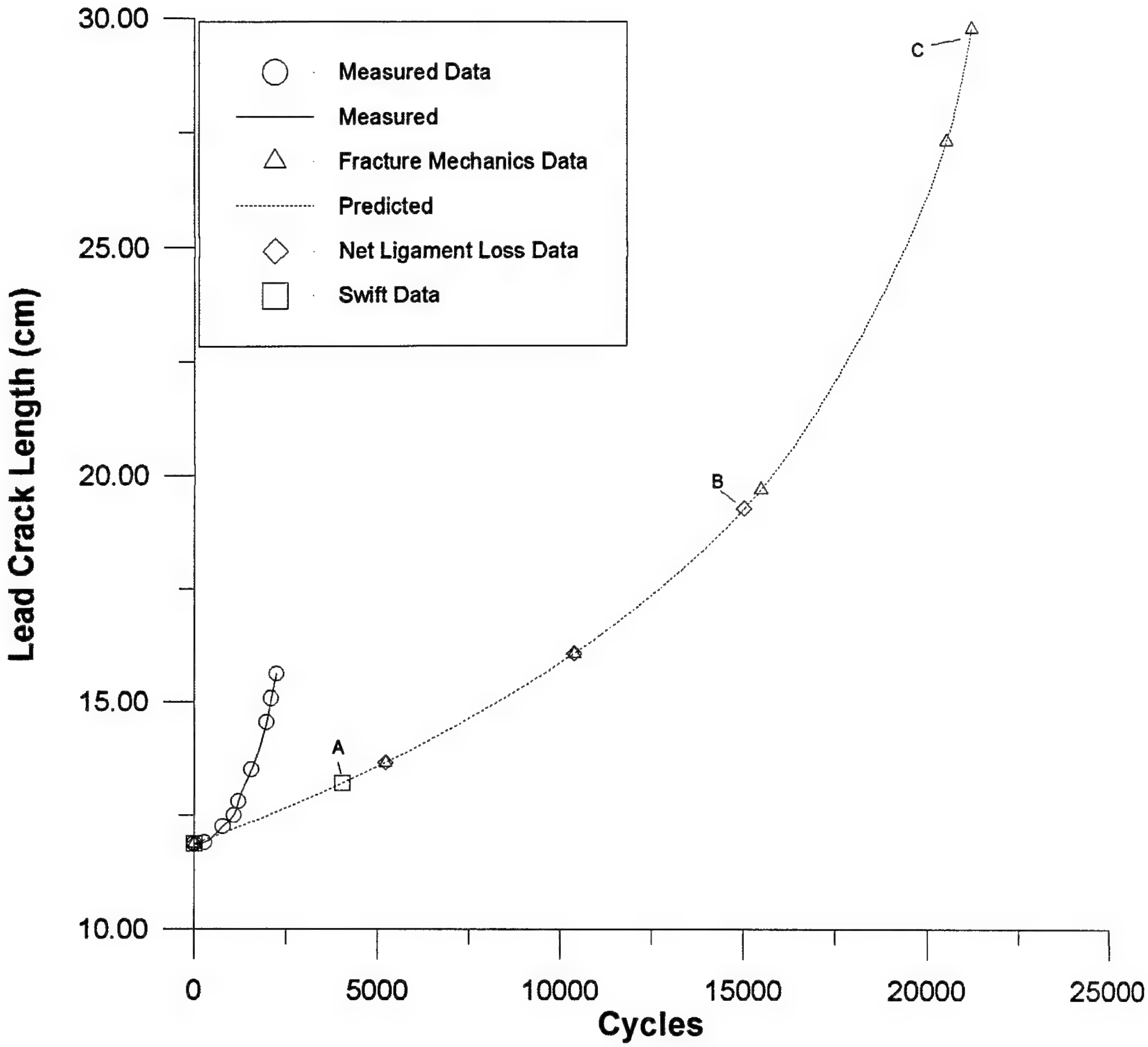

Note: A - maximum predicted fatigue life with Swift criterion
B - maximum predicted fatigue life with Net Ligament Loss criterion
C - maximum predicted fatigue life with Fracture Mechanics criterion

Figure 33. **Specimen FAT 01C**: Fatigue Life Results, With Interaction Effects 40% (t)

Appendix D: Moukawsher's (18) Results

The following are tables of results of experiments performed by Moukawsher on small specimens of 2024-T3. The tables of residual strength and fatigue results are presented for comparison with results of this study.

Table 14. **Moukawsher's Residual Strength Results**

Specimen	MSD/ Holes	Measured Load (ksi)	CALCULATED *P_{kapp} (ksi)	*P_{net} (ksi)	*P_{swift} Ult St (ksi)	*P_{swift} Flow St (ksi)	*P_{avgst} (ksi)	*P_{avgd} (ksi)
RS 01a	MSD	20.20	25.00	25.22	23.58	21.34	17.74	9.94
RS 01b	MSD	23.25	25.60	26.37	25.81	23.36	18.74	10.59
RS 01c	MSD	19.82	25.20	23.01	23.20	21.00	19.18	10.78
RS 04a	MSD	12.91	21.20	18.11	19.18	17.36	17.09	8.66
RS 04b	MSD	17.15	21.20	19.92	19.68	17.81	16.07	8.11
RS 04c	MSD	16.26	20.40	19.78	19.96	18.07	15.99	8.70
RS 04d	MSD	15.59	19.80	19.41	18.25	16.52	15.08	8.03

PERCENT ERROR* (%) Specimen	P_{kapp}	P_{net}	P_{swift} Ult	P_{swift} Fl	P_{avgst}	P_{avgd}
RS 01a	23.76	24.85	16.73	5.64	-12.18	-50.79
RS 01b	10.11	13.42	11.01	0.47	-19.40	-54.45
RS 01c	27.14	16.09	17.05	5.95	-3.23	-45.61
RS 04a	64.21	40.28	48.57	34.47	32.38	-32.92
RS 04b	23.62	16.15	14.75	3.85	-6.30	-52.71
RS 04c	25.46	21.65	22.76	11.13	-1.66	-46.49
RS 04d	27.00	24.50	17.06	5.97	-3.27	-48.49
Average Error for Type B specimens	28.76	22.42	21.13	9.64	-1.95	-47.35

* Equations 4, 6, 9, 11, 12, used to calculate predicted failure load

Table 15. **Moukawsher's (18) Fatigue Life Results**

Specimen	Measured Fat Life (cycles)	Best Prediction (cycles)
MSD 10	36020	44430
MSD 11	215680	257700
MSD 06	16853	24977
Specimen		Prediction
MSD 10		23.35
MSD 11		19.48
MSD 06		48.21
Average Error		30.35

Note: MSD10 has equivalent configuration as FAT 01A for this study
MSD 11 has equivalent configuration as FAT 01B and FAT 02B for this study
MSD 06 has equivalent configuration as FAT 01C for this study
Moukawsher did not state what failure criterion or interaction configuration was used to produce the most accurate predictions of fatigue life.

Bibliography

1. Actis, R. L., and Szabo, B. A. "Computation of Stress Intensity Factors for Panels with Multi-site Damage," Paper Presented at the U.S. Air Force Structural Integrity Conference, San Antonio, Texas, December 1992.

2. Atluri, S. N., and Tong, P. "Computational Schemes for Integrity Analyses of Fuselage Panels in Aging Airplanes," Structural Integrity of Aging Airplanes, S.N. Atluri, S.G. Sampath, P. Tong, Editors, Springer-Verlag, Berlin, Heidelberg, 1991.

3. Bannantine, J.A., Comer, J.J., and Handrock, J.L. *Fundamentals of Metal Fatigue Analysis*. Prentice Hall, New Jersey, 1990.

4. Broek, D. *Elementary Engineering Fracture Mechanics, Fourth Revised Edition*. Dordrecht: Kluwer Academic Press, 1991.

5. Cole, J., and Carey, S. "Jurassic Jets," Wall Street Journal, 3 November 1994.

6. Dawicke, D.S., and Newman, J. C. " Analysis and Prediction of Multiple-Site Damage (MSD) Fatigue Crack Growth," NASA Technical Paper 3231, 1992.

7. De la Motte, E. B., and Opalski, F. A. "MSD: Where We Are and Where We Should Go," Paper Presented at the U.S. Air Force Structural Integrity Conference, San Antonio, Texas, December 1993.

8. Derriso, M. "Static Program," Air Force Institute of Technology (AU), Wright-Patterson AFB, OH, 1993.

9. Dowling, N. E. "Notched Member Fatigue Life Predictions Combining Initiation and Propogation," Fracture of Engineering Materials and Structures, Vol 2, 1979, pp 129 - 138.

10. Fuchs, H. O., and Stephens, R. I. *Metal Fatigue in Engineering*. John Wiley & Sons, New York, 1980.

11. Gallagher, J. P., Dhar, S., Berens, A. P., and Burns, J. G. "A Comparison of Fracture Criteria for Crack Coalescence and Other Observations Based on Residual Strength Calculations," Paper Presented at the U.S. Air Force Structural Integrity Conference, San Antonio, Texas, December 1993.

12. Harris, C. E., and Heyman, J. S. "Overview of NASA Research Related to the Aging Commercial Transport Fleet," Journal of Aircraft, Vol. 30, No. 1, Jan.-Feb. 1993, pp. 64-68.

13. Jeong, D.Y., and Brewer, J.C. "On the Linkup of Multiple Cracks," Engineering Fracture Mechanics, Vol 51, No. 2, 1995, pp. 233-238.

14. Kamei, A., and Yokobori, T. "Two Collinear Asymmetrical Elastic Cracks," Report of the Research Institute for Strength and Fracture of Materials, Tohoku University, Vol. 10, Section 1-4, pp 41-42, December 1974.

15. Luzar, J. Engineer, Boeing Wichita, 28 March 1995.

16. Mar, J.W. "Structural Integrity of Aging Airplanes: A Perspective," Structural integrity of Aging Airplanes, S.N. Atluri, S.G. Sampath, P. Tong, Editors, Springer-Verlag, Berlin, Heidelberg, 1991.

17. "Metallic Materials and Elements for Aerospace Vehicle Structures," Mil-HDBK-5F, Department of Defense, Washington D.C., November 1990.

18. Moukawsher, E. J. "Fatigue Life and Residual Strength of Panels with Multiple Site Damage," Master of Science Thesis, Purdue University, 1282 Grissom Hall, West Lafayette, Indiana, 47907-1282, May 1993.

19. Newman, J. C., Dawicke, D. S., Sutton, M. A. Begelow C. A. "A Fracture Criterion for Widespread Cracking in Thin-Sheet Aluminum Alloys," Presented to International Committee on Aeronautical Fatigue, Stockholm, Sweden, June 1993.

20. Park, J.H., and Atluri, S. N. "Fatigue Growth of Multiple-Cracks Near a Row of Fastener-Holes in a Fuselage Lap-Joint," Paper Presented at the U.S. Air Force Structural Integrity Conference, San Antonio, Texas, December 1992.

21. Partl, O., Schijve, J. "Multiple-site-damage in 2024-T3 alloy sheet," Delft University of Technology Report LR-660. January 1992.

22. Rooke, D. P., and Cartwright, D. J. *Compendium of Stress Intensity Factors*. Her Majesty's Stationery Office, London, 1976.

23. Sanders, B. P. *Characterization of Fatigue Behavior in a Metal Matrix Composite (SCS-6/Ti-15-3) at Elevated Temperature*. Doctoral Dissertation, AFIT/DS/ENY/92J. School of Engineering, Air Force Institute of Technology (AU), Wright-Patterson AFB, OH, January 1992.

24. "Standard Test Method for Measurement of Fatigue Crack Growth Rates", ASTM E647-93, American Society for Testing and Materials, June 1993.

25. Stevens, K. K. *Statics and Strength of Materials*. Prentice-Hall, Inc., Englewood Cliffs, New Jersey, 1987.

26. Swift, T. "Damage Tolerance in Pressurized Fuselages', 11th Plantema Memorial Lecture, Presented at the 14th Symposium of the International Committee on aeronautical Fatigue (ICAF), Ottawa, Canada, June 1987.

27. Swift, T. "Effect of MSD on Residual Strength", from a presentation given at the U.S. Air Force Symposium on Multi-Site Damage, February 1992.

28. Swift, T. "Widespread Fatigue Damage Monitoring Issues and Concerns," Paper Presented at the 5th International Conference on Structural Airworthiness of New and Aging Aircraft, Hamburg, Germany, June 1993.

29. "Test Methods of Tension Testing of Metallic Materials", ASTM E8-94C, American Society for Testing and Materials, July 1994.

30. Tong, P., Arin, K., Jeong, D.Y., Greif, R., Brewer, J.C., and Bobo, S.N., "Current DOT Research on the Effect of Multiple Site Damage on Structural Integrity," Paper Presented at 1991 International Conference on Aging Aircraft and Structural Airworthiness, 19 - 21 Nov 1991.

Vita

Captain Mark C. Cherry was born 6 September 1969 in Limestone, Maine. He graduated from Robinson High School, in Fairfax, Virginia, in 1987. That summer he entered the United States Air Force Academy where he graduated with a degree of Bachelors of Science in Engineering Mechanics. Upon his graduation from USAFA in 1991, he was assigned to Maxwell AFB Gunter Annex in Montgomery, Alabama. There he served as the Deputy Program Manager for Requirements for the Air Force Command and Control Networking System Program Office. He entered the Air Force Institute of Technology in July 1994.

Permanent Address: 30 Knob Hill St.
Sharon, MA 02067

REPORT DOCUMENTATION PAGE

Form Approved
OMB No. 0704-0188

1. AGENCY USE ONLY *(Leave blank)*

2. REPORT DATE
December 1995

3. REPORT TYPE AND DATES COVERED
Master's Thesis

4. TITLE AND SUBTITLE
INVESTIGATION OF RESIDUAL STRENGTH AND FATIGUE LIFE OF UNSTIFFINED ALUMINUM PANELS WITH MULTIPLE SITE DAMAGE

5. FUNDING NUMBERS

6. AUTHOR(S)
Mark C. Cherry, Captain, USAF

7. PERFORMING ORGANIZATION NAME(S) AND ADDRESS(ES)
Air Force Institute of Technology, WPAFB, OH 45433-6583

8. PERFORMING ORGANIZATION REPORT NUMBER
AFIT/GAE/ENY/95D-06

9. SPONSORING/MONITORING AGENCY NAME(S) AND ADDRESS(ES)

WL/FIBEC
Wright-Patterson AFB, OH 45433

10. SPONSORING/MONITORING AGENCY REPORT NUMBER

11. SUPPLEMENTARY NOTES

12a. DISTRIBUTION/AVAILABILITY STATEMENT

Approved for public release; Distribution Unlimited

12b. DISTRIBUTION CODE

13. ABSTRACT *(Maximum 200 words)*

This study investigated the effects of Multiple Site Damage (MSD) on unstiffined panels of 2024-T3 Aluminum 1.016 mm (0.04 in) thick. The objective of the study was to test the validity of the available analytical methods to predict the residual strength and fatigue life of panels with MSD. Residual strengths of large specimens with MSD were measured in two different configurations to test the applicability of five failure criteria. These configurations were prepared by either fatiguing MSD damage, or simulating fatigue damage by sawcuts at each hole. When specimens were assumed to behave in a linear elastic manner, failure criteria overestimated the residual strength of specimens. Failure criterion which included consideration for crack interaction effects consistently predicted conservative failure loads. Fatigue tests were also conducted in three configurations to test the ability of three analytical methods to predict fatigue life. When linear elastic assumptions were made fatigue life was overestimated by failure criteria. A failure criteria that accounted for crack interaction effects as well as the MSD cracks plastic zone size produced the better prediction of fatigue life.

14. SUBJECT TERMS

Multiple Site Damage (MSD), Fatigue Life, Residual Strength

15. NUMBER OF PAGES
132

16. PRICE CODE

17. SECURITY CLASSIFICATION OF REPORT	18. SECURITY CLASSIFICATION OF THIS PAGE	19. SECURITY CLASSIFICATION OF ABSTRACT	20. LIMITATION OF ABSTRACT
UNCLASSIFIED	UNCLASSIFIED	UNCLASSIFIED	UL

GENERAL INSTRUCTIONS FOR COMPLETING SF 298

The Report Documentation Page (RDP) is used in announcing and cataloging reports. It is important that this information be consistent with the rest of the report, particularly the cover and title page. Instructions for filling in each block of the form follow. It is important to ***stay within the lines*** to meet ***optical scanning requirements***.

Block 1. Agency Use Only *(Leave blank)*.

Block 2. Report Date. Full publication date including day, month, and year, if available (e.g. 1 Jan 88). Must cite at least the year.

Block 3. Type of Report and Dates Covered. State whether report is interim, final, etc. If applicable, enter inclusive report dates (e.g. 10 Jun 87 - 30 Jun 88).

Block 4. Title and Subtitle. A title is taken from the part of the report that provides the most meaningful and complete information. When a report is prepared in more than one volume, repeat the primary title, add volume number, and include subtitle for the specific volume. On classified documents enter the title classification in parentheses.

Block 5. Funding Numbers. To include contract and grant numbers; may include program element number(s), project number(s), task number(s), and work unit number(s). Use the following labels:

C -	Contract	**PR** -	Project
G -	Grant	**TA** -	Task
PE -	Program Element	**WU** -	Work Unit Accession No.

Block 6. Author(s). Name(s) of person(s) responsible for writing the report, performing the research, or credited with the content of the report. If editor or compiler, this should follow the name(s).

Block 7. Performing Organization Name(s) and Address(es). Self-explanatory.

Block 8. Performing Organization Report Number. Enter the unique alphanumeric report number(s) assigned by the organization performing the report.

Block 9. Sponsoring/Monitoring Agency Name(s) and Address(es). Self-explanatory.

Block 10. Sponsoring/Monitoring Agency Report Number. *(If known)*

Block 11. Supplementary Notes. Enter information not included elsewhere such as: Prepared in cooperation with...; Trans. of...; To be published in.... When a report is revised, include a statement whether the new report supersedes or supplements the older report.

Block 12a. Distribution/Availability Statement. Denotes public availability or limitations. Cite any availability to the public. Enter additional limitations or special markings in all capitals (e.g. NOFORN, REL, ITAR).

DOD - See DoDD 5230.24, "Distribution Statements on Technical Documents."
DOE - See authorities.
NASA - See Handbook NHB 2200.2.
NTIS - Leave blank.

Block 12b. Distribution Code.

DOD - Leave blank.
DOE - Enter DOE distribution categories from the Standard Distribution for Unclassified Scientific and Technical Reports.
NASA - Leave blank.
NTIS - Leave blank.

Block 13. Abstract. Include a brief *(Maximum 200 words)* factual summary of the most significant information contained in the report.

Block 14. Subject Terms. Keywords or phrases identifying major subjects in the report.

Block 15. Number of Pages. Enter the total number of pages.

Block 16. Price Code. Enter appropriate price code *(NTIS only)*.

Blocks 17. - 19. Security Classifications. Self-explanatory. Enter U.S. Security Classification in accordance with U.S. Security Regulations (i.e., UNCLASSIFIED). If form contains classified information, stamp classification on the top and bottom of the page.

Block 20. Limitation of Abstract. This block must be completed to assign a limitation to the abstract. Enter either UL (unlimited) or SAR (same as report). An entry in this block is necessary if the abstract is to be limited. If blank, the abstract is assumed to be unlimited.